

Development of a multiplexed RNAi-coupled sensor assay to study neuronal function on the large-scale

Dissertation

for the award of the degree

"Doctor rerum naturalium"

of the Georg-August-University Göttingen

within the doctoral program

GGNB Molecular Physiology of the Brain

of the Georg-August University School of Science (GAUSS)

submitted by

Alexander Herholt

from Bielefeld, Germany

Göttingen, 2016

Thesis Committee:

Prof. Dr. Moritz Rossner

Molecular Neurobiology, Department of Psychiatry, LMU München

Prof. Dr. Nils Brose

Department of Molecular Neurobiology, MPI of Experimental Medicine Göttingen

Dr. Camin Dean

Trans-synaptic Signaling, European Neuroscience Institute Göttingen

Members of the Examination Board:

Prof. Dr. Moritz Rossner (Referee)

Molecular Neurobiology, Department of Psychiatry, LMU München

Prof. Dr. Nils Brose (2nd Referee)

Department of Molecular Neurobiology, MPI of Experimental Medicine Göttingen

Dr. Camin Dean

Trans-synaptic Signaling, European Neuroscience Institute Göttingen

Further members of the Examination Board:

Prof. Dr. Martin Göpfert

Department of Cellular Neurobiology, Georg-August-University Göttingen

Prof. Dr. Mikael Simons

Cellular Neuroscience, MPI of Experimental Medicine Göttingen

Institute of Neuronal Cell Biology, DZNE, München

Prof. Dr. Michael Sereda

Molecular and Translational Neurology, Department of Neurogenetics,

MPI of Experimental Medicine Göttingen

Date of oral examination: 10.08.2016

Declaration

Herewith I declare that I prepared the PhD thesis entitled: 'Development of a multiplexed RNAi-coupled sensor assay to study neuronal function on the large-scale' on my own and with no other sources and aids than quoted.

Alexander Herholt

31st Mai, 2016

Göttingen

Contents

Contents	i
List of Figures	iv
List of Tables	iv
1. Abstract	1
2. Introduction	2
2.1. Synaptic plasticity and excitation-transcription coupling in higher brain function	2
2.1.1. Forms of synaptic plasticity	2
2.1.2. Synapse-to-nucleus signaling	4
2.2. Synaptic dysfunction as a converging point of psychiatric diseases	8
2.2.1. Evidence at the circuit level	8
2.2.2. Evidence at the cellular level	9
2.2.3. Evidence at the molecular level	10
2.3. Inventory of the high-throughput toolbox in neuroscience	13
2.3.1. Cellular systems	13
2.3.2. High-content screens	15
2.4. Functional genomics	15
2.4.1. Genetic perturbation by RNA interference and CRISPR-Cas9	16
2.4.2. Advances through molecular barcoding and its application	20
2.4.3. Pooled RNAi/CRISPR-Cas9 screenings	21
2.5. Objectives	24
3. Materials	25
3.1. Equipment	25
3.2. Chemicals and consumables	26
3.2.1. Drugs used in experiments	26
3.2.2. Antibodies and cell stains	26
3.2.3. Commercial kits	27
3.2.4. NGS Reagents & Chips	27
3.2.5. Enzymes	27
3.3. Eukaryotic cell lines	28

3.4. Bacterial strains.....	28
3.5. Buffers and solutions.....	29
3.5.1. Solutions for western blotting.....	29
3.5.2. Solutions for luciferase assays	29
3.5.3. Solutions and media for cell culture	30
3.6. Oligonucleotide	31
3.7. Plasmids.....	33
4. Methods.....	34
4.1. Culturing of eukaryotic cell lines	34
4.2. Primary neuron culture.....	34
4.3. AAV production	35
4.4. Rotenone dose-response cell viability assay.....	37
4.5. Multiplexed <i>cis</i> -regulatory sensor assay	37
4.6. Luciferase assays	39
4.7. Protein detection by immunocytochemistry	40
4.8. Protein detection by western blot.....	41
4.9. RNA detection by reverse transcription and qRT-PCR.....	41
4.10. Design and cloning of the PATHscreeener library.....	42
4.11. Pooled RNAi screen in primary neurons.....	44
4.12. Cloning individual shRNAs and sgRNAs	48
5. Results	50
5.1. General considerations for a pooled RNAi screen in neurons.....	50
5.2. A reporter for neuronal activity.....	52
5.3. Vector design for sensor-based RNAi screenings	56
5.3.1. The principle of the screening approach.....	56
5.3.2. The shRNA expression cassette.....	58
5.3.3. Combining sensor and shRNA expression	61
5.4. Library cloning strategy	63
5.5. Sensor-based pooled RNAi screen in primary neurons.....	65
5.5.1. Proof-of-concept screen for regulators of neuronal excitation	65

5.5.2. Quality controls within the screening pipeline	66
5.5.3. Hit nomination by enhanced Z-score ranking and DESeq2 analysis	67
5.5.4. Hit ranking to biological function by KEGG and Reactome analyses	70
5.5.5. Reproducibility of the screen.....	73
5.5.6. Screening for negative regulators of neuronal excitation.....	75
5.6. Adaptation towards CRISPR-Cas9-based screening in primary neurons	76
6. Discussion.....	78
6.1. Advancing the current screening strategies.....	78
6.2. Assay validity	79
6.2.1. Identification of genes with known function in synaptic plasticity	79
6.2.2. Hits with association to psychiatric disorders.....	80
6.2.3. Chemokine signaling: Growing evidence for its role in neuronal activity.....	81
6.2.4. Comparison with the screen by Parnas et al.	82
6.3. Limitations of the approach	83
6.4. Future aspects of pooled genetic screens in neuroscience.....	83
6.4.1. Importance for psychiatric drug discovery	84
7. Abbreviations	86
8. References.....	88
9. Acknowledgement.....	107
Curriculum vitae	108

List of Figures

Figure 1: Regulatory pathways in synaptic plasticity and activity-dependent gene expression.	7
Figure 2: Alteration in cortical circuit function in schizophrenia.	9
Figure 3: Summary of genetic associations for MDD, BPD, ASD, and SZD.	12
Figure 4: Maturation stages of murine primary neurons.	14
Figure 5: Gene silencing by RNAi.	18
Figure 6: Overview of CRISPR-Cas9 applications.	20
Figure 7: Current paradigms for pooled genetic screens.	23
Figure 8: AAV infection rate.	36
Figure 9: Cellular RNA content is a more sensitive indicator of neuronal viability in the dish than DNA.	51
Figure 10: Multiplexed <i>cis</i> -regulatory sensor assay in response to neuronal silencing and synaptic stimulation.	54
Figure 11: Genomic architecture of the murine <i>Arc</i> promoter.	55
Figure 12: Design and characterization of the artificial E-SARE sensor.	56
Figure 13: Principle of the sensor-based genetic interference screen.	58
Figure 14: Efficient mRNA knockdown by hU6 promoter-driven shRNAs in neuronal cells. .	60
Figure 15: Functional validation of the PATHscreener vector.	62
Figure 16: Generation of the PATHscreener library.	64
Figure 17: Screening design and workflow.	66
Figure 18: Quality control measures from the pooled RNAi screen.	67
Figure 19: Enhanced Z-score and DESeq2 analysis of the pooled RNAi screen A.	69
Figure 20: Individual validation of selected candidates.	70
Figure 21: Screening hits along the synapse-to-nucleus pathway.	73
Figure 22: Reproducibility of the pooled RNAi screen in primary neurons.	74
Figure 23: Comparison of identified negative regulators in screen A, B, and C.	75
Figure 24: Adaptation towards an AAV CRISPR screening vector.	77

List of Tables

Table 1: Complexity of the PATHscreener library.	65
Table 2: Screens in this thesis: A / B / C.	66
Table 3: KEGG Pathway analysis for the Top140 positive regulators.	71
Table 4: Reactome Pathway analysis for the Top140 positive regulators.	72

1. Abstract

Psychiatric diseases such as schizophrenia, bipolar disorder and autism spectrum disorders are considered neurodevelopmental synaptopathies. Compelling evidence obtained from large-scale genome-wide association studies, identified a plethora of genetic variations within hundreds of genes encoding components of the post-synaptic compartment and calcium signaling mediating excitation-transcription-coupling. This synapse-to-nucleus signaling is thought to be particularly important for synaptic plasticity and learning and memory. In the last decade, tremendous progress has been made in neuroscience research when employing an array of molecular and cellular techniques to study the impact of individual genes on synaptic plasticity. Nevertheless, neuroscience methodology lags behind the field of cancer research in terms of large scale functional genetic screens, e.g. mediated by RNA interference (RNAi). The underlying cause is likely due to both the difficulties of culturing post-mitotic neurons and the phenotypic complexity. In this regard, comprehensively identifying genes involved in neuronal excitation and synapse-to-nucleus signaling may not only deepen our understanding of the corresponding biological processes, but might also be key in unearthing promising targets for psychiatric drug discovery.

I have developed a functional genomics tool that is applicable to primary neurons and combines the throughput of a pooled RNAi screen with the sensitivity of a pathway reporter assay based on the synaptic activity-response element, modified from the *Arc* enhancer. This thesis describes a proof-of-concept study in which an AAV-based RNAi library was screened for regulators of neuronal excitation and synapse-to-nucleus signaling. The assay principle relies on molecular barcodes, which serve as quantitative reporters, while at the same time also functioning as unique identifiers of the targeted genes. Upon synaptic stimulation, the screen identified a multitude of known genes involved in glutamatergic synapse-to-nucleus signaling, as well as previously unknown candidates like the chemokine receptor XCR1. The technical approach's reproducibility has been verified by substantial overlap of gene hits during three independent screens. Later in the thesis, I also present the principal applicability of CRISPR-Cas9 tools in neurons, which may improve performance for genetic interference screens in the near future.

This assay seeks to enhance the analytic toolbox used for analyzing regulatory processes during neuronal signaling and for the identification of novel targets in psychiatric drug discovery.

2. Introduction

2.1. Synaptic plasticity and excitation-transcription coupling in higher brain function

The human brain contains over 80 billion neurons (Azevedo et al., 2009). Those neurons are connected with each other via thousands of synaptic connections in order to transmit electrical signals for communication (Williams and Herrup, 1988). During brain development neurons of various types organize into distinct brain regions (e.g. cortex and hippocampus) and form local circuits (Hensch, 2005). Spatially separated circuits are connected by hubs of neurons that mediate long-range communication (Bullmore and Sporns, 2009). Although the exact mechanisms by which information is stored and processed in the brain is still unknown, neuronal plasticity is key to higher brain function during learning and memory (Amtul and Atta-Ur-Rahman, 2015). This involves strengthening of synaptic contacts, their maintenance as well as their weakening. Neuronal plasticity thereby modulates the intrinsic excitability of neurons and the strength of their synaptic connections. The persistence of such modifications at the cellular level depends on whether the intensity and duration of activity triggers a transcriptional response and the expression of new synaptic proteins (Kandel, 2001). The molecular mechanisms of this excitation-transcription coupling are intensively studied and key players have been identified (Bading, 2013; Greer and Greenberg, 2008; West et al., 2002). Emphasizing the importance of neuronal plasticity for higher brain function, it is not surprising that many neuropsychiatric diseases are associated with synaptic dysfunction (West and Greenberg, 2011).

2.1.1. Forms of synaptic plasticity

Synaptic plasticity integrates various kinds of responses to activity leading to changes in synaptic strength and efficacy. Such modifications play a key role during experience-driven information-processing and -storage in the brain. In general, one can categorize the synaptic modifications into forms of short-term and long-term synaptic plasticity (Citri and Malenka, 2008).

Although, the presented study mainly deals with the molecular program leading to long-lasting synaptic changes, concepts of short-term plasticity will be introduced briefly for the sake of completeness. Short-term plasticity covers changes that persist for milliseconds to several minutes and they mainly involve modifications of the neurotransmitter release probability at the presynaptic terminal (Thomson, 2000). The release probability can be either facilitated or depressed as a consequence of trains of stimuli and this seems to depend on the frequency of stimuli and the recent history of stimulation at the synapse

(Zucker and Regehr, 2002). Stimulation in short intervals of less than 20 ms commonly elicit a reduced response to the second stimuli compared to the first one, a phenomenon called paired-pulse depression. The counterpart, paired-pulse facilitation can occur at longer intervals of 20-500 ms. Furthermore, facilitation is rather observed if the synapse had a low neurotransmitter release probability prior to the stimulus and vice versa for depression (Dobrunz and Stevens, 1997). Regulators of the release property are, for example, presynaptic ionotropic receptors, such as the kainate receptor and the nicotinic acetylcholine receptor, which act as autoreceptors by sensing the neurotransmitter content at the synaptic cleft and eliciting feed-back mechanisms (Engelman and MacDermott, 2004). In addition, postsynaptic depolarization can lead to the release of retrograde messengers (e.g. dopamine, glutamate, BDNF, oxytocin, and endocannabinoids) from the postsynaptic compartment to modify presynaptic properties (Kombian et al., 1997; Nagappan and Lu, 2005; Nugent et al., 2007; Zilberter, 2000). The regulation of neurotransmitter release probability seems to play an important role as high-pass- and low-pass filters during information processing (Abbott and Regehr, 2004).

Long-term plasticity refers to mechanisms which result in synaptic remodeling that persist for hours, days, and longer (Citri and Malenka, 2008). Hence, these mechanisms are crucial for the development of neuronal circuits and for information storage as long-term memory (Segal, 2005). The two most studied phenomena of long-term plasticity are long-term potentiation (LTP) and long-term depression (LTD). Both have been primarily investigated at glutamatergic synapses in the CA1 region of the hippocampus, which involve activation of *N*-methyl-D-aspartate (NMDA) receptors (NMDARs) (Lüscher and Malenka, 2012; Martin et al., 2000). Important for the induction of LTP and LTD are the different channel properties of α -amino-3-hydroxy-5-methyl-4-isoxazole propionic acid (AMPA) receptors (AMPA receptors) and NMDARs, the two major ionotropic glutamate receptors at excitatory synapses (Benke et al., 1998; Mayer et al., 1984). Activation of AMPARs by presynaptic glutamate release leads to an influx of the monovalent cations sodium and potassium and generates the excitatory postsynaptic response. NMDARs, in contrast, are blocked by magnesium at resting membrane potential and this block is only released upon strong depolarization of the postsynaptic membrane and simultaneous activation by glutamate (1984; Nowak et al., 1984). If this occurs, sodium and calcium can pass the NMDAR channel into the postsynaptic compartment. It is believed that the level of calcium within the dendritic spine regulates the switch between depression and potentiation (Malenka and Nicoll, 1993). High-frequency synaptic stimulation leads to a strong increase in calcium concentration and the induction of LTP, whereas repetitive low-frequency stimulation causes a moderate increase in calcium and finally LTD (Sabatini et al., 2002). A crucial switch might be the timing of presynaptic action potential input and the backpropagating potential coming from the dendrites. LTP is evoked if the presynaptic spike slightly precedes the backpropagating

action potential at the synapse, and vice versa for LTD (Stuart et al., 1997; Waters et al., 2005). Calcium inside the dendritic spine triggers a number of signaling events leading to rapid changes in postsynaptic AMPAR content ('early-phase' response) and with some delay to local dendritic protein synthesis and induction of gene expression in the nucleus ('late-phase' response) (Greer and Greenberg, 2008; Henley and Wilkinson, 2016). The latter will be discussed in more detail below.

2.1.2. Synapse-to-nucleus signaling

Long-term potentiation is thought to be a molecular correlate of learning and memory and long-term memory consolidation requires 'late-phase' LTP including gene expression (Adams and Dudek, 2005). This excitation-transcription coupling makes it inevitable that the signal generated during synaptic transmission is propagated to the nucleus in order to induce the expression of activity-dependent genes. The communication between the synapse and the nucleus is of great importance and multiple routes have been identified (Bading, 2013; Nakamura et al., 1999; Xia et al., 1996) (illustrated in figure 1). As mentioned earlier, neurotransmitter release at glutamatergic synapses can elicit a calcium influx into the postsynaptic compartment through the opening of the NMDAR channel. Although this rise in calcium concentration through NMDARs mainly remains restricted to the dendritic spine, several lines of evidence indicate that calcium is the key second messenger for communication between synapse and nucleus (Bading et al., 1997; Chawla, 2002; Greer and Greenberg, 2008; Redmond, 2008; Sheng and Greenberg, 1990). Furthermore, experiments with nuclear calcium indicators demonstrated that changes in nuclear calcium concentration correlate with synaptic activity and specific quenching of nuclear calcium prevented the induction of 43% of all activity-dependent genes (Bengtson et al., 2010; Hardingham et al., 1997; Zhang et al., 2009). Thus, by which mechanisms does the calcium signal propagate to the nucleus and what are alternative routes? The first mechanism involves voltage-gated calcium channels (VGCC). Upon membrane depolarization those channels open and calcium fluxes into the cell (Fatt and Katz, 1953; Llinás et al., 1976). Calcium influx through VGCCs located in the membrane of the cell soma and the dendrites rapidly increases the intracellular calcium concentration caused by a steep gradient across the membrane (McBurney and Neering, 1987). Calcium can enter the nucleus by diffusion and activate downstream effectors such as calcium/calmodulin-dependent protein kinase IV (CaMK4). Through phosphorylation, CaMK4 passes the signal to cAMP-responsive element-binding protein (CREB), one of the key activity-dependent transcription factors, and its interaction partner CREB-binding protein (CBP) (Chawla et al., 1998; Impey et al., 2002). Together, they induce expression of a huge set of activity-dependent genes (e.g. *FOS*, *ARC*, *BDNF*) (Kim et al., 2010; Pfenning et al., 2007). Recent data suggest that the CaMK2

subunits alpha, beta, and gamma are playing an important role for inducing neuronal plasticity-coupled gene expression as well. In this model, calcium influx through the VGCC Cav1.2 first mobilizes actin-bound CaMK2 α/β and, subsequently, a voltage-dependent conformational change of the channel causes an accumulation of CaMK2 α/β (Li et al., 2016). This in turn activates CaMK2 γ by phosphorylation and CaMK2 γ shuttles calcium-loaded calmodulin (CaM) into the nucleus where it induces CREB-CBP activation via CaMK4 (Ma et al., 2014). Voltage-dependent calcium channels are not the only regulators of intracellular calcium concentrations. The calcium signal might be amplified from the endoplasmic reticulum (ER), which can function as a high capacity calcium store (Berridge, 1998). For instance, ryanodine receptors can release calcium from the ER (Kuwajima et al., 1992). In addition, inositol triphosphate (IP3) receptors line up at the ER membrane along the dendrites and sequential receptor activation might generate a propagating calcium wave through calcium release from the ER. Activation of IP3 receptors occurs when synaptic transmission activates G-protein coupled receptors (GPCRs) which stimulate the generation of IP3 and diacylglycerol (DAG) via phospholipase C (PLC) (Jaffe and Brown, 1994; Nakamura et al., 1999; Watanabe et al., 2006). After a calcium wave has occurred, cytoplasmic calcium concentrations are brought back to a low level by exporting calcium through calcium ATPases and sodium-calcium exchangers located at the plasma membrane and via sarcoendoplasmic reticulum calcium ATPases into the ER (Verkhatsky, 2004).

CREB-dependent gene expression upon synaptic stimulation may also be induced by cAMP, another prominent second messenger (Mayr and Montminy, 2001; Montminy, 1997). It is produced by adenylate cyclases and the activation of some adenylate cyclases is dependent on calcium/CaM signaling (e.g. Adyc8) (Nicol and Gaspar, 2014). cAMP activates protein kinase A (PKA) thereby stimulating CREB-mediated transcription. Pharmacological and genetic perturbations of the cAMP pathway *in vivo* caused deficits in cognitive tasks, thus establishing a link between cAMP signaling and learning and memory (Wang and Storm, 2003). However, to what extent cAMP signaling is contributing to activity-dependent gene expression remains unclear.

Calcium flux through NMDARs and VGCCs also activates the mitogen-activated protein kinase (MAPK) cascade including the key players ERK1/2 (Dolmetsch et al., 2001; Hardingham et al., 2001; Xia et al., 1996). Besides calcium/calmodulin-dependent kinases and PKA, MAPKs are the third kinase class that is important for long-term synaptic plasticity (Shalin et al., 2006; Sindreu et al., 2007). Entry-point for the MAPK pathway is the small GTPase Ras and evidence suggests that Ras is activated by Ras guanyl-nucleotide releasing factors (Ras-GRFs) complexed with calcium-loaded CaM (Ebinu et al., 1998; Farnsworth et al., 1995). Ras activity in the postsynapse is controlled by the CaMK2-dependent Ras-GTPase activating protein SynGAP, a risk gene for intellectual disability, epilepsy and autism spectrum disorders (ASD) in humans (Jeyabalan and Clement, 2016).

Active Ras induces indirectly the phosphorylation of Raf isoforms (e.g. ARAF) which in turn phosphorylate MEK1/2. Unphosphorylated MEK1/2 traps ERK1/2 in the cytoplasm, but phosphorylation releases ERK1/2 and activates it. ERK1 and ERK2 have multiple cellular substrates, such as ribosomal protein S6 kinase 2 (RSK2), mitogen- and stress-activated kinase 1 (MSK1), and Elk-1 a transcriptional co-factor of serum-response-factor (SRF) (Arthur et al., 2004; Gille et al., 1995; Xing et al., 1996). Activation of MAPK-signaling upon synaptic stimulation is reported to have local and global effects on neuronal function (Wiegert and Bading, 2011). As pointed out earlier, calcium influx through synaptic NMDARs remains locally confined to the dendritic spine. This is also observed for activated ERK1/2 at the synapse which have been shown to participate in the regulation of AMPAR cycling between the PSD and endosomes (Kim et al., 2005; Zhu et al., 2002). In addition, MAPK signaling at the soma and inside the nucleus is also required for synaptic plasticity and memory formation (Shalin et al., 2006; Sindreu et al., 2007). However, little is known how synaptic activity is connected to active ERK1/2 in the soma and nucleus. A possible scenario may involve a rise in somatic and nuclear calcium concentrations upon opening of VGCCs leading to a global activation of MAPK signaling (Adams and Dudek, 2005; Wiegert et al., 2007). A cytoplasmic substrate of activated ERK1/2 is for example RSK2 which induces CREB-dependent gene expression. Besides its role in transcription factor activation, nuclear ERK1/2, together with MSK1, also regulates activity-dependent gene expression more broadly by chromatin remodeling through histone 3 phosphorylation (Brami-Cherrier et al., 2007).

At last, the induction of activity-dependent genes occurs downstream of the presented signaling pathways from the synapse to the nucleus. Description of the activity-dependent transcriptome and epigenome by RNA-seq and ChIP-seq, respectively, provided insight into the transcriptional program underlying long-term synaptic plasticity (Kim et al., 2010; Malik et al., 2014; Zhang et al., 2009). The transcriptional response itself has multiple layers. Signals from the synapse are activating pre-existing transcription factors (e.g. CREB, MEF2, SRF) and chromatin remodeling factors (West et al., 2002). This regulates the expression of immediate-early-genes (IEGs), a class that contains multiple transcription factors itself (e.g. FOS, EGR1, c-JUN) (Murphy et al., 1991). Subsequently, those IEG transcription factors induce the expression of late-response genes (e.g. BDNF, HOMER1) which function at the synapse and thus exert long-lasting modulations of synaptic contacts in neuronal circuits during LTP and LTD (Barco et al., 2005; Sala et al., 2003). Recent findings indicate that particularly the late response gene expression differs between excitatory- and inhibitory neurons due to different sets of active enhancer regions (Spiegel et al., 2014). How exactly differential signaling and the combinatorial action of various transcription factors dictate the cellular response to experience-driven activity remains elusive and requires further investigation. Furthermore, it is likely that so far unrelated protein networks directly or

indirectly contribute to the regulation of neuronal function and thus represent an untouched pool of potential targets for drug discovery in the field of central-nervous system (CNS) diseases.

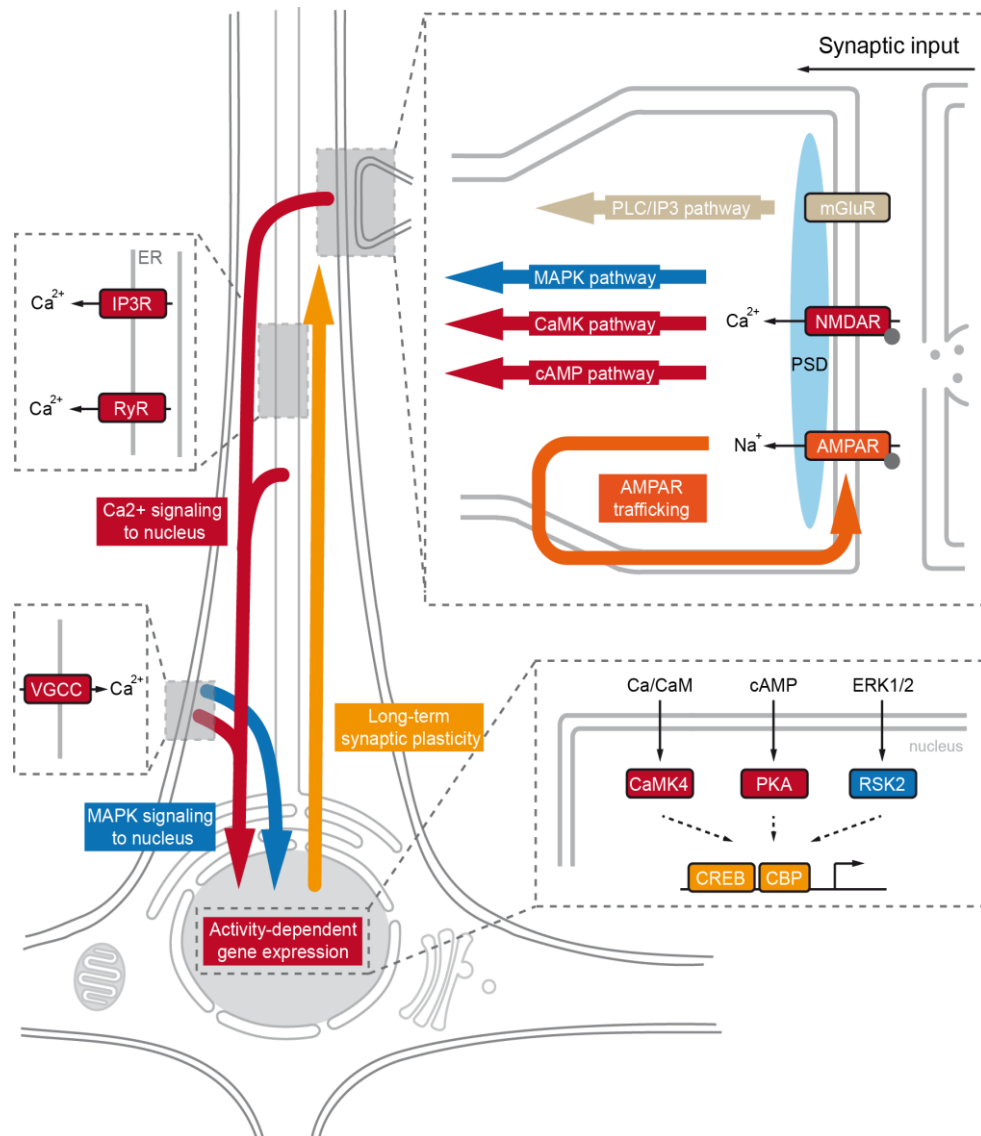


Figure 1: Regulatory pathways in synaptic plasticity and activity-dependent gene expression.

Presynaptic release of glutamate can initiate multiple signaling cascades in the postsynaptic neuron. Trafficking of AMPARs at the postsynapse directly modulates synaptic strength during LTP and LTD. Long-term synaptic plasticity requires activity-dependent gene expression of synaptic proteins. Calcium is thought to be the main second messenger from the synapse to the nucleus, for instance via calcium/calmodulin-dependent kinases (CaMK). The calcium signal might be enhanced through calcium influx from the ER or by voltage-gated calcium channels (VGCC) located in the plasma membrane. Kinases, such as CaMK4, PKA, and RSK2, phosphorylate various regulators of the activity-dependent gene expression program, like CREB and CBP (for citations see main text). Adapted from (Bading, 2013; Ebert and Greenberg, 2013).

2.2. Synaptic dysfunction as a converging point of psychiatric diseases

The etiology of psychiatric disorders like schizophrenia, bipolar disorder (BPD) and ASD remains in large parts unknown although great progress has been made over the last decade in the field of brain imaging and risk factor identification (Ripke et al., 2013; Sarkar et al., 2015). In addition, neurons established from induced pluripotent stem cells (iPSC) represent a new source to explore molecular and cellular processes that might be altered in patients (Haggarty et al., 2016). A substantial body of evidence from various methodologies suggests that synaptic dysfunction and calcium-signaling play a central role in multiple psychiatric diseases (West and Greenberg, 2011). The following sections review findings at different levels starting with alterations in neuronal circuit function and ending with the multitude of genetic mutations accounting for disease susceptibility.

2.2.1. Evidence at the circuit level

Studies that aimed to decode the structural and functional connectivity of the brain using imaging (functional MRI) and electrophysiological (EEG/MEG) techniques suggest that the brain connectome has small-world topology (Uhlhaas and Singer, 2012). This implicates that neuronal micro-networks in spatially distant brain areas communicate via few highly connected hubs (Bullmore and Sporns, 2009). Communication between prefrontal cortex and hippocampus, for instance, is thought to be required for information processing and long-term storage (Brincat and Miller, 2015; Igarashi, 2015). Such higher brain functions are dependent on various kinds of oscillatory activity of neuronal groups and their synchronization over short and long distances (Varela et al., 2001). While long-range communication rather involves theta (4-7 Hz), alpha (8-12 Hz), and beta (13-25 Hz) oscillations, local oscillatory activities tend to be at higher gamma-band frequencies (25-200 Hz) (von Stein and Sarnthein, 2000). Electrophysiological studies with schizophrenia patients have revealed reduced cortical gamma-oscillations during cognitive tasks like working memory (Haenschel et al., 2009) (Figure 2). In addition, altered theta- and alpha-oscillations have been recorded during sensory-gating in patients with schizophrenia (Hong et al., 2010). Oscillatory activity is the result of a precisely tuned interplay between groups of excitatory neurons and inhibitory interneurons within neuronal circuits (Wang and Buzsáki, 1996). In the cerebral cortex such circuits are formed by excitatory glutamatergic pyramidal cells and inhibitory GABAergic interneurons (Whittington et al., 1995). Those inhibitory neurons, in particular fast-spiking parvalbumin (PV) positive interneurons, are responsible for the fine-tuning of gamma-frequency oscillations during cognitive tasks (Bartos et al., 2007). The physiological basis for impaired high-frequency gamma-oscillations in schizophrenia patients is therefore likely a dysbalance between excitation and inhibition (E/I) (Sohal et al., 2009).

This causality is supported by various studies in pharmacological rodent models for symptoms of schizophrenia. Administration of the NMDA receptor antagonists Ketamine or MK-801 into the prefrontal cortex of mice and rats leads to decreased evoked gamma-oscillations and finally a schizophrenia-like phenotype (Homayoun and Moghaddam, 2007a; Saunders et al., 2012). Notably, it has been observed that a NMDA receptor hypofunction leads to reduced inhibitory control of glutamatergic output neurons, resulting in cortical excitation (Homayoun and Moghaddam, 2007b). Finally, optogenetic elevation of the E/I balance within the prelimbic/infralimbic cortex of mice caused impairments during learning and social behavior paradigms (Yizhar et al., 2011). Taken together, these findings indicate that the modulation of glutamatergic neurotransmission might be relevant for the treatment of schizophrenia and ASD.

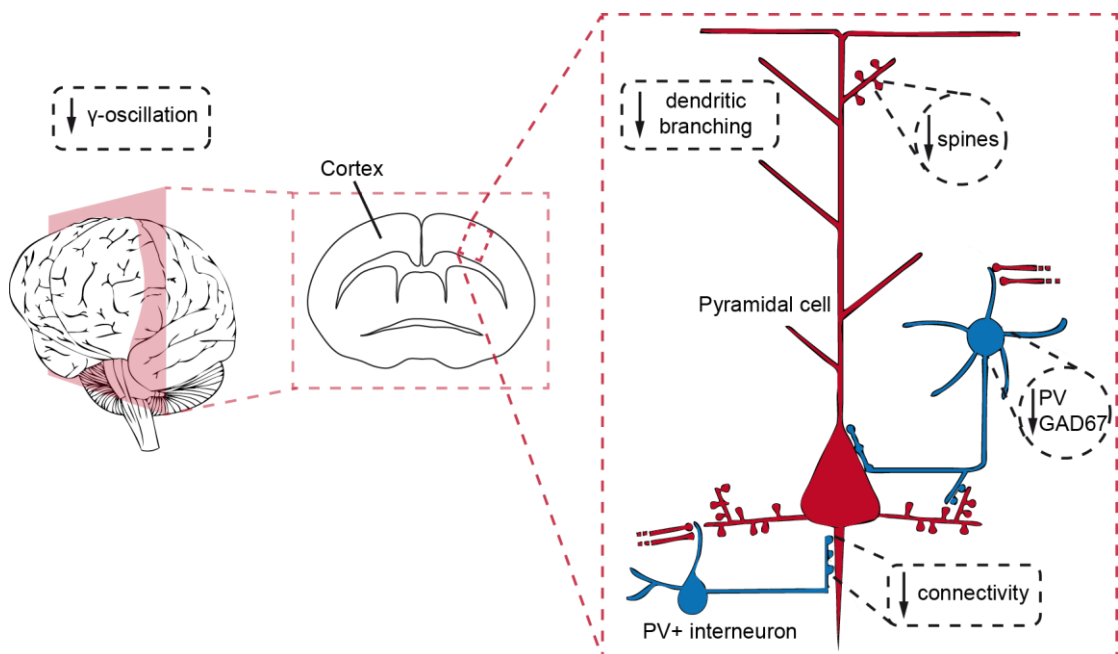


Figure 2: Alteration in cortical circuit function in schizophrenia.

Schizophrenia patients are showing morphological and cellular hallmarks of disturbed neurodevelopment and circuit formation such as decreased dendritic arborization, reduced spine density, and decreased interneuron-marker (PV, GAD67) expression (for citations see main text). Adapted from (Marín, 2012; Pratt et al., 2012).

2.2.2. Evidence at the cellular level

At the cellular level multiple studies provide evidence for alterations in neuronal maturation and synaptic plasticity in schizophrenia patients (Penzes et al., 2011). Schizophrenia subjects show shorter and less branched dendrites (Black et al., 2004; Guidotti et al., 2000;

Selemon and Goldman-Rakic, 1999). Furthermore, a reduced spine density has been observed on pyramidal neurons of the primary auditory cortex and on CA3 dendrites of the hippocampus (Kolomeets et al., 2005; Steen et al., 2006; Sweet et al., 2009) (Figure 2). Until recently, psychiatric research was strongly limited by the unavailability of neuronal material from patients and restricted to postmortem tissue and pharmacologic as well as genetic mouse models. The seminal work by Takahashi and Yamanaka, who for the first time reprogrammed human fibroblasts into iPSCs, paved the way towards patient-derived induced neurons (iNeurons) (Takahashi and Yamanaka, 2006). Such iNeurons harbor the complex genetic burden of the patient and thus represent a unique cellular model to study neuropathology. A study by Brennand and colleagues provided the first evidence that iNeurons established from schizophrenia patients reflect cellular correlates of the disease (Brennand et al., 2011). Those cultures showed reduced connectivity compared to iNeurons from healthy controls and decreased expression of synaptic proteins like PSD-95 and glutamate receptor subunits (GRIK1, GRIK4, GRM7, GRIN2A). In addition, dysregulated cAMP and WNT signaling activity was detected (Brennand et al., 2011). Moreover, altered energy metabolism has been reported for schizophrenia patient-derived neuronal progenitor cells and glutamatergic neurons derived from patients suffering from BPD (Mertens et al., 2015; Paulsen et al., 2013). Cultures from patients with a *DISC1* (Disrupted-in-Schizophrenia 1) loss-of-function mutation showed neurodevelopmental abnormalities, synaptic deficits and gene expression changes (Wen et al., 2014).

Taken together, current evidence from various sources of morphological studies highlight that schizophrenia, BPD, and ASD are most likely neurodevelopmental disorders with a significant synaptopathology. As a consequence, disturbed neuronal circuit function and unbalanced E/I are detected, which seem to be putative causes for symptoms like cognitive deficits, social isolation, and hallucination. A major challenge still is to decipher the link between genetic susceptibility for psychiatric disorders and the occurrence of symptoms as well as the response to medications. Psychiatric genomics made great progress in the identification of risk loci over the last years and current knowledge will be discussed in the following chapter.

2.2.3. Evidence at the molecular level

In schizophrenia and BPD both genetic and environmental factors have an impact on disease vulnerability. Family and twin studies have estimated a heritability of ~80% and ~60% for schizophrenia and BPD, respectively (Song et al., 2015; Sullivan et al., 2003) (Figure 3). Attempts to link genetic variations to schizophrenia by classical human genetics delivered only few solid associations. Worth mentioning in that context are the 22q11.2

micro-deletion and the involvement of *DISC1*. The 22q11.2 micro-deletion, which in most of the cases occurs *de novo*, results in the disruption of 30-60 genes on chromosome 22 and leading to a high risk of 25% to develop schizophrenia (Bassett et al., 2008; Karayiorgou et al., 2010). *DISC1* was linked to schizophrenia in a genetic study of a Scottish family that had an unusual number of cases with mental illness (St Clair et al., 1990). A chromosomal translocation was detected which disrupts the *DISC1* gene. Great progress has been made in the field of psychiatric genetics since the advent of genome-wide-association-studies (GWAS) and in particular with the collaborative approach by the Psychiatric Genomics Consortium (PGC). This permitted screening of a sufficient number of patients and healthy controls to detect associations between common variants (frequency >1-5% in the population) and psychiatric disorders at genome-wide significance (Cross-Disorder Group of the Psychiatric Genomics Consortium et al., 2013; Ripke et al., 2013). It became apparent that the genetic background of schizophrenia is highly heterogeneous and polygenic (Schizophrenia Working Group of the Psychiatric Genomics Consortium, 2014). Thus, so far undetermined combinations of multiple genetic variants seem to build the genetic vulnerability, where each variant only has a small effect size (Franke et al., 2016). In the case of schizophrenia the latest release from the PGC describes 108 loci which reach genome-wide significance by comparing 36,989 cases with 113,075 controls (Schizophrenia Working Group of the Psychiatric Genomics Consortium, 2014) (Figure 3). Since most of those loci lie within regulatory and not exonic regions, usually the proximal genes are reasoned to be involved in disease susceptibility (Maurano et al., 2012). The GWAS data is an excellent basis for studies on disease etiology and drug discovery for psychiatric disorders and it is now required to analyze putative risk genes in greater depth. This might finally bridge the gap between genetic susceptibility and the clinical symptoms. As a first step, genes at or near associated loci for schizophrenia have been analyzed whether they converge into common biological processes. The most recent releases of the PGC report on an enrichment of genes affecting calcium signaling (e.g. *CACNA1C*, *CACNAB2*, *CACNA1I*), glutamatergic transmission and synaptic plasticity (e.g. *GRM3*, *GRIN2A*, *SRR*, *GRIA1*) and targets of *MIR137* (e.g. *TCF4*) (Ripke et al., 2013; Schizophrenia Working Group of the Psychiatric Genomics Consortium, 2014). Furthermore, the major histocompatibility complex (MHC) locus, comprising over 200 genes with known functions in T-cell immune response, has been the first and since then the strongest genetic risk association for schizophrenia (Charles A Janeway et al., 2001; Stefansson et al., 2009). Overall, enhancers that are active in tissues with immune function harbored an enriched number of schizophrenia associations, however, it has long been elusive what kind of role these common variants play in the pathophysiology of schizophrenia (Ripke et al., 2013; Schizophrenia Working Group of the Psychiatric Genomics Consortium, 2014). Recently, complement component 4 (*C4*), a member of the classical component cascade, was identified as the main schizophrenia risk

gene at the MHC locus and a function in synapse elimination during postnatal development has been reported (Sekar et al., 2016).

Similar to the blurred boundaries between symptomatic manifestations of various psychiatric disorders, genetic data is challenging the distinction as the genetic correlations between schizophrenia, BPD and major depressive disorder (MDD) is in the range of 0.4-0.6 (Maier et al., 2015). Besides common variants, rare copy number variations (CNVs), which are less frequent but have higher penetrance, seem to play an important role in disease etiology for schizophrenia and also for ASD (Figure 3). Such structural variants (SV), including microdeletions and microduplications of more than 500 kilobases, affect the expression of dozens of genes (Levinson et al., 2011; Vacic et al., 2011). Figure 3 summarizes the current data for heritability, GWAS loci, and structural variants for four major mental illnesses (Geschwind and Flint, 2015).

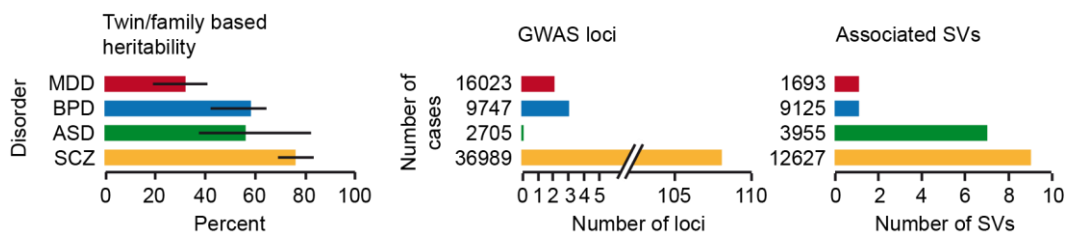


Figure 3: Summary of genetic associations for MDD, BPD, ASD, and SZD.

Left, estimated heritability from twin and family studies. Errorbars (sem). MDD, major depressive disorder; BPD, bipolar disorder; ASD, autism spectrum disorder; SCZ, schizophrenia. Middle/right, the number of identified genome-wide significant loci and associated structural variants (SV). The number of analyzed patients within the largest study for a disorder is given on the y-axis. Adapted from (Geschwind and Flint, 2015).

A systematic detection of rare variants (allele frequency <0.5-1%) within protein-coding regions by exome sequencing (exome-seq) is now possible, as costs for next-generation-sequencing are falling. However, similar to GWAS, large sample numbers are inevitable to gain statistical power (Tennessen et al., 2012). Two recent large scale exome-seq projects have identified a significant enrichment of disruptive rare variants within sets of voltage-gated calcium ion channel genes (e.g. *CACNA1C*, *CACNA1B*, *CACNA1H*), genes of the post-synaptic density (PSD), and genes of the ARC-complex and the NMDAR-complex (e.g. *DLG1*, *DLG2*, *CaMK2A/2B*, *SLC25A3*, *ABLIM1*, *SYNGAP1*) (Fromer et al., 2014; Purcell et al., 2014). In addition, target genes of the ASD-associated RNA-binding protein FMRP, which controls translation at the synapse, have been enriched significantly (Darnell et al., 2011; Tang et al., 2015). The concept that many psychiatric disorders primarily represent synaptopathies is further supported by a thorough characterization of the human synapse

proteome. A mapping to known disease-associated mutations revealed that over 200 genes connected to the synapse cause changes in synapse physiology, and are related to over 130 human brain diseases (Bayés et al., 2011).

In conclusion, genetic studies on psychiatric disorders are revealing the highly complex polygenicity for disorders like schizophrenia and BPD. The genetic associations are enriched within synaptic genes, genes involved in calcium signaling and immune function and the overlap, both in terms of genetics as well as symptoms, is high for schizophrenia, BPD, and MDD. Hence, it is likely that assay development for research on neuronal function will have an impact on a broad range of CNS diseases in general, and neuropsychiatric disorders in particular.

2.3. Inventory of the high-throughput toolbox in neuroscience

Development of high-throughput methods for applications in neuroscience is generally lagging behind other biomedical research areas like oncology. This is not surprising as the cellular systems as well as the phenotypes of interest are highly specialized. Nonetheless, immense progress has been made to increase, for example, the throughput through advanced high-content assays, but pooled genetic assays are still absent from the high-throughput toolbox in neuroscience.

2.3.1. Cellular systems

Neurons are highly specialized cells which is reflected by the complexity of regulatory physiological processes and how frequent perturbations lead to pathological states. Given its unique repertoire of cellular functions it is inevitable that the regulation of neuronal excitation and synapse-to-nucleus signaling needs to be studied in a differentiated and mature neuron population. This has also been only recently acknowledged by the pharmaceutical industry after suffering a series of failures during clinical trials for drugs that originated from classical biochemical target-based drug discovery projects (Scannell and Bosley, 2016). In this scenario, the predictive validity of an *in vitro* assay, which is the ability to yield good answers and good treatments based on, for example, profiles of cellular activities, is strongly dependent on the biological relevance of the cell culture system (Vincent et al., 2015).

Primary neurons from mice and rats are for a long time a well-established cellular system to study neuronal differentiation and signaling in the dish. Neuronal maturation in this system is relatively fast, resulting in an extensive network with functional synaptic connections already at day-in-vitro (DIV) 12-15 (Figure 4) (Baj et al., 2014). At that time, spontaneous network

activity can be recorded and synaptic activity can be strongly induced by blocking the inhibitory input of the network using the GABA_A-receptor antagonist bicuculline (BIC). In addition, for functional genomics studies, it is of advantage that sufficient cell numbers of high purity can be obtained from embryonic animals.

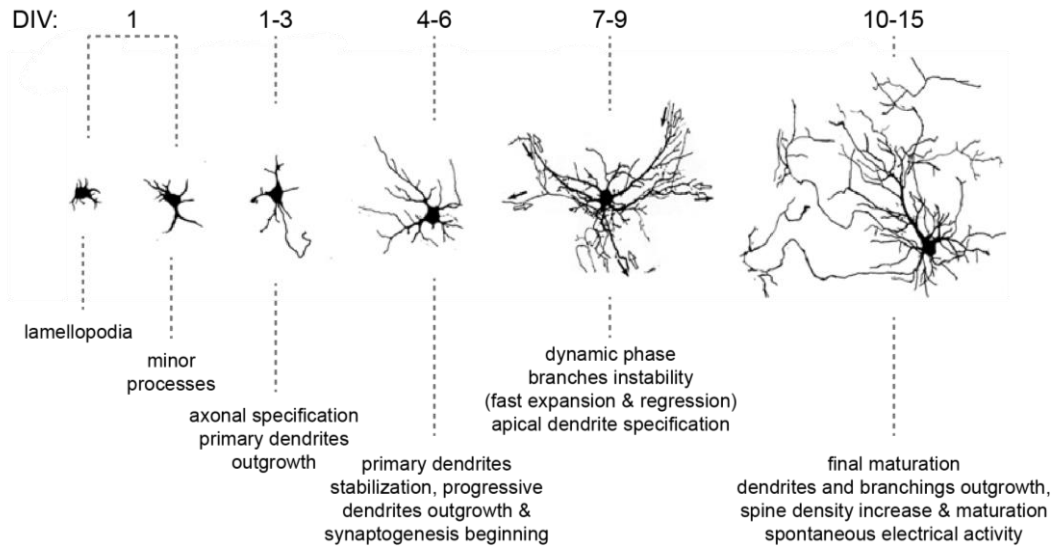


Figure 4: Maturation stages of murine primary neurons.

Maturation stages of primary neuron from DIV 1 till 15. Staging was done using murine primary hippocampal neurons, but is most likely similar for cortical neuron cultures. Within two weeks mature neuronal cultures are generated. Adapted from (Baj et al., 2014).

An alternative and highly valued source for neuronal cell culture assays are iNeurons, which have been differentiated from iPSCs of a given human donor (Dimos et al., 2008). This technique has attracted much attention as it allows studying cell biology of a neuron that harbors the genetic information of the donor (Mertens et al., 2016). Thus, it represents a unique source for cells with the highly complex set of genetic variations present in a psychiatric patient (Brennan et al., 2011; Habela et al., 2016; Haggarty et al., 2016; Krey et al., 2013; Topol et al., 2015; Wen et al., 2014). However, this method is relatively new and a variety of iNeuron-differentiation protocols are available which strongly differ in cell yield, purity, and maturation state of the culture (Mertens et al., 2016). In general, human-derived iNeurons tend to differentiate and mature much slower compared to rodent primary neurons and a decent extent of functionally mature synapses is usually only achieved by co-culture with astrocytes over several weeks (Nicholas et al., 2013). Nevertheless, differentiation protocols are improving rapidly and as soon as yield, purity, and the number of functional

synapses have increased, iNeurons will likely become the cell-type of choice for functional genomics screens in neuropsychiatric research.

2.3.2. High-content screens

High-content assays are one of the most advanced high-throughput assays in general and in particular in neuroscience. Their power lies in the multi-parametric analysis of cellular phenotypes using automated microscopy (Boutros et al., 2015). However, assay design is not trivial as the molecular correlates of a given phenotype need to be stained with high specificity or transgenic labels must be available in order to enable robust segmentation of cellular features by automated image analysis. The most frequently used marker is neuronal viability and thus neuroprotection has been the main focus so far (Anderl et al., 2009; Schulte et al., 2011). More sophisticated parameters are neurite length and arborization as well as changes in synapse number (Harrill et al., 2011; Ofengeim et al., 2012; Radio, 2012). In the last years significant progress has been made in order to streamline and facilitate the image acquisition (Caicedo et al., 2016). This has led to a growing number of users and the pharmaceutical industry is using high-content assays in phenotypic drug discovery for CNS diseases (Haggarty et al., 2016; Hunsberger et al., 2015). While high-content compound screens are feasible with neuronal cultures, genetic interference screens are more challenging (Harrill et al., 2011; Ofengeim et al., 2012). A reason is the poor transfectability of primary neurons, which as a consequence implies the use of viral transduction. However, the generation of large-scale arrayed viral libraries for the expression of thousands of shRNAs (short hairpin RNA) or cDNAs is extremely expensive and laborious and usually not feasible for a single academic group. To my knowledge, only one single high-content RNAi has been published until now with primary neurons (Nieland et al., 2014). This screen used a relatively small scale arrayed lentiviral RNAi library of 607 shRNA vectors to screen for regulators of synaptogenesis. High-content assays and pooled genetic screens can be considered somewhat as complementary. A high-content screen using the top hits from a pooled genetic screen may, for example, represent a very powerful orthogonal secondary validation tool.

2.4. Functional genomics

Functional genomics is a research field that is investigating the impact of the genotype on molecular or cellular phenotypes at genome-scale. This involves for example the study of dynamic changes in the transcriptome, the proteome, and the epigenome as well as large-scale loss- and gain-of-function studies. In recent years functional genomics approaches in

neuroscience have delivered a wealth of data about the neuronal activity-dependent transcriptome and epigenome, as well as the cellular and synaptic proteome (Bayés et al., 2011; Kim et al., 2010; Malik et al., 2014; Sharma et al., 2015; Zhang et al., 2009). Systematic large-scale approaches to study gene function during neuronal activity are, however, missing.

2.4.1. Genetic perturbation by RNA interference and CRISPR-Cas9

Understanding gene function is one major quest in molecular biology. Early after the discovery of the post-transcriptional mRNA abundance control mechanism called RNAi in the nematode *Caenorhabditis elegans* in 1998 and later in mammals, RNAi became the prime method for loss-of-function studies (Jinek and Doudna, 2009; Winter et al., 2009)(Fire et al., 1998). The endogenous RNAi pathway takes place within the nucleus and the cytoplasm and involves two major cleavage steps (illustrated in figure 5). miRNAs are typically transcribed as gene-clusters by RNA polymerase II (Borchert et al., 2006; Lee et al., 2004). The generated transcripts, termed primary miRNA (pri-miRNA), are capped, polyadenylated, and usually comprise several hundred nucleotides in length. Pri-mRNAs fold into characteristic hairpin structures containing imperfectly base-paired stems (Carthew and Sontheimer, 2009). The fold of the transcript is important for its proper processing. The first of the two major maturation steps occurs within the nucleus where the stem-loop (hairpin) of the pri-miRNA is cleaved-off by a microprocessor complex containing the RNase III enzyme Droscha (Lee et al., 2003). This cleavage occurs co-transcriptionally and generates the miRNA precursor (pre-miRNA) which is ~70 nt in length and consists of a stem which harbors the crucial ~22 nt miRNA sequence and a terminal loop. The pre-miRNA is exported into the cytoplasm by the transport factor Exportin-5 in complex with Ran-GTP (Yi et al., 2003; Zeng and Cullen, 2004). Thus, the second major processing step occurs in the cytoplasm and involves the multi-protein RISC loading complex (RLC) (Gregory et al., 2005). The RLC consists of the RNase III Dicer, the double-stranded RNA-binding proteins TRBP (Tar RNA binding protein), PACT (protein activator of PKR), and the core component Argonaute-2 (Ago2). The terminal loop of the pre-miRNA is cleaved-off by Dicer, creating the mature ~22 nt long miRNA duplex (Chendrimada et al., 2005). This double-stranded RNA consists of the guide strand and the passenger strand. While the guide strand contains the sequence complementarity to the mRNA target and thus has to be used for gene regulation, the passenger strand must be degraded. After cleavage of the pre-miRNA, Dicer and its interactors TRBP and PACT dissociate from the miRNA duplex. The active RNA-induced silencing complex (RISC) is formed by an asymmetric guide strand selection by Ago2 (Frank et al., 2010; Khvorova et al., 2003; Schwarz et al., 2003). The active RISC is then guided to its mRNA target mainly by position 2 to 8 of the guide strand which is defined as the seed

region of the miRNA (Rajewsky, 2006). The extent of complementarity of miRNA and mRNA are thought to be a key determinant of the regulatory mechanism. While a perfect match induces Ago2-mediated cleavage of the mRNA, central mismatches rather promote repression of mRNA translation (Filipowicz et al., 2008).

The usage of RNAi for loss-of-function studies is easy and fast. Usually, short double-stranded RNA molecules are transfected into cells where they are processed into small interfering RNAs (siRNAs) of about 22 nucleotides in length. These siRNAs can silence gene expression in a sequence specific manner. A second strategy is based on the expression of shRNAs, an endogenous-like early intermediate RNA of the RNAi pathway. These shRNAs can be expressed from RNA polymerase II promoters or RNA polymerase III promoters (e.g. human U6 promoter) (Li et al., 2007; Mohr et al., 2014). This feature was a critical milestone for the development of pooled RNAi screens, as it allows viral delivery and stable shRNA expression over long cultivation periods. The principle of pooled genetic screens will be discussed in chapter 2.4.3.

Introduction

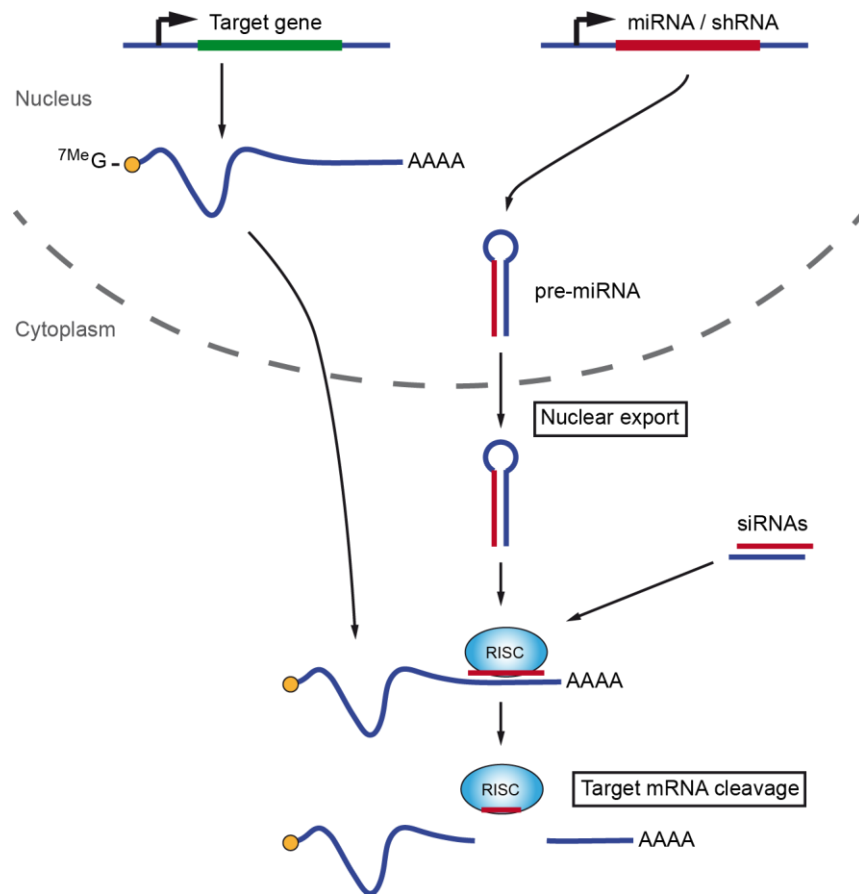


Figure 5: Gene silencing by RNAi

Exogenous RNAi reagents like shRNAs and siRNAs can enter the endogenous RNAi pathway at different steps. shRNAs are expressed from plasmids or viral genomes and mimic precursor miRNAs (pre-miRNAs). Therefore, they need to be processed by the RNase III Dicer (not shown) before the guide RNA (in red) gets incorporated into the RNA-induced silencing complex (RISC). siRNAs are RNA duplexes which can be delivered by transfection. They directly enter RISC, but only allow transient gene silencing. In case of perfect complementarity of the guide strand to the target mRNA, the target transcript is cleaved. Otherwise, translational repression is triggered by a partial complementarity (not shown). Adapted from (Mohr et al., 2014).

In 2011, a groundbreaking publication by Charpentier and colleagues described how the prokaryote *Streptococcus pyogenes* uses clustered regularly interspaced short palindromic repeats (CRISPR) as a defense mechanism against invading prophage DNA (Deltcheva et al., 2011). This mechanism has evolved into a new tool for genome editing and gene expression regulation (Jinek et al., 2013). The CRISPR locus of *Streptococcus pyogenes* is transcribed into a precursor CRISPR RNA (pre-crRNA), which is processed by RNase III enzymes into short CRISPR RNAs (crRNA). A second small RNA, called trans-activating crRNA (tracrRNA), brings the crRNA and the Cas endonuclease together to form a trimeric complex. Guided by the crRNA towards invading prophage-DNA, Cas protein cleaves the foreign DNA and thereby protects the bacterium (Deltcheva et al., 2011). Somewhat

afterwards, additional work figured out that Cas9 is the only Cas protein required for this mechanism and that the tracrRNA and the crRNA can be fused into a single short guide RNA (sgRNA) (Jinek et al., 2012). The sgRNA harbors a 20 nucleotide long sequence complementary to the target DNA and a hairpin-forming region for Cas9 binding. Cas9 itself contains two critical endonuclease domains (HNH and RuvC-like), which cleave both strands of the target DNA (Jinek et al., 2012). Another important feature of the system is the protospacer-adjacent-motif (PAM). The PAM represents just a few bases adjacent to the target sequence and is recognized by Cas9 directly. Studies on other prokaryotes revealed that CRISPR-Cas is a conserved bacterial defense system and each Cas9 orthologue has its own PAM sequence specificity (Leenay et al., 2016). Thus, on-target specificity results from the interplay between sgRNA-target complementarity and the PAM sequence. The in-depth knowledge about sgRNA and Cas9 function made the CRISPR-Cas9 system the next-generation tool for genome engineering. To date a variety of applications using CRISPR-Cas9 exist (Hsu et al., 2014). The most classical is to induce a double-strand break at the gene-of-interest in order to trigger non-homologous end-joining which can lead to a gene knock-out or to create a knock-in by homologous recombination of a donor DNA fragment (Figure 6A) (Jinek et al., 2013). Characterization of the endonuclease domains of Cas9 led to Cas9 mutants (D10A, H840A) without endonuclease activity, so called dead-Cas9 (dCas9) (Qi et al., 2013). The dCas9 variant can be used to shuttle additional effector domains to a specific genomic locus (Figure 6B). By fusing transcriptional activators (e.g. VP64) or repressors (e.g. KRAB) to Cas9 and targeting the fusions close to the transcriptional-start-site it is possible to regulate the expression of virtually any gene-of-interest. These applications are also referred to as CRISPR activation (CRISPRa) and CRISPR interference (CRISPRi) (Gilbert et al., 2014; Larson et al., 2013). Recent advancements allow enhancing the regulatory effect through targeting multiple effector domains to a single locus (Konermann et al., 2015; Tanenbaum et al., 2014). One interesting tool is the synergistic-activation-mediator (SAM) system, that uses engineered sgRNAs (sgRNA2.0) containing two additional hairpin-structures (MS2 stem-loops), which act as RNA aptamers and bind the corresponding RNA-binding domain (MCP domain) (Konermann et al., 2015). Multiple effector domains can be fused to the RNA-binding domain for strong regulatory effects (Figure 6C).

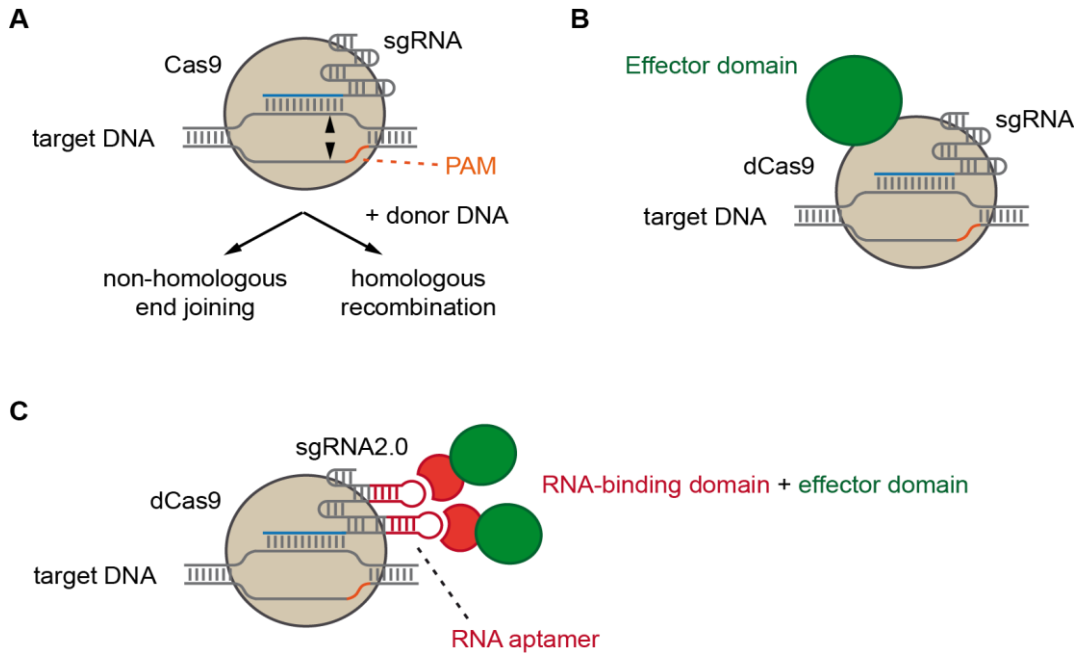


Figure 6: Overview of CRISPR-Cas9 applications

A. Ternary complex of Cas9 protein, sgRNA and target DNA including the PAM sequence. Cas9 cleaves the target DNA at both strands (arrowheads). The cell will repair this double-strand break either by non-homologous end-joining or if a donor DNA fragment is present by homologous recombination. **B.** Fusion of an effector domain to Cas9 without endonuclease activity (dCas9) allows visualization (e.g. GFP fusion) or gene expression regulation (e.g. VP64 or KRAB fusion) at a specific genomic site. **C.** The SAM system recruits effector domains via sgRNAs containing RNA aptamers (e.g. MS2 stem-loop) that recruit proteins containing specific RNA-binding domains (e.g. MCP). Modified from (Shalem et al., 2015).

2.4.2. Advances through molecular barcoding and its application

The ability of viral delivery and long-term expression of shRNAs was not the only important milestone towards pooled genetic screenings. A second major advancement was the development of oligonucleotide arrays and later the progress in next-generation sequencing (NGS). Oligonucleotide arrays are glass slides onto which thousands of defined single-stranded DNA oligonucleotides are printed using a high-definition inkjet DNA synthesis procedure. Prior to next-generation-sequencing, such arrays have been used as microarrays to study differential gene expression by hybridization of fluorescently labeled cDNA to the arrayed immobilized oligonucleotides (Schena et al., 1995). Notably, it is also possible to release the synthesized oligonucleotides from the glass slide, thereby creating an enormous pool of synthetic DNA bricks for gene synthesis or large-scale shRNA/sgRNA and molecular barcode libraries (Bassik et al., 2009; Collins et al., 2009; Tian et al., 2009). Currently, all academic and commercial pooled shRNA/sgRNA libraries have been created by parallelized on-chip synthesis of custom designed shRNA or sgRNA sequences.

Molecular barcoding describes a methodology which uses unique synthetic DNA sequence tags, coupled to a second functional genetic element, for an unambiguous parallelized readout. Already over 20 years ago this method was used to analyze bacterial virulence genes in a parallelized manner by insertional mutagenesis of transposons carrying a DNA barcode (Hensel et al., 1995). Only slightly later, a similar approach has proven to be useful for the generation of a library of yeast gene-deletion mutants covering 96 % of all annotated *Saccharomyces cerevisiae* open reading frames. Each deleted gene was replaced by a DNA barcode sequence to identify individually deleted strains within a pooled quantitative survival assay (Giaever et al., 1999, 2002; Winzeler et al., 1999). Years later, the concept of a pooled loss-of-function assay was brought into mammalian cells by using pooled lentiviral shRNA libraries (Ngo et al., 2006; Paddison et al., 2004; Schlabach et al., 2008; Silva et al., 2008). Here, either a DNA barcode linked to the shRNA or one half of the shRNA hairpin was read in order to deconvolute the pooled assay. In the early days this was done using DNA microarrays and later by next-generation sequencing.

A second application for molecular barcodes are multiplexed cis-regulatory reporter assays. In this approach, RNA barcode reporters, which are under control of regulatory promoter elements (e.g. enhancers, transcription-factor binding sites, minimal promoters), replace classical protein reporters like GFP and luciferase. This enables tremendous multiplexing and principally activity measurements of all annotated cis-regulatory elements in a single experiment. Barcoded reporters have been first used to profile pathway activities downstream of ERBB signaling, an approach named EXTassay (Botvinnik et al., 2010). Later by the use of on-chip oligonucleotide synthesis of thousands of enhancer fragments, it was used as massively-parallel reporter assays (MPRAs) to dissect the activities of enhancers (Melnikov et al., 2012). During this project, a pooled cis-regulatory reporter gene assay has been used to compare the response of multiple barcoded sensors to synaptic activity.

2.4.3. Pooled RNAi/CRISPR-Cas9 screenings

Pooled genetic screens were invented to circumvent the highly laborious, time-consuming and expensive working steps associated with arrayed screens. As pointed before, pooled screens allow rapid generation of viral shRNA libraries for loss-of-function studies at genome-wide scale. Additionally, well-to-well variability is eliminated since all knockdowns are examined under the very same experimental conditions.

To date, three different screening paradigms exist. These have been very much influenced by the needs in cancer research, as first screens were performed in this field and still the majority of published screens are related to cancer (Ngo et al., 2006; Paddison et al., 2004;

Schlabach et al., 2008; Silva et al., 2008). The three screening paradigms are hereafter called 'rescue screen', 'drop-out screen', and 'FACS-based screen' and the key steps are illustrated in figure 7 (Shalem et al., 2015). A rescue screen aims to discover genes which confer resistance to a cytotoxic treatment. Hence, those genes are potentially required for sensitivity to the treatment. In drug discovery, this assay is frequently used to identify the target or mode-of-action (MoA) of a compound (Deans et al., 2016; Fennell et al., 2014; Wagner and Schreiber, 2016). The second paradigm, a drop-out screen, is performed to identify essential genes for cell survival and proliferation. As the name suggests, its goal is to remove those cells from the test population where the knockdown impairs viability (Shalem et al., 2015). This usually requires long-time culture periods in order to gain sensitivity. An interesting and often used subtype of a drop-out screen is a synthetic-lethal screen, a method aiming to unravel combinatorial effects of the knockdown and a second genetic or pharmacological perturbation, for example an oncogenic mutation or a compound (Luo et al., 2009). FACS-based genetic interference screens represent a class that differs from the first two paradigms by its ability to study phenotypes other than cell viability or proliferation. Here, the cell pool is treated with a stimulus and the cellular response might be captured by an endogenous marker or a fluorescent reporter. The cell pool is then sorted into bins of strong- and weak-responding cells. If a knockdown is interfering with signal propagation of the stimulus to the downstream marker or reporter, the corresponding cells are expected to be enriched in the weak-responding cell population (Parnas et al., 2015). Conversely, cells where the knockdown results for example in an enhanced response to the stimulus should be rather enriched in the strong-responding cell pool. This paradigm has been used recently to dissect the response of dendritic cells to bacterial LPS (lipopolysaccharide) at unprecedented accuracy (Parnas et al., 2015). In all three paradigms, the genomic DNA of the cell pools is extracted and the shRNA/sgRNA abundances are determined by next-generation sequencing. In rescue- and drop-out screens, the endpoint sample is usually compared to an initial reference sample for the identification of hits. In FACS-based screens, the strong- and weak-responding cell pools are compared directly for hit nomination.

Overall, pooled genetic interference screens have demonstrated its value for the discovery of new putative drug targets, MoA identification and pathway deconvolution. Recently, the methodology made an important move from the dominating cancer field to primary cells (Parnas et al., 2015). However, to date, no pooled screening strategy has been described for post-mitotic primary neurons to identify regulators of neuronal plasticity.

Introduction

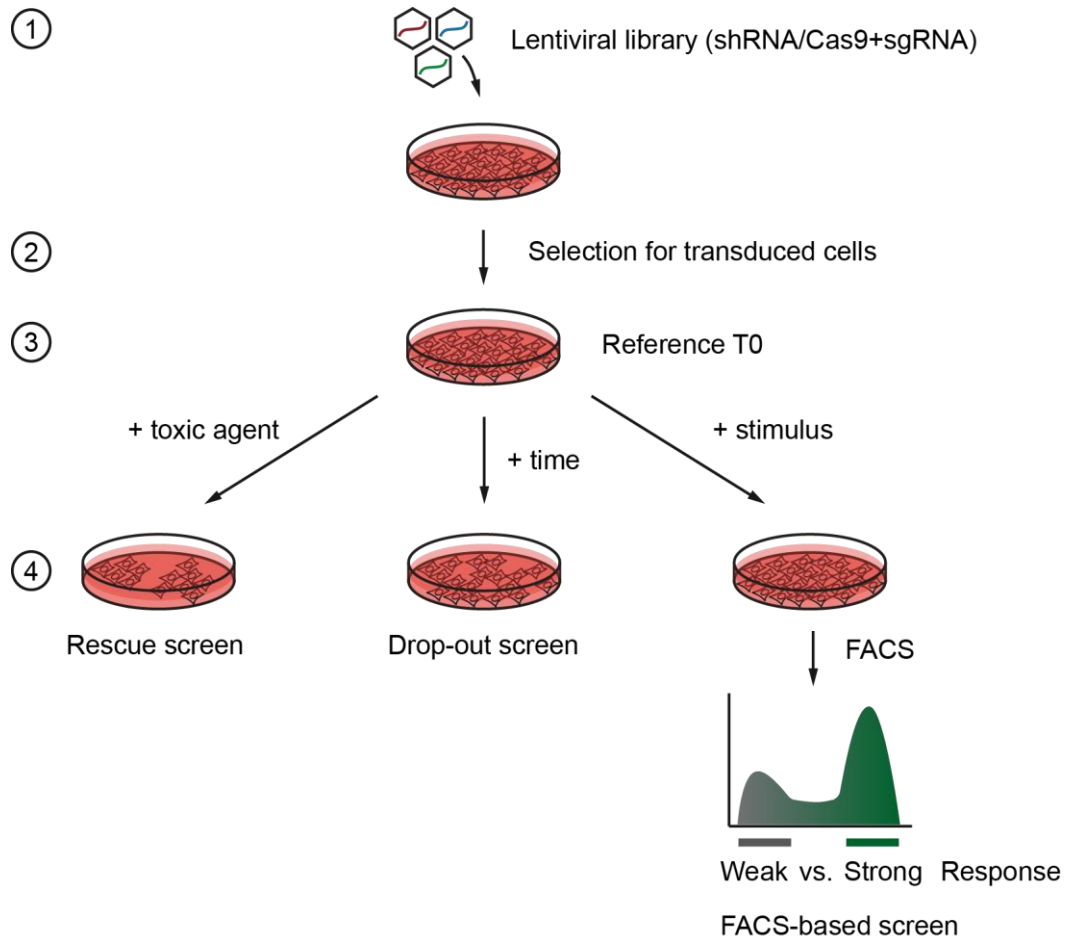


Figure 7: Current paradigms for pooled genetic screens.

Three general paradigms for pooled genetic screens have been described: (i) rescue-, (ii) drop-out-, and (iii) FACS-based screens. All methods share steps of infecting cell pools with a lentiviral shRNA/sgRNA library (step 1) and selecting for positively transduced cells (step 2). The cell pool after selection represents the reference sample (step 3). For a rescue screen, cells are treated with a toxic agent and only cells with a shRNA/sgRNA-mediated resistance remain in the cell pool (step 4, left). A drop-out screen can identify essential genes as the cells with the corresponding perturbation are lost over time from the population (step 4, middle). In a FACS-based screen, cells are stimulated and sorted based on their response (step 4, right). Finally, relative shRNA/sgRNA abundances will be determined by NGS. For rescue- and drop-out screens, endpoint samples are compared to reference samples, and for FACS-based screens, the strongly responding candidates are compared to the weakly responding ones (for citations see main text).

2.5. Objectives

Pooled RNAi screens represent a powerful tool to investigate gene function at the systems level. Its full potential to dissect any relationship between genotype and phenotype has so far only partially been addressed. The lack of innovative strategies to study phenotypes other than cell survival or proliferation precluded the development of resourceful experimental approaches for a long time. The aim of this thesis is to break this deadlock by combining the throughput of a pooled RNAi screen with the sensitivity of a genetic sensor that regulates the defined expression of molecular RNA barcode reporters. The hypothesis is that this approach could broaden the application spectrum of pooled genetic screens in terms of cell-types and the cellular phenotype of interest in general. For a proof-of-concept study primary neurons were selected as a challenging and meaningful cellular system that is of particular relevance for plasticity-related as well as neurodegenerative disorders. Moreover, primary cultured neurons are, because of technical reasons, a mainly untouched landscape for high-throughput assays in the field of drug discovery. Genome-wide association studies in psychiatric disorders, like schizophrenia, BPD, and ASD, have uncovered a plethora of risk genes that mainly converge into pathways involved in synaptic plasticity and calcium-mediated synapse-to-nucleus signaling. Current neuropharmacology is, however, only focusing on a few targets, for example the dopamine 2 receptor in the case of anti-psychotics. Hence, it was the aim to develop an assay that can dissect the networks underlying neuronal excitation-transcription coupling, which in the future hopefully brings new potential drug targets into focus. In addition, psychiatric drug discovery is increasingly focusing on hit identification by phenotypic compound screens. Those assays might have a better predictive validity than classical biochemical assays, but the protein target of a drug is often unknown. Thus, there is a strong need for assays that allow target identification and pathway activity deconvolution. Pooled RNAi screen are already used for this purpose in different disease areas and the sensor-coupled pooled RNAi screen might enable target identification of drugs for CNS diseases.

At the time when the project was launched RNAi was the well characterized gold-standard technique for loss-of-function studies in cell culture systems. Recent studies of CRISPR-Cas9-mediated genetic perturbation argue to integrate this tool into the barcoded sensor assay introduced here. A process that has been initiated in this thesis.

3. Materials

3.1. Equipment

Arium 611 Water Purification System	Sartorius
Picodrop Spectrophotometer	Picodrop Limited
Vortex Genie 2	Bender + Hobein
Mini Centrifuge Model sprout	Biozym
Heraeus Centrifuge Fresco 17	Thermo Fisher Scientific
Heraeus Megafuge 16	Thermo Fisher Scientific
Thermomixer BioShake iQ	Biometra
Thermocycler T3000	Biometra
Thermocycler TGradient	Biometra
Rotor-Gene Q cycler	Qiagen
Electrophoresis power supply	Pharmacia LKB
UV Gel documentation system	INTAS
Genepulser Xcell Elektroporationsgerät	BioRad
Ultra-low temperature lab freezer U725	New Brunswick Scientific

Cell culture

Hera Cell incubator	Thermo Fisher Scientific
Hera Safe Workbench	Thermo Fisher Scientific
Nalgene freezing Container "Mr. Frosty"	Sigma-Aldrich
Microscope Axiovert 25	Zeiss
Microscope Observer Z1	Zeiss

Luciferase measurements

Tumbling Table WT17	Biometra
Microplate Reader Mithras LB 940	Berthold Technologies
32-Channel Luminometer LumiCycle 32	ActiMetrics

Next-generation-sequencing

Ion OneTouch2 System	Ion Torrent
Ion Personal Genome Machine (PGM)	Ion Torrent
Ion Proton	Ion Torrent
Ion Torrent Server	Ion Torrent
Ion Torrent Server	Ion Torrent
Qubit 2.0 Fluorometer	Invitrogen
UV Airclean Workstation	LTF Labortechnik

Software

Microsoft Windows Professional 7	Microsoft
Microsoft Office 2007	Microsoft
Acrobat Reader 9.5	Adobe
Illustrator CS5	Adobe
Photoshop CS5	Adobe
Lasergene 8.0	DNA Star Inc.
MicroWin 2000	Berthold Technologies
Fiji ImageJ	Freeware
R Version 3.2.3	Freeware
R-studio Version 0.99.484	Freeware
Tinn-R Editor Version 2.3.7.1	Freeware
Lumicycle Version 1.4	ActiMetrics
Zotero	https://www.zotero.org

3.2. Chemicals and consumables

3.2.1. Drugs used in experiments

4-aminopyridine (4-AP)	Abcam (ab120122)
D-APV	Tocris (0106)
(-)-Bicuculline methiodide (BIC)	Abcam (ab120108)
Glycine	Abcam (ab120050)
Phorbol-12-myristat-13-acetat (PMA)	
Rotenone	Sigma (R8875)
Strychnine hydrochloride	Abcam (ab120416)
Tetrodotoxin (TTX)	Abcam (ab120055)

3.2.2. Antibodies and cell stains

Rat anti-HA	Roche (11867423)
Mouse anti-Flag-M2	Sigma (3165)
Rabbit anti-synaptophysin	Abcam (ab52636)
Mouse anti-Map2	Sigma (M1406)
Goat Alexa488 anti-mouse	Dianova (115-545-006)
Goat Alexa647 anti-rabbit	Life Technologies (A21245)
Goat Cy3 anti-rat	Dianova
HRP-goat-a-mouse monoclonal IgG (H+L)	

Materials

HRP-goat-a-rat monoclonal IgG (H+L)	Jackson Immuno Research Labs
Prolong Gold Antifade reagent	Jackson Immuno Research Labs
Hoechst 33342	Thermo Fisher Scientific
	Life Technologies

3.2.3. Commercial kits

Direct-zol RNA MiniPrep Kit	Zymo Research
Qiagen AllPrep DNA/RNA Mini Kit	Qiagen
NucleoSpin Plasmid Quick Pure	Macherey-Nagel
NucleoBond PC100 Midiprep	Macherey-Nagel
NucleoSpin Gel and PCR Clean-up	Macherey-Nagel

3.2.4. NGS Reagents & Chips

Qubit dsDNA HS Assay Kit	Invitrogen
Ion PGM Template OT2 200 Kit	Ion Torrent
Ion PGM Sequencing 200 Kit v2	Ion Torrent
Ion PGM Hi-Q™ OT2 Kit	Ion Torrent
Ion PGM Hi-Q™ Sequencing Kit	Ion Torrent
Ion PI™ Template OT2 200 Kit v3	Ion Torrent
Ion PI™ Sequencing 200 Kit v3	Ion Torrent
Ion Sphere Quality Control Kit	Ion Torrent
Dynabeads MyOne Streptavidin C1	Invitrogen
DNA LoBind Tubes (1.5 ml)	Eppendorf
Ion 318 Chip Kit v2	Ion Torrent
Ion PI™ Chip Kit v2	Ion Torrent

3.2.5. Enzymes

HotStarTaq Plus DNA Polymerase	Qiagen
PWO Polymerase	Roche
BP Clonase II	Thermo Fisher Scientific
LR Clonase II	Thermo Fisher Scientific

Materials

LR Clonase II Plus	Thermo Fisher Scientific
SuperScript III Reverse Transcriptase	Thermo Fisher Scientific
TURBO DNase	Thermo Fisher Scientific
Restriction enzymes	New England Biolabs
2x RotorGene SYBRgreen PCR Master Mix	Qiagen
NEBNext High-Fidelity 2x PCR Master Mix	NEB
T4 DNA ligase	NEB
Benzonase	Sigma
Proteinase K	Roth

3.3. Eukaryotic cell lines

PC12 tetOFF

Rat adrenal pheochromocytoma cell line expressing tetracycline regulated transactivator tTA (Clonetechn)

HEK293wt

Human Embryonic Kidney immortalized cell line (ATTC)

HEK293FT

Human Embryonic Kidney immortalized cell line (ATTC)

SH-SY5Y

Human neuroblastoma cell line

N2a

Murine neuroblastoma cell line

3.4. Bacterial strains

***Escherichia coli* transformation competent cells:**

MegaX DH10B electro-competent cells	Thermo Fisher Scientific
One Shot Mach1 chemical-competent cells	Thermo Fisher Scientific
One Shot ccdB survival 2 T1R chemical-competent cells	Thermo Fisher Scientific
Mach1 chemical-competent cells	Self-made

3.5. Buffers and solutions

AAV cell lysis buffer

150 mM NaCl
50 mM Tris-HCl (ph 8.5)

ICC blocking solution

2 g BSA in 80 ml dH₂O, 2 ml FBS, 2 ml fishgelatine, 10 ml 10x PBS
add up to 100 ml with dH₂O

3.5.1. Solutions for western blotting

Triton-X Lysis buffer

50 mM Tris pH7.5
150 mM NaCl
1% Triton-X100
1 mM EGTA

Protease inhibitors: Complete tablet (Roche), 10 mM NaF, 1 mM ZnCl₂, 1 mM Na₃VO₄, 4.5 mM Na₄P₂O₇

3.5.2. Solutions for luciferase assays

Firefly luciferase assay buffer

20 mM Tricine
1.07 mM (MgCO₃)₄*Mg(OH)₂*5H₂O
2.67 mM MgSO₄
0.1 mM EDTA
33.3 mM DTT

Materials

270 μ M Coenzyme A

470 μ M D-Luciferin, free base

530 μ M ATP

For dissolving of magnesium carbonate titrate the pH with HCl until the solution is clear. Then adjust the pH to 7.8 with NaOH. Add luciferin and ATP at last and control the pH. The buffer is stored at -20°C in the dark and thawed at room temperature.

Renilla luciferase assay buffer

Prepare K_2PO_4 (pH 5.1) solution: adjust the pH of 1 M KH_2PO_4 solution to 5.1 using 2 M KOH.

1.1 M NaCl

2.2 mM $\text{Na}_2\text{-EDTA}$

0.22 M K_2PO_4 (pH 5.1)

0.44 mg/ml BSA

1.3 mM NaN_3

Adjust the pH to 5.0 with KOH. Then add 1.43 mM Coelenterazine (dissolved in 100% EtOH). The buffer is stored at -20°C in the dark and thawed at room temperature.

3.5.3. Solutions and media for cell culture

NeuroCulture medium

Neurobasal medium, 2% B27, 1% GlutaMax

HEK293/N2a medium

DMEM(4.5 g/l glucose), 10% FBS, 1% GlutaMax (maintenance medium)

DMEM(4.5 g/l glucose), 1% FBS, 1% GlutaMax (starvation medium)

PC12 medium

DMEM(1 g/l glucose), 10% FBS, 5% HS, 1% GlutaMax (maintenance medium)

Materials

DMEM(1 g/l glucose), 1% FBS, 1% GlutaMax (starvation medium)

SH-SY5Y medium

50% DMEM(4.5 g/l glucose), 50% F12, 10% FBS, 1% GlutaMax (maintenance medium)

50% DMEM(4.5 g/l glucose), 50% F12, 1% FBS, 1% GlutaMax (starvation medium)

3.6. Oligonucleotide

Oligonucleotides were made by the AGCTlab of the MPI of Experimental Medicine in Göttingen or purchased from Eurofins in Munich.

cDNA synthesis:

Oligo(dT)	PHO-TTTTTTTTTTTTTTTTTTTTTTTT
Random nonamer (N9)	NNNNNNNNNN

qRT-PCR:

Tcf4 fwd (Mm)	CTGGAGCAGCAAGTTCGAG
Tcf4 rev (Mm)	TTCTCTTCCTCCCTTCTTTTCA
Arc fwd (Mm)	AGGGGCTGAGTCCTCACA
Arc rev (Mm)	GACTTCTCAGCAGCCTTGAGAC
Rpl13a fwd (Mm)	ATCCCTCCACCCTATGACAA
Rpl13a rev (Mm)	GCCCCAGGTAAGCAAACCTT
WPRE fwd	
WPRE rev	ACTGTGTTTGCTGACGCAAC
hU6p fwd	AGTCCCGAAAGGAGCTG
hU6p rev	tttcaagttacgtaagcatatgatagt caaggctgtagagagataattggaat

IonTorrent sequencing:

qDec1.2 fwd	CCGAGTAGAATTAACCCTCACTAAA
qDec2.2. rev	CGCGTCTACTAATACGACTCAC
Dec fwd	AGCTAGTTGCTAAGTCTGCCGAGTAG
Dec rev	TCGTACATGCATTGACTCGCGTCTAC
PGM_A_IXcodeX_AFA_s	CCATCTCATCCCTGCGTGTCTCCGACTCAGNNNNNNNNNNNNNTCCTC ACTAAAGGGTAGGTGACAC

Materials

shRNA library cloning:

hU6 fwd	TCTCagagagagacagagacagatcc
Dec rev	GTAGACGCGAGTCAATGCATGTACGA
BC35 rev	GAGActtaagatATCGGATCCAGCTAGTTGC
SpA	GTAGACGCGAGTCAATGCATGTACGATCTAGACAATAAAAGATCTTT ATTTTCATTAGATCTGTGTGTTGGTTTTTTGTGTGACTAGTCTCGTA TGCCGTCTTTTGCTTGCC
BC35	cttaagatATCGGATCCAGCTAGTTGCTAAGTCTGCCGAGTAGAATT AACCCCTACTAAAGGGTAGGTGACACTATHHHGHHHHGHHHHGNN TVVVTVVVTVVVTVVVTCCTATAGTGAGTCGTATTAGTAGACGCGAG TCAATGCATGTACGATCTAGAC
PGM_trP1_hU6_as	CCTCTCTATGGGCAGTCGGTGATccttgtggaaggacgaaacacc

shRNAs:

Tcf4 (target sequence)	TTCTAATTACCGGATATTGAAT
Adcy3	CCGGGCCATCTTTCTCAGGTTATTTGTTAATATTCATAGCAAATGACCT GGGAAAGATGGCTTTTTTT
Il2rb	CCGGCCCTCCAAACTTAATTATCCAGTTAATATTCATAGCTGGATGATT AAGTTTGGAGGGTTTTTTT
Camk2d	CCGGGACGGGATGTTCTATGCAAATGTTAATATTCATAGCGTTTGCATG GAACATCCCGTCTTTTTTT
Cacna1f	CCGGCCCTCATCTACTGCTTAATAAGTTAATATTCATAGCTTATTGAGC AGTAGATGAGGGTTTTTTT
Bhlhe40	CCGGGTCAGCACAATTAAGTAAGAAGTTAATATTCATAGCTTCTTGCTT AATTGTGCTGACTTTTTTT
Calm1	CCGGGCCGCTATACTTCTTTATTATGTTAATATTCATAGCATAATAAAG AAGTATAGCGGCTTTTTTT
Tacr2	CCGGCCACAGGCAATGTTGATATAAGTTAATATTCATAGCTTGTATCAG CATTGCCTGTGGTTTTTTT
Gphn	CCGGGCATACAAGATAGTACTAGATGTTAATATTCATAGCATCTGGTAC TATCTTGTATGCTTTTTTT
Disc1	CCGGGACTGGCTTATTTGAGAGAAAGTTAATATTCATAGCTTCTCTCG AATAAGCCAGTCTTTTTTT
Cacna1h	CCGGGCTAGAATGTAGTGAGGATAAGTTAATATTCATAGCTTATCCTCG CTGCATTCTAGCTTTTTTT

Materials

sgRNAs:	Target sequence
SV40-promoter	GAATAGCTCAGAGGCCGAGG
Arc-promoter	CCTACTCGCTCCCCTCCCGT

3.7. Plasmids

ID: AAV production:

V1739	pFdelta6 (adenoviral helper proteins)
V1740	pRV1 (serotype 2 capsid protein)
V1741	pH21 (serotype 1 capsid protein)

Luciferase assays:

V66	phRL-TK
-----	---------

***cis*-regulatory sensor assay:**

V825	pAAVspace_DEST_luc2_WPRE	Cloning vector
------	--------------------------	----------------

SARE sensor:

	pAAV_SARE-ArcMin-luc2_WPRE_pA	1-6x SARE
--	-------------------------------	-----------

PATHscreeener:

V1337	Cellecta Decipher Mouse Module 1 library	
V1338	AAV E-SARE PATHscreeener (with shRNA)	Library or single shRNA
V1301	AAV E-SARE PATHscreeener (shRNA stuffer)	Non-targeting control

CRISPR-Cas9:

V1785	pAAV_Syn1p-dCas9
V1787	PATHscreeener2.0 (sgRNA stuffer)
	sgRNA-SV40
	pSV40-luc2

4. Methods

4.1. Culturing of eukaryotic cell lines

The cell lines PC12, SH-SY5Y, N2a, HEK293, and HEK293FT were cultured in the appropriate growth medium at 37°C in a humidified incubator at 5% CO₂. After reaching 80-90% confluency, cells were passaged using standard protocol including treatment with 0.05% trypsin-EDTA. For all experiments, cells were seeded into the appropriate cell culture plate one day prior to the beginning of the experiment. Maintenance of the cell culture stocks, including passaging and test for mycoplasma contamination, has been done with the help of Beate Kauschat and Nadia Gabellini (Molecular Neurobiology, Department of Psychiatry, LMU Munich).

4.2. Primary neuron culture

Primary mouse cortical neurons were prepared from E15.5 C57BL/6 mice embryos. Culture dishes were freshly coated with poly-L-lysine (PLL, 0.1 mg/ml in dH₂O) overnight at room temperature. Dishes were washed twice with dH₂O. For immunocytochemistry, acid-treated glass coverslips were placed into the culture dish and coating was done with PLL (0.1 mg/ml in borate buffer). Coverslips were washed twice with PBS. Immediately after washing, half of the final culture medium volume of neuronal plating medium (containing 5% FBS) was added to the coated culture dishes and placed into a cell culture incubator at 5 % CO₂. In case of 96-well plates, FBS was omitted from the initial plating in order to avoid the complete medium exchange on DIV1. Mouse cortices were dissected in cold HBSS/5 mM HEPES. Up to 16 pairs of cortices were dissociated in 2 ml pre-warmed Neurobasal medium containing Papain (20 U/ml) at room temperature for 13 min. Papain treatment was terminated by adding 10 ml pre-warmed and pH equilibrated DMEM(4.5 g/l glucose)/10 % FBS. The medium was replaced once with new 10 ml pre-warmed and pH equilibrated DMEM(4.5 g/l glucose)/10 % FBS and then with 2 ml pre-warmed and pH equilibrated neuronal plating medium. Cells were gently triturated with a P1000 pipette. The cell suspension was transferred through a 40 µm mesh (BD Cell strainer) to remove any cell clumps. Next, cell concentration was determined by counting trypan blue negative cells using a Neubauer cell counting chamber. Finally, cells were plated by adding the second half of the final culture medium volume to the cell culture dish. In all experiments a cell density of ~500 cells/mm² was used.

Except for experiments in 96-well plates, where serum-free medium was used from the beginning, culture medium was completely replaced by serum-free neuronal culture medium on DIV1. Feeding of the neuronal cultures was done on DIV6-7 for the first time by replacing

half volume with pre-warmed and pH equilibrated neuronal culture medium. From then on, cultures were fed every 3-4 days until the end of the experiment.

4.3. AAV production

The production of AAV particles was done following the general published guidelines with the assistance of Beate Kauschat (Molecular Neurobiology, Department of Psychiatry, LMU Munich) (McClure et al., 2011). In detail, this included the following steps:

Transfection

AAVs were produced using HEK293FT cells. For a single virus preparation, 12×10^6 cells were seeded onto one PLL (0.02 mg/ml)-coated 15 cm cell culture dish the day before transfection. One hour prior to the transfection, the cell culture medium was replaced by 15 ml HEK293 medium. The transfection mix was prepared as followed: Per 15 cm dish, 10 μ g pFdelta6, 3.75 μ g pRV1, 3.75 μ g pH21, and 4 μ g pAAV (i.e. the custom AAV plasmid) were mixed in 0.5 ml OptiMEM medium. Polyethyleneimine (PEI) was used as a transfection reagent and added to the DNA/OptiMEM mix in a PEI:DNA ratio of 4:1. The transfection mix was thoroughly mixed and incubated at room temperature for 10 minutes. Next, the transfection mix was added drop wise to the cells. Four hours post-transfection, 15 ml HEK293 medium were added. The mix of two AAV capsid expressing plasmids pH21 (serotype 1) and pRV1 (serotype 2) results in AAV particles with mixed capsid proteins form AAV serotype 1 and 2. This mix was determined to have superior infection efficiencies compared to either serotype alone (data not shown).

AAV harvest

Three days post-transfection, AAV particles were harvested from the culture. Therefore, the cells were detached from the cell culture dish by rigorous pipetting and the cell suspension was transferred into a 50 ml tube. Next, cells were pelleted by centrifugation at 1000 rpm for 5 minutes and the supernatant was aspirated. The cell pellet was resuspended in 5 ml of AAV cell lysis buffer and cells were lysed by three freeze-thaw cycles between -80°C and 37°C . In order to digest the genomic DNA, the cell lysate was incubated with benzonase (50 U/ml) at 37°C for 30 minutes. Subsequently, the cell lysate was centrifuged at 1000 rpm for 15 minutes to pellet the cell debris. Afterwards, the AAV-containing supernatant was passed through a $0.45 \mu\text{m}$ filter and transferred into an Amicon Ultra-15 centrifugal filter unit (100 kDa membrane cutoff, Millipore) in order to ultra-filtrate and concentrate the viral particles. During this procedure 10 ml cold PBS was added twice to the AAV solution to exchange the buffer. The final volume after concentration was 0.25-0.5 ml and aliquots of the virus were frozen and stored at -80°C until usage.

Absolute quantification of the AAV genomic copies (GC) by quantitative PCR (qPCR)

The quantification of the AAV GCs served as an approximate value to control the infection rate between experiments. For the quantification by PCR, the AAV genomes were first purified from the AAV preparation. Therefore, 5 μ l AAV stock was mixed with 84 μ l dH₂O, 10 μ l 10x Turbo DNase buffer and 1 μ l Turbo DNase (2 U/L) to digest residual pAAV plasmid DNA. The mix was incubated at 37°C for 15 minutes and the TurboDNase was subsequently inactivated at 95°C for 5 minutes. Next, 5 μ l proteinase K (10 mg/ml) were added and incubated at 55°C for 10 minutes to digest the AAV capsid and release the AAV genomic DNA. The AAV genome was purified using the NucleoSpin Gel and PCR Clean-up kit (Macherey&Nagel) and eluted in 200 μ l elution buffer.

Absolute quantification was done on a Qiagen Rotor-Gene cyler using the 2x RotorGene SYBRgreen PCR Master Mix and the hU6p qRT-PCR primer pair. A pAAV plasmid serial dilution (1e+03 - 1e+06 copies/ μ l, plus non-template control) was used as a standard and always ran in parallel to the AAV genome sample. Final AAV GC titers in the range of 1e+09-1e+10 GC/ μ l were usually obtained.

Determination of the infectious AAV titer

In order to correlate the AAV GC titer to the infection rate of murine primary neurons, cortical cultures were infected with a serial dilution of a GFP expressing AAV and GFP positive cells were counted by a microscopic analysis (Figure 8). This correlation was used to adjust the infection rate of the AAV shRNA library to a level where it can be assumed that the great majority of infected cells are only transduced by a single AAV particle.

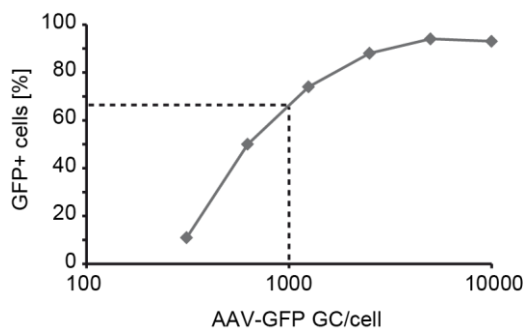


Figure 8: AAV infection rate

AAV infection rate for primary neurons determined using a serial dilution of a GFP expressing AAV vector.

4.4. Rotenone dose-response cell viability assay

The response of primary neurons to various rotenone concentrations was determined by microscopy counting of cell nuclei, as well as quantification of genomic DNA (gDNA) and total RNA. Primary neurons were seeded onto PLL-coated 6-well plates. Rotenone was diluted in half-logarithmic steps in DMSO as 100x solutions (from 3.16e-07 M to 3.16e+10 M) and 1/100 volume of the final cell culture volume was added to the cells in duplicates or triplicates at DIV7. Cells were incubated at 37 °C in a humidified incubator at 5 % CO₂ until DIV14.

For the microscopic counting, cell nuclei were stained on DIV14 using Hoechst dye. Using a Zeiss Observer Z1 microscope, three images of the nuclear stain per well were acquired. Subsequently, the neuron cultures were lysed and gDNA as well as total RNA was isolated using the Qiagen AllPrep DNA/RNA Mini Kit. The gDNA and total RNA concentrations were determined using a UV spectrophotometer. The images of the nuclear stain were further analyzed using Fiji ImageJ software. For counting of all cell nuclei the Analyze Particle function was used, generating an output file with the individual nucleus areas. Discrimination between live and dead cells was done by applying a filter for pyknotic (dead) and non-pyknotic (live) nuclei. First, the mean nucleus areas of pyknotic and non-pyknotic nuclei were determined manually and then used as thresholds to filter the microscopic nuclei count. Dose-response curves of all measurements were done using the R package drc.

4.5. Multiplexed *cis*-regulatory sensor assay

Cloning of the cis-regulatory sensor library

The AAV-based *cis*-regulatory sensor library was cloned and provided by Dr. Ben Brankatschk (Molecular Neurobiology, Department of Psychiatry, LMU Munich). The general design is based on the previously published EXTassay approach, where *cis*-regulatory sensors drive the expression of unique molecular barcodes, so called EXTs (Botvinnik et al., 2010). In brief, *cis*-regulatory sensors consist either of clustered transcription factor binding sites and response elements upstream of the minimal adenoviral major late promoter (minMLP) (termed *cis*-element-based sensors), or of 1-1.5 kb long endogenous promoter fragments which harbor the transcription start site (termed promoter-based sensors). The corresponding sequences were either synthesized by Genscript or PCR amplified from genomic DNA. Cloning was done using the MultiSite Gateway pro plus kit (Invitrogen) according to the manufacturer's instructions. Thereby, three insert fragments were cloned into the pAAVspace_DEST_luc2_WPRE (V825) vector by recombination. For *cis*-element-based sensor, the three fragments consist of the (i) clustered *cis*-element, (ii) the minMLP,

Methods

and (iii) the molecular barcode. In case of a promoter-based sensor, the three fragments are (i) a stuffer sequence, (ii) the promoter, and (iii) the molecular barcode (see figure 10A). All constructs were verified by restriction digest and sequencing of the insert.

Cell culture

E15.5 wt primary cortical mouse neurons were seeded in 6-well plates at 0.5 million cells/well. Cultures were infected on DIV5 with the AAV *cis*-regulatory sensor library with 2500 AAV GCs per cell. A duplicate sample was silenced by treatment with 1 μ M TTX and 100 μ M APV on DIV12. On DIV14, a duplicate sample was harvested as an untreated reference. The remaining samples were stimulated with 50 μ M BIC, 100 μ M 4-AP, 100 μ M glycine, and 1 μ M strychnine for 2, 4, and 8 hours in duplicates. All samples were finally harvested using Qiazol reagent. The RNA was purified using the Zymo Direct-zol RNA MiniPrep kit. Subsequently, the purified RNA was treated with TurboDNase to digest residual AAV genomes and cleaned up by a second column purification using the Zymo Direct-zol RNA MiniPrep kit according to the manufacturer's instructions.

The purified RNA was reverse transcribed as followed:

Total RNA	4.5 μ l
Random nonamer primer (120 μ M)	1 μ l
dNTPs (10 mM each)	0.5 μ l
5 minutes at 65°C, followed by 1 minute on ice. Then add per reaction:	
5x First-strand reaction buffer	2 μ l
DTT (0.1 M)	1 μ l
SuperScript III RT	1 μ l
Incubate first at 50°C for 30 minutes, followed by 15 minutes at 70°C.	

Following the cDNA synthesis, barcodes were amplified by PCR with Dec1/2 primers (250 nM each) using HotStar Taq plus DNA polymerase (Qiagen). The cDNA input was 1 μ l of a 1/10 dilution into a 20 μ l PCR reaction. In addition, an external barcode mix was added to the PCR reaction, which can be used for calibration between samples. The PCR was performed with an annealing temperature of 59°C and 30 cycles. The PCR product was verified by agarose gel-electrophoresis.

In a second PCR, the adapter sequences for Ion Torrent sequencing were fused to the barcodes. The forward code primer contained the Ion-A adapter sequence required for Ion Torrent sequencing and a 12bp code sequence for multiplexing of samples in a single sequencing run. The reverse primer contained the Ion-P1 adapter sequence required for Ion

Torrent sequencing. The PCR was done using HotStar Taq plus DNA polymerase (Qiagen). The PCR product was verified by agarose gel-electrophoresis. The final PCR products were pooled and purified using the NucleoSpin Gel and PCR Clean-up kit (Macherey&Nagel).

Barcode libraries were sequenced on an Ion Torrent PGM sequencer using the 318 chip. The sequencing service was provided by Stefanie Behrens and Dr. Sabrina Galinski (Molecular Neurobiology, Department of Psychiatry, LMU Munich). All template preparations and enrichments were done according to the manufacturer's protocols for the Ion PGM Template OT2 200 kit. Sequencing was done according to the manufacturer's protocols for the Ion PGM Sequencing 200 v2 kit. Processing of the raw data was done in collaboration with Dr. Sven Wichert (Molecular Neurobiology, Department of Psychiatry, LMU Munich) using custom shell and R scripts. First, raw reads were split into individual samples using the 12 bp code and subsequently mapped to a reference barcode library using a local BLAST. Thereby, reads were counted. Next, read counts were normalized to total read numbers per sample. Normalized read counts were standardized to read counts of a sensor which contains only the minMLP, but no *cis*-regulatory element. Finally, data was presented as a heatmap of log₂-transformed fold changes relative to the untreated reference sample.

4.6. Luciferase assays

Firefly luciferase reporter gene assays were performed during the development and validation of the PATHscreener and PATHscreener2.0 vector and for the validation of individual candidates from the screen.

Multiplate luciferase assays

For multiplate assays, cells were seeded into 96-well plates and either transfected (for cell lines) or infected (for primary neurons). Cells were transfected using Lipofectamine2000 (Invitrogen) according to the manufacturer's instructions or infection by an E-SARE-luciferase containing AAV. Infection was done with 500-1000 AAV GCs per cell. The assay always compares an unstimulated response with a stimulated response.

Validation of individual shRNAs was done with primary neurons in 24-well plates. Neurons were infected with AAV PATHscreener vectors either expressing an shRNA or a non-targeting control RNA. Cultures were treated the same way as the screening samples (BIC/4-AP vs. TTX/APV). At the end of the assay, cells were lysed using Passive lysis buffer (Promega). The luciferase activity was measured by a Mithras LB 940 Microplate Reader (Berthold Technologies) and the software MicroWin2000.

Luciferase assays using a 32-channel luminometer

Live cell luciferase activity was measured using the LumiCycle 32 apparatus. Therefore, primary neurons were seeded onto 3.5 cm culture dishes. The medium was supplemented with 1/1000 luciferin (Promega).

4.7. Protein detection by immunocytochemistry

Immunocytochemistry was used to quantify synapses in maturing primary neuron cultures and to verify the expression of CRISPR-Cas9 components. Therefore, primary neurons were grown on glass coverslips. The entire staining procedure was performed at room temperature. First, 1 vol. of 4% paraformaldehyde (PFA) was added to the cell culture medium for fixation and incubated for 15 minutes. Next, the neurons were washed three times with PBS. Neurons were permeabilized with 0.1% Triton-X-100 in PBS for 1 minute, followed by three washes with PBS. Subsequently, ICC blocking solution was applied for 30 minutes. The neurons were then incubated with the primary antibody in 0.1% ICC blocking solution for one hour. Afterwards, neurons were washed three times for 5 minutes each with PBS. The secondary fluorescently labeled antibody was applied for one hour in 0.1% ICC blocking solution. Finally, the coverslips were washed three times with PBS for 5 minutes each, briefly rinsed in dH₂O, and mounted onto glass slides using Prolong Gold Antifade reagent (containing DAPI for nuclei staining).

Synapse staining

Primary antibodies: mouse anti-MAP2 (1:200); rabbit anti-synaptophysin (1:250)

Secondary antibodies: Alexa488 anti-mouse (1:500); Alexa647 anti-rabbit (1:500)

CRISPR-Cas9 staining

Primary antibodies: mouse anti-FLAG-M2 (1:100); rat anti-HA (1:100)

Secondary antibodies: Alexa488 anti-mouse; Cy3 anti-rat (both 1:500)

Image acquisition and analysis

Images were acquired using a Zeiss Observer Z1 microscope in combination with the Zeiss Zen 2012 software. For the synapse quantification, images were analyzed with Fiji ImageJ using the 'Find Maxima' function. The synapse count was normalized to the mean intensity of the MAP2 staining.

4.8. Protein detection by western blot

Western blotting was used to verify the expression of the CRISPR-Cas9 components dCas9 (HA-tagged) and MS2-p65-VP64 (FLAG-tagged) in HEK293 cells. Therefore, HEK293 cells were seeded into 6-well plates (0.5 million/well) and transfected either with V1785 or V1787 using Lipofectamine2000 (Invitrogen) according to the manufacturer's protocol. The western blot was performed by Barbara Meisel (Molecular Neurobiology, Department of Psychiatry, LMU Munich). In brief, cells were washed once with PBS on ice and harvested by lysis in 1% Triton-X protein lysis buffer (containing protease inhibitors). The lysate was transferred into a reaction tube and centrifuged at 13,000 rpm for 10 minutes at 4°C to clear cell debris. Next, the protein samples were mixed with Loading/reducing buffer and proteins were denatured at 70°C for 10 minutes. Proteins were separated on a Mini-PROTEAN TGX, 4-15% gel (Biorad) prior to blotting onto a PVDF transfer membrane Hybond P (GE Healthcare). Afterwards, the blot was first incubated with blocking solution (5% milk powder in TBS-T) followed by the primary antibody and the secondary HRP-conjugated antibody. Imaging of the blots was done using the ECL ChemoCam Imager (INTAS).

Primary antibodies: rat anti-HA (1:1000), mouse anti-FLAG-M2 (1:5000), mouse anti-GAPDH (loading control, 1:1000)

Secondary antibodies: anti-rat-HRP (1:5000), anti-mouse-HRP (1:5000)

4.9. RNA detection by reverse transcription and qRT-PCR

Relative mRNA quantification was used to determine the knockdown of an shRNA or the activation of gene expression by CRISPRa. In both cases, total RNA was isolated using the Zymo Direct-zol RNA MiniPrep kit according to the manufacturer's instructions, including an on-column DNA digest. The first-strand cDNA synthesis was done using SuperScript III reverse transcriptase kit (Invitrogen). qRT-PCR assay primers were designed using the Roche Universal Probe Library assay design center. qRT-PCRs were performed on a Qiagen Rotor-Gene cycler using the 2x Rotogene SYBR green Master Mix. Rpl13a was used as a reference gene. The relative quantification was done with the Qiagen Rotogene software using the $\Delta\Delta C_t$ -method (Schmittgen and Livak, 2008).

4.10. Design and cloning of the PATHscreeener library

Insert preparation

The shRNA library template for the insert has been the Decipher Mouse Module 1 shRNA library by Collecta. The insert was prepared by two consecutive PCRs in order to add the synthetic polyA signal (SpA) and the random barcode (BC35).

PCR#1

Decipher shRNA library (10 ng/μl)	1 μl
SpA oligo (2 nM)	1 μl
Dec rev primer (10 μM)*	0.5 μl
hU6 fwd primer (10 μM)*	0.5 μl
dH ₂ O	7 μl
2x PWO Master Mix	10 μl

* add after first 5 cycles

PCR parameters: 95°C 2 min, 95°C 20 sec, 59°C 20 sec, 72°C 30 sec (5 cycles), 95°C 20 sec, 55°C 20 sec, 72°C 30 sec (20 cycles)

The PCR product has been purified using the NucleoSpin Gel and PCR Clean-up kit (Macherey&Nagel) and validated by 2% agarose gel-electrophoresis.

PCR#2

Product PCR#1 (2e+09 molecules/μl)	1 μl
BC35 oligo (4e+09 molecules/μl)	1 μl
BC35 rev primer (10 μM)	0.5 μl
hU6 fwd primer (10 μM)	0.5 μl
dH ₂ O	7 μl
2x PWO Master Mix	10 μl

PCR parameters: 95°C 2 min, 95°C 20 sec, 55°C 20 sec, 72°C 30 sec (10 cycles)

The PCR product has been purified using the NucleoSpin Gel and PCR Clean-up kit (Macherey&Nagel) and validated by 2% agarose gel-electrophoresis.

The purified product of PCR#2 was digested with BamHI and ClaI for 2 hours at 37°C and subsequently purified using the NucleoSpin Gel and PCR Clean-up kit (Macherey&Nagel). The final insert concentration was determined using the Picodrop spectrophotometer.

Vector preparation

The empty PATHscreener vector (V1301, 10 µg) was digested with BamHI and ClaI for 6 hours at 37°C and purified by 1% agarose gel-electrophoresis and the NucleoSpin Gel and PCR Clean-up kit (Macherey&Nagel). Additionally, the linearized vector was purified by phenol/chloroform/ethanol extraction. Therefore, 1 vol. of phenol was added, the solution was mixed by shaking for 20 times and centrifuged at full speed for 5 minutes. The upper layer was transferred to a new tube and 100 µl TE buffer was added to the phenol phase for re-extraction. Afterwards the two upper layers were pooled and the procedure was repeated with 1 vol. of chloroform. Finally, the linearized vector DNA was precipitated by adding 1/10 vol. of 3 M sodium-acetate pH 5.2 and 2.5 vol. 100% ethanol. For precipitation it was vortexed and kept at -20°C for 1 hour. Subsequently, the DNA was pelleted by full speed centrifugation at 4°C for 10 minutes. The supernatant was removed and the pellet was washed once with cold 70% ethanol. After this washing step the pellet was air-dried for 5 minutes and resuspended in 20 µl TE buffer.

Ligation

Ligation was done with 500 ng linearized vector and a vector:insert ratio of 1:3. Prior to the ligation, the mix of vector and insert was heated up to 55°C for 2 minutes and then snap-frozen at -20°C for 10 minutes followed by thawing on ice. Next, 1 µl 10x T4 ligase buffer (NEB) and 1.4 µl T4 DNA ligase (NEB) was added (final vol. 10 µl) and the ligation reaction was incubated at 16°C over night. Before transformation, 10 µl H₂O were added to the reaction in order to reduce the salt concentration and the T4 ligase was heat inactivated at 65°C for 10 minutes.

Transformation

Transformation was done by electroporation. MegaX Dh10b E.coli (20 µl) were added to 2 µl ligation reaction. The mix was gently pipetted up and down and transferred to an ice-cold electroporation cuvette. Immediately the electroporation was done the bacteria were recovered by adding 1ml pre-warmed Recovery medium (included with MegaX Dh10b E.coli). The electroporated bacteria were incubated at 37°C for 1 hour with shaking. A dilution series from 1-10 µl was spread onto 10 cm LB-agar (ampicillin) plates for colony counting the next day. Twelve mini cultures were inoculated with individual colonies in order to verify the cloning. Colony number per volume was calculated and the volume for ~10,000 colonies was spread onto a 15cm LB-agar (ampicillin) plate. In total 3 plates were inoculated in order to get a maximum number of ~30,000 different barcodes within the library. The next day, colonies from all 3 plates were collected and plasmid DNA was purified using the NucleoBond PC100 Midiprep Kit (Macherey-Nagel).

Sequencing of shRNA and barcode

In order to assign the barcode sequence to the shRNA the region encoding the barcode and the shRNA was amplified by PCR using primers with Ion Torrent sequencing adapters (PGM_A_IXcode3_AFA_s fwd primer / PGM_trP1_hU6_as rev primer). The PCR product has a size of 345 bp and was sequenced on an Ion Torrent PGM sequencer using the 318 chip. The sequencing service was provided by Stefanie Behrens and Dr. Sabrina Galinski (Molecular Neurobiology, Department of Psychiatry, LMU Munich). All template preparations and enrichments were done according to the manufacturer's protocols for the Ion PGM Template OT2 400 Kit. Sequencing was done according to the manufacturer's protocols for Ion PGM Hi-Q Sequencing Kit.

The analysis was done using a custom R script which included the following steps: Raw reads were filtered by length (>231 bp) in order to cover the barcode sequence and the shRNA antisense strand. Using the Biostrings function `matchLRPatterns()` filtered raw reads were scanned for the barcode (left pattern) and the 8 bp adjacent to the shRNA antisense strand (right pattern). 5 mismatches were allowed in the left pattern without indels and 3 mismatches in the right pattern with indels. Thereby, barcode sequences and shRNA antisense strand sequences were extracted. Next, shRNA antisense strand sequences were aligned by BLAST to the *Cellecta* shRNA library reference list. At this stage, a matrix with a barcode ID, the barcode sequence, the shRNA sequence, and the shRNA ID, and the Refseq ID of the shRNA target was created. This matrix was finally filtered for barcodes that were coupled to the same shRNA in more than 80% of the cases. The final barcode library was aligned to itself using a local megablast with varying parameters to determine optimal megablast stringency for barcode discrimination during the screen. These were an e-value threshold of $1e-10$ and a word-size of 12.

4.11. Pooled RNAi screen in primary neurons

Cell culture

Primary cortical neuron cultures were prepared from E15.5 wt mice. Neurons from 16-24 embryos were pooled per screen. Per sample, 10 million or 5 million cells were seeded onto PLL-coated 15 cm or 10 cm tissue culture dishes, respectively. In parallel, PLL-coated 3.5 cm dishes were seeded with 0.5 million cells to record the treatments in the Lumicycler. 2-4 replicate cultures were prepared per treatment condition. Seeding was done in Neurobasal medium supplemented with 5% FBS, 2% B27, and 1% GlutaMax. On DIV1, the medium was replaced by Neurobasal medium supplemented with 2% B27 and 1% GlutaMax (NeuroCulture medium; 20ml per 15cm dish, 10ml per 10cm dish). On DIV6, cultures were

Methods

infected with the AAV-PATHscreener library at an AAV particle to cell ratio of 1000:1. Simultaneously, cultures were fed by adding pre-warmed NeuroCulture medium (5 ml per 15 cm dish, 2.5 ml per 10 cm dish, and 0.5 ml per 3.5 cm dish). On DIV10, all cultures were fed with pre-warmed NeuroCulture medium (5 ml per 15cm dish, 2.5 ml per 10 cm dish, 0.5 ml per 3.5 cm dish) and half of the cultures were in addition treated with 1 μ M TTX and 100 μ M APV to silence neuronal activity. The culture for real-time luciferase recordings were in addition supplemented with the firefly luciferase substrate luciferin and the recording using the Lumicycler was started. On DIV12, the cultures which have not been silenced were stimulated with a cocktail containing 50 μ M BIC, 100 μ M 4-AP, 100 μ M glycine, 1 μ M strychnine for 4 hours.

Harvest

For cell harvest of silenced and stimulated cultures the culture medium was aspirated and cells were rinsed once with cold PBS. Subsequently, QIAzol cell lysis reagent was applied for lysis (5 ml for 15 cm dishes, 2.5 ml for 10 cm dishes). Cell lysate was scraped from the dishes and transferred into a 15 ml tube. The lysate was kept at -80°C until RNA isolation.

Total RNA isolation

Lysates were thawed at room temperature and cell debris was pelleted by centrifugation at 4000 rpm for 5 minutes. The supernatant was transferred into a new 15ml tube and the total RNA was isolated using the Zymo Direct-zol RNA MiniPrep kit according to the manufactures instructions with the following modifications. The lysate from 10 million cells was split onto 2 RNA purification columns in order to not exceed the RNA binding capacity of a column. Elution was done in 50 μ l RNase-free H₂O per column and the two eluates from 10 million cells were pooled afterwards.

The total RNA was quantified using a Picodrop spectrophotometer. ~60 μ g or ~30 μ g total RNA was obtained from 10 million or 5 million cells, respectively.

In order to digest traces of co-isolated AAV genomes, total RNA was treated with TurboDNase for 30 minutes at 37°C. For ~60 μ g total RNA this was done in a volume of 300 μ l using 6 μ l TurboDNase. With less total RNA input the reaction was scaled down accordingly. The DNase-digested total RNA was subsequently cleaned-up by adding 1 vol. of 100% ethanol and using the Zymo Direct-zol RNA MiniPrep Kit for purification. One column was used per sample. Elution in 25 μ l RNase-free H₂O. Total RNA was again quantified using a Picodrop spectrophotometer.

Methods

cDNA synthesis

The first-strand cDNA synthesis was done using the Invitrogen SuperScript III reverse transcriptase. The entire total RNA was reverse transcribed in multiple 20 μ l reactions containing 5 μ g total RNA each and using oligo(dT) primer. The reaction protocol was as followed:

Total RNA	5 μ g
Oligo(dT) primer (50 μ M)	1 μ l
dNTPs (10 mM each)	1 μ l
H2O	Up to 13 μ l

5 minutes at 65°C, followed by 1 minute on ice. Then add per reaction:

5x First-strand reaction buffer	4 μ l
DTT (0.1 M)	1 μ l
H2O	1 μ l
SuperScript III RT	1 μ l

Incubate first at 50°C for 30 minutes, followed by 15 minutes at 70°C.

Barcode quantification by qRT-PCR

In order to validate the sensor induction during the screen, RNA barcode expression was quantified relative to Rpl13a expression or absolute using a plasmid standard with $1e+02$ copies – $1e+05$ copies/ μ l. Primer pairs were qDec1.2/qDec2.2 for the barcode and the plasmid standard and qRT-PCR primer for Rpl13a. Analysis was done using the Qiagen Rotor-Gene Software with the $\Delta\Delta$ Ct-method for relative quantification.

2x RotorGene SYBRgreen PCR Master Mix	5 μ l
Fwd primer (10 μ M)	1 μ l
Rev primer (10 μ M)	1 μ l
cDNA (pre-diluted 1:100)	3 μ l

Default qRT-PCR cycling parameters.

Dec PCR

The 'Dec PCR' amplifies the barcode from the cDNA sample. Prior to the 'Dec PCR', the entire cDNA was purified using the Macherey&Nagel PCR clean-up kit und eluted with 20 μ l elution buffer. Per sample 100 μ l reactions were prepared, split into 2x 50 μ l reactions for PCR and pooled again afterwards.

Methods

cDNA (purified)	10 μ l
qDec1.2 fwd primer (10 μ M)	1.25 μ l
qDec2.2 rev primer (10 μ M)	1.25 μ l
H ₂ O	37.5 μ l
NEBNext 2x PCR MasterMix	50 μ l
PCR parameters: 98°C 30sec, 98°C 10sec, 59°C 30sec, 72°C 30sec (20 cycles)	

The PCR product was confirmed by 2% agarose gel-electrophoresis.

Code PCR

The 'Code PCR' fuses sample specific 12bp code sequences to the 'Dec PCR' product in order to pool samples for next-generation sequencing. The forward code primer contains the Ion-A adapter sequence required for Ion Torrent sequencing and the 12bp code sequence. The reverse primer contains the Ion-P1 adapter sequence required for Ion Torrent sequencing. Code PCR reaction per screen sample:

Dec PCR product (pre-diluted 1:10)	5 μ l
Code fwd primer (10 μ M)	0.625 μ l
Code rev primer (10 μ M)	0.625 μ l
H ₂ O	18.75 μ l
NEBNext 2x PCR MasterMix	25 μ l
PCR parameters: 98 °C 30 sec, 98 °C 10 sec, 58 °C 30 sec, 72 C 30 sec (10 cycles)	

The PCR product was confirmed by 2% agarose gel-electrophoresis.

20-40 μ l per sample were pooled subsequently and purified using the NucleoSpin Gel and PCR Clean-up kit (Macherey&Nagel).

Next-generation sequencing of barcodes

Barcode libraries were sequenced on an Ion Torrent Proton sequencer using the PI chip. The sequencing service was provided by Stefanie Behrens and Dr. Sabrina Galinski (Molecular Neurobiology, Department of Psychiatry, LMU Munich). All template preparations and enrichments were done according to the manufacturer's protocols for the Ion PI Template OT2 200 v3 kit. Sequencing was done according to the manufacturer's protocols for the Ion PI Sequencing 200 v3 kit. One PI chip delivered on average 100 million raw reads.

Processing of the raw data was done in collaboration with Dr. Sven Wichert (Molecular Neurobiology, Department of Psychiatry, LMU Munich) using custom shell and R scripts. First, raw reads were split into individual samples using the 12 bp code and subsequently mapped to a reference barcode library using a local BLAST. Thereby, reads were counted

and assigned to shRNAs and gene targets. Next, read counts were normalized to total read numbers per sample. If multiple barcodes are assigned to the same shRNA, corresponding read counts were summed. To control the correlation between replicates, similarities between all samples were estimated using pair-wise Pearson correlation coefficient and plotted as a heatmap with hierarchical clustering. Analysis was then continued by enhanced Z-score ranking or using the DESeq2 R package (Love et al., 2014).

For the enhanced Z-score analysis, normalized read counts of replicates were collapsed to mean count values and log₂ transformed. Log₂ ratios were calculated between stimulated and silenced samples and normalized to enhanced Z-scores. In order to collapse to gene level, the barcode/shRNA with the strongest effect towards the positive- (for negative regulators) or negative direction (for positive regulators) was selected to represent a certain gene.

The DESeq2 package allows testing for differential expression of a gene or in this case of a barcode. Therefore, normalized read count data with all replicates for the stimulated and silenced conditions was first processed using the `DESeqDataSetFromMatrix()` function. Next, data was analyzed using the `DESeq()` function which includes the Wald test for differential expression and correction by multiple testing using the Benjamini-Hochberg method (Benjamini and Hochberg, 1995).

KEGG and Reactome pathway analysis

Pathway analysis of the top positive regulators from the enhanced Z-score ranking was done using the KEGG database and the Reactome database (Fabregat et al., 2016; Ogata et al., 1998). The KEGG analysis was done via the WEBGESTALT homepage (<http://bioinfo.vanderbilt.edu/webgestalt/>) and the Reactome analysis was done using the analysis function of the Reactome Pathway Browser (<http://www.reactome.org/PathwayBrowser/>).

4.12. Cloning individual shRNAs and sgRNAs

In order to validate screen results, selected shRNAs from the library were individually cloned into the AAV E-SARE PATHscreeener vector (V1301). Pairs of oligonucleotides were synthesized by Eurofins with Agel and EcoRI-compatible overhangs and annealed as followed. In 50 µl volume, 2.5 µg of each oligonucleotide were mixed together with 5 µl 10x T4 DNA ligase buffer (NEB). The mix was incubated at 90°C for 2 minutes and then slowly cooled down to room temperature to allow annealing of the two shRNA strands. The annealed oligonucleotides were diluted to 5 ng/µl and ligated into the linearized AAV E-SARE PATHscreeener vector.

Methods

shRNA oligonucleotide pairs were designed as followed:

Forward: 5'-CCGG-shRNA forward sequence-3'

Reverse: 5'-AATT-shRNA reverse sequence-3'

Cloning of sgRNAs into the linearized PATHscreeener2.0 vector was done using the same protocol as for shRNAs. For linearization, the PATHscreeener2.0 vector was digested with BbsI, creating overhangs for the ligation.

sgRNA oligonucleotide pairs were designed as followed:

Forward: 5'-ACCG-sgRNA target sequence-3'

Reverse: 5'-AAAC-sgRNA reverse target sequence-3'

5. Results

5.1. General considerations for a pooled RNAi screen in neurons

Until now the majority of pooled functional genetic screens (RNAi or CRISPR-Cas9) have been performed in oncology (Diehl et al., 2014; Shalem et al., 2015). This has an obvious impact on existing protocols and plasmid libraries. In oncology, the general goal is to screen for modifiers of cell proliferation/survival. To achieve the desired segregation of 'hit-cells' from 'non-hit-cells' in terms of cell numbers within the total cell population, long cultivation periods over multiple passages are required. This implies the use of lentiviral libraries (shRNA or sgRNA) to generate stable integrations in the genome of the mitotic cell line of interest (Rubinson et al., 2003; Stewart et al., 2003). The long selection procedure in order to get a strong phenotype finally allows isolating the genomic DNA and counting the number of integrations per shRNA by next-generation sequencing. An alternative approach involves the use of reporter cell lines and flow cytometry as a strategy to segregate different phenotypes at the endpoint of the screen and to focus the readout to cellular functions other than proliferation/survival (Parnas et al., 2015). This strategy is closest to the technology presented within the following chapters.

The aim to perform a pooled RNAi screen in a post-mitotic cell type, such as primary neurons, required certain adjustments to the classical protocols. Standard cell culture protocols for primary mouse neurons allow cultivation for not more than a few weeks and viability usually declines after two weeks in culture. Thus, the time window to produce a strong cell survival phenotype is relatively short. Nevertheless, to screen for modifiers of cell survival would be of great interest in terms of neurodegenerative diseases. Therefore, it has been initially tested how genomic DNA and total RNA abundance changes in response to cytotoxic stress within a primary neuron population. Cultures were treated with the electron transport chain inhibitor rotenone at different concentrations for 7 days and cell number, genomic DNA and total RNA was quantified. Surprisingly, the total nuclei count was only modestly reduced even at high rotenone concentrations (>100nM), although quantification of viable cells, by filtering out all pyknotic nuclei, revealed the toxicity of rotenone with an IC₅₀ of 14 nM (Figure 9A). This already indicated that an analysis based on a DNA barcode readout might lack the required sensitivity in a cell viability paradigm. In accordance to the cell count, it has been observed that only at rotenone concentrations above 100nM a reduction of the genomic DNA content by ~40% could be detected (IC₅₀ 40 nM). However, a more sensitive change in total RNA content with an IC₅₀ (15 nM) comparable to the live cell count and a higher dynamic range compared to genomic DNA was measured (Figure 9B). Taken together, this indicated that without long-term culturing including cell passaging, a segregation of viable and non-viable cell pools based on a DNA reporter is not feasible.

Results

Furthermore, RNA-based barcode readouts seem to be preferable in the case of primary neurons.

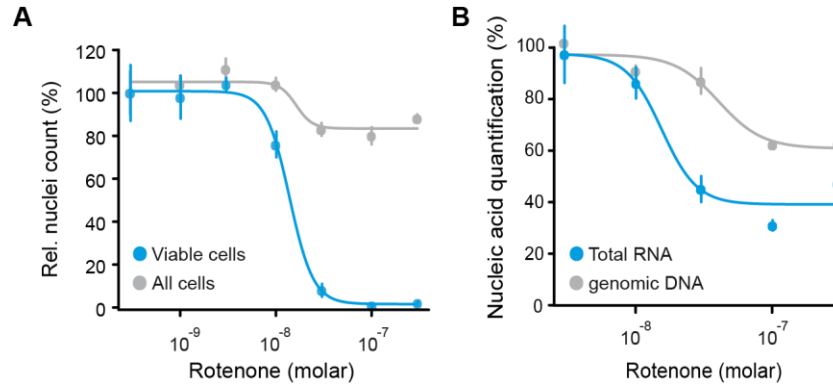


Figure 9: Cellular RNA content is a more sensitive indicator of neuronal viability in the dish than DNA.

A. Rotenone killing-curve. Primary neurons were treated with the indicated Rotenone concentrations from DIV7 till DIV14. Cells were counted by nuclear Hoechst stain. Either all Hoechst positive nuclei were quantified (All cells) or only non-pyknotic nuclei to discriminate viable from non-viable cells (Viable cells) (n=3 +-sem). **B.** Quantification of total RNA and genomic DNA content from primary neuron cultures in response to metabolic stress by Rotenone treatment (n=2 +-sem).

A second modification to current protocols was the viral system used to transduce primary neurons for a pooled RNAi screen. Primary neurons are post-mitotic cells and thus integration of the shRNA library is not needed for stable long-term transgene expression. Since the readout does not require stable barcode integration as well, it has been decided to use recombinant Adeno-associated virus (AAV). This has several practical and experimental advantages. AAVs require less safety precautions and are structurally more robust than lentiviruses (Bouard et al., 2009). More importantly, however, is that AAVs produced with certain capsid serotypes (e.g. serotype 1 and 2) have a natural tropism for neuronal cells and do not trigger a cellular immune response (McCown, 2005). Within the cell the AAV genome preferentially persists extrachromosomally (Nakai et al., 2001). This might reduce the risk of integration locus effects on shRNA and barcode expression and eliminates the possibility that coding or regulatory regions in the genome are destroyed due to integration (Moiani et al., 2012).

However, the first attempt to use a pooled shRNA library in order to screen for modifiers of neuronal survival highlighted that the assay transfer from oncology to neuroscience is not trivial. The cytotoxic stress paradigm did not lead to a strong quantitative shift of the shRNA-coupled barcode abundances within the neuron population after one week of treatment (data

not shown). This emphasized that a highly sensitive readout is absolutely necessary for successful pooled loss-of-function screenings in primary neurons. Therefore, it has been hypothesized that a more promising readout option would be the use of a reporter which monitors a cellular state (e.g. pathway activity). This might not only improve sensitivity and robustness of the screen but would provide proof-of-principle for an interference assays that leverages a sensor-assisted approach (since sensors can be flexibly exchanged) to dissect signaling networks principally in any genetically amenable cell type with pathway specificity and at a genomic scale.

5.2. A reporter for neuronal activity

The response to synaptic stimulation involves a cascade of cellular events which propagate the signal from the synapse to the nucleus. Stimulation of excitatory synapses causes an influx of calcium through NMDA receptors and L-type voltage-gated calcium channels (Dolmetsch, 2003). The main signaling routes to the nucleus involve calcium-dependent activation of calcium/calmodulin-dependent protein kinases and of adenylate cyclases (Greer and Greenberg, 2008). This results in activation of CaMK4 and PKA. Activated PKA and CaMK4 phosphorylate a set of pre-existing transcription factors (e.g. CREB, MEF2) (Flavell et al., 2006; Hardingham et al., 1997). These transcription factors induce expression of activity-dependent immediate early genes (e.g. *Fos*, *Arc*, *Npas4*). This activity-dependent gene expression program has been studied in great depth using RNA-seq and ChIP-seq technologies (Kim et al., 2010; Malik et al., 2014; Zhang et al., 2009). However, already during the pre-omics era activity-dependent genes have been studied and the transcription factor *Fos* was one of the first identified immediate early gene that is induced by neuronal excitation (Greenberg et al., 1985; Morgan et al., 1987; Sheng and Greenberg, 1990). Since then, the *Fos* gene product or the *Fos* promoter (~1kb upstream sequence of the transcription start site) coupled to a reporter (e.g. GFP) have been extensively used to label and identify activated neurons (Garner et al., 2012; Schilling et al., 1991). While the induction of the *Fos* promoter is sufficient to discriminate cell populations of activated versus silent neurons, its dynamic range is relatively small and thus probably not sensitive enough as a quantitative readout for a high-throughput RNAi screen.

In order to identify a genetic sensor with a wide dynamic range upon synaptic stimulation, a multiplexed *cis*-regulatory sensor assay was performed. Each sensor within this assay either consists of a clustered transcription factor binding sites (*cis*-element) coupled to a minimal adenoviral major late promoter (minMLP) or a ~1 kb promoter fragment (Figure 10A). During the assay sensors are driving the expression of unique molecular RNA barcodes in response to cellular signaling events. Barcode transcripts are finally isolated and decoded by NGS in

Results

order to measure sensor activities (Figure 10B). For the identification of a synaptic activity sensor, primary cortical neurons were infected with the AAV pool of 70 sensor vectors and the sensor activities were measured at DIV14 under neuronal silencing conditions, basal activity (i.e. untreated), and synaptic stimulation. Silencing of neuronal activity has been achieved through the application of the voltage-gated sodium channel inhibitor tetrodotoxin (TTX) in combination with the NMDAR antagonist D-(-)-2-Amino-5-phosphonopentanoic acid (APV) (McLennan, 1981; Narahashi et al., 1966). Neuronal activity of the culture has been evoked by blocking inhibitory synaptic transmission using the GABA_A receptor antagonist bicuculline (BIC). In all experiments, BIC has been supplemented with the potassium channel blocker 4-Aminopyridine (4-AP), the NMDAR co-agonist glycine, and the glycine receptor antagonist strychnine (Curtis et al., 1970; Meves and Pichon, 1975). This stimulation cocktail is referred to as BIC/4-AP. Multiple sensors qualified as synaptic activity reporters as they showed reduced activity in silenced neurons and increased barcode expression after synaptic stimulation (Figure 10C). The largest dynamic range between synaptic silencing and stimulation was measured for a sensor consisting of an enhancer from the murine *Arc* promoter, called synaptic activity-responsive element (SARE) (Kawashima et al., 2009). The SARE sensor outperformed classical neuronal activity reporters such as the endogenous promoters of *Fos* and *Egr1* (Figure 10C).

Results

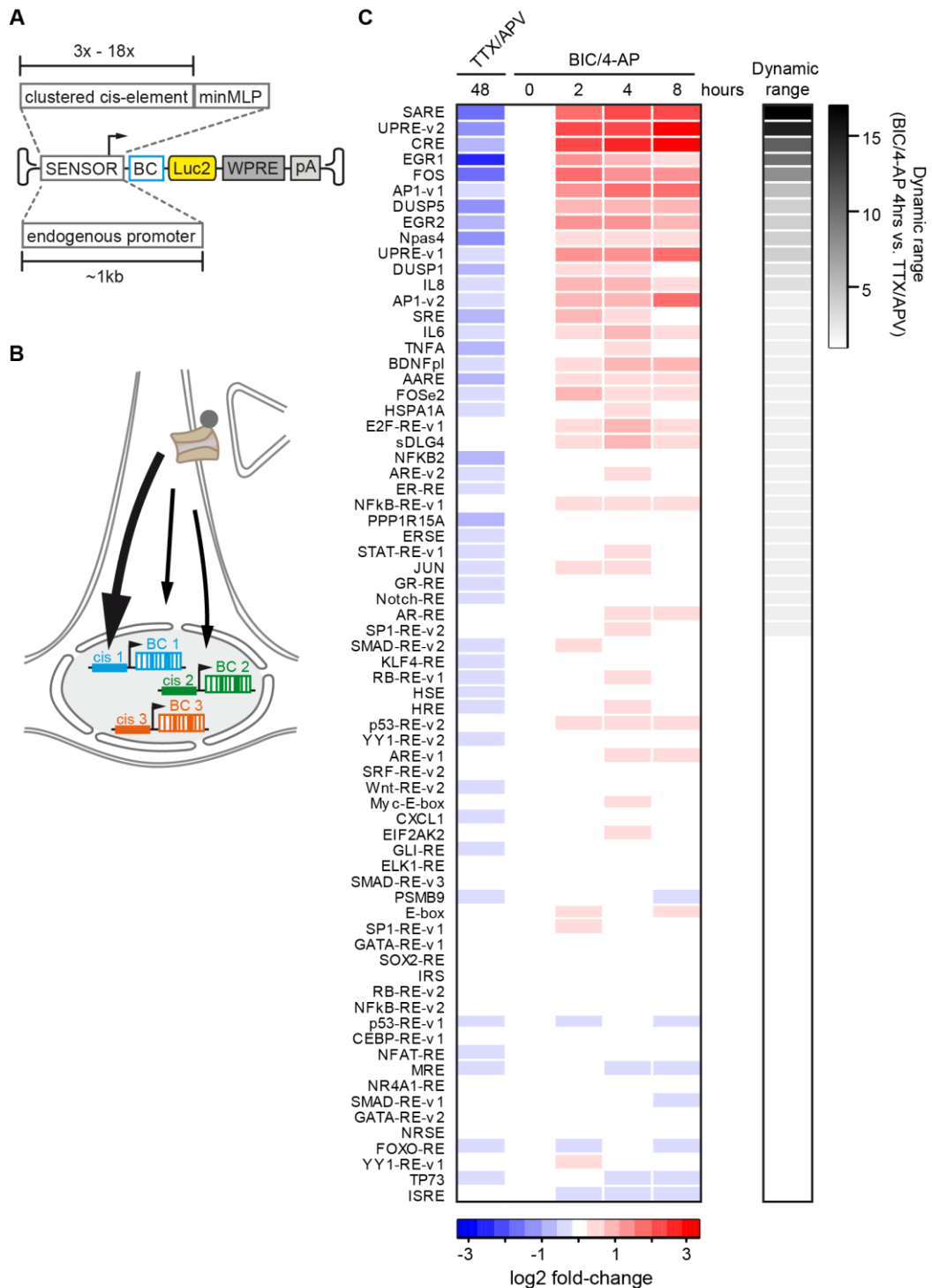


Figure 10: Multiplexed *cis*-regulatory sensor assay in response to neuronal silencing and synaptic stimulation.

A. Schematic map of the *cis*-regulatory sensor vector. The barcode (BC) and the firefly luciferase (*luc2*) are driven by clustered transcription factor binding site (*cis*-elements) or endogenous promoters. **B.** Illustration of the assay design. Neuronal cultures are infected by a pool of sensor vectors packaged into AAV particles and the sensor response is measured by NGS of the barcode pool. **C.** Heatmap of 70 sensor responses to TTX/APV or BIC/4-AP at the indicated hours of treatment (\log_2 fold changes). Sensors are ranked by dynamic range of BIC/4-AP (4hrs) vs. TTX/APV (right heatmap).

The SARE enhancer is a ~100 bp sequence localized >6 kb upstream of the *Arc* gene and contains binding sites for three activity-dependent transcription factors (CREB, MEF2 and SRF) (Figure 11). The *Arc* gene is expressed in response to neuronal activity and ARC protein is enriched at the post-synaptic density of dendritic spines and exerts functions during synaptic plasticity via regulation of AMPA receptor endocytosis (Chowdhury et al., 2006; Plath et al., 2006; Shepherd et al., 2006). Kawashima and colleagues have originally identified the SARE enhancer and characterized its sensitivity to synaptic stimulation (Kawashima et al., 2009). A genome-wide bioinformatics search for SARE-like sequences has revealed that this arrangement of transcription factor binding sites is not unique for the *Arc* promoter, but is found in promoter regions of many other neuronal activity-dependent genes (Rodríguez-Tornos et al., 2013).

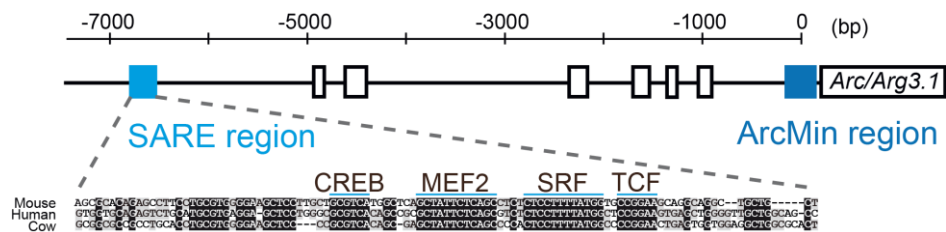


Figure 11: Genomic architecture of the murine *Arc* promoter.

Top, the SARE and ArcMin regions are indicated by blue boxes. Evolutionarily conserved genomic regions are represented by white boxes. Bottom, sequence alignment of the SARE region between mouse, human and cow. Sequences of high conservation are highlighted in black boxes. Binding sites for CREB, MEF2 and SRF/TCF are indicated. Modified from (Kawashima et al., 2013).

During the development of the sensor pool for the cis-regulatory assay, the SARE sensor has been optimized for highest signal-to-noise ratio by clustering of multiple SARE repeats in front of a 420bp minimal *Arc* promoter (ArcMin), similar to work by Kawashima and colleagues (Kawashima et al., 2013). Sensors with one, three, four, five, and six SARE repetitions were tested for a maximal dynamic range in the neuronal cell line SH-SY5Y upon stimulation with PMA (phorbol-12-myristat-13-acetat). A cluster of four SARE repetitions gave highest fold inductions and was therefore used in all subsequent experiments (Figure 12A). This composite promoter is hereafter named enhanced SARE (E-SARE) sensor, in line with the nomenclature used by Kawashima and colleagues, although their construct contains five SARE repetitions. Next, the E-SARE sensor was further characterized in primary cortical neurons. Longitudinal recordings of E-SARE-driven luciferase activity from untreated, maturing primary neurons revealed that the baseline E-SARE activity recapitulates the course of increasing synaptogenesis, as determined by staining the presynaptic marker synaptophysin in maturing cultures (Figure 12B). The kinetics also match the staging by Baj

Results

and colleagues shown in figure 4 (Baj et al., 2014). Finally, the E-SARE sensor not only responds to neuronal silencing (TTX/APV) and synaptic stimulation (BIC/4-AP), but can also be induced by brain-derived neurotrophic factor (BDNF) which is a well-established stimulus with functions in neuronal differentiation and plasticity (Figure 12C) (Park and Poo, 2013). The optimized and validated E-SARE sensor has been subsequently used for developing the pooled RNAi screen in primary neurons.

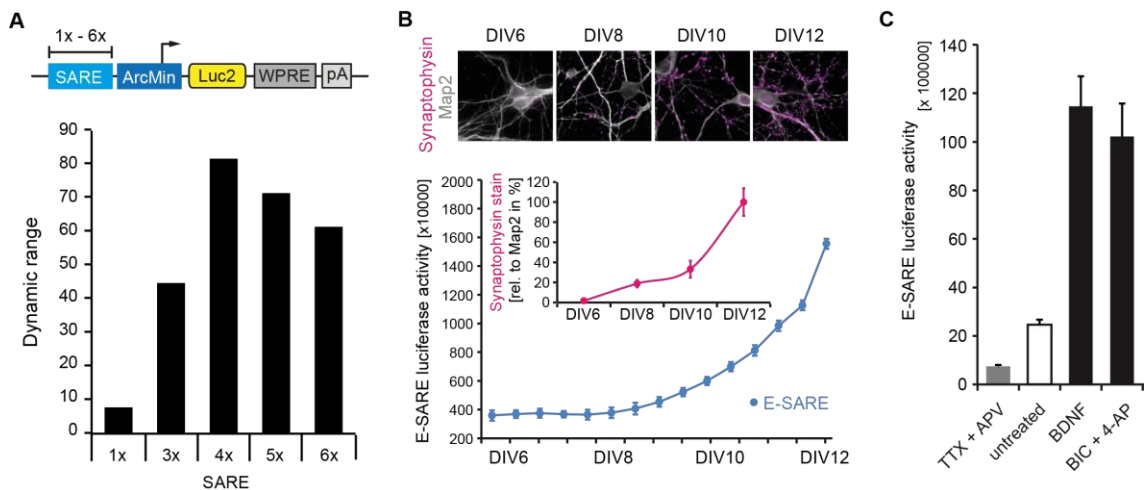


Figure 12: Design and characterization of the artificial E-SARE sensor.

A. Top, Schematic map of the sensor-luciferase vector with clustered SARE enhancers. Bottom, Comparison of luciferase activity of clustered SARE reporters after stimulation with PMA in SH-SY5Y cells (n=6). A cluster of four SARE is hereafter called enhanced SARE (E-SARE) sensor. **B.** Longitudinal measurement of basal E-SARE activity in maturing primary neurons from DIV6-12 (n=3 +-sem). Inset, Synapse quantification by staining of the presynaptic marker synaptophysin (n=3 +-sem). Top, representative images of primary neurons (DIV6-12) stained with antibodies against synaptophysin and MAP2. **C.** E-SARE activity in primary neurons upon silencing (TTX/APV), basal activity (untreated), and stimulation (BDNF, BIC/4-AP) at DIV14 (n=6 +-sd).

5.3. Vector design for sensor-based RNAi screenings

5.3.1. The principle of the screening approach

The presented study aimed to combine a pooled shRNA screen with a sensitive and robust genetic sensor. This sensor should consist of an optimized synthetic promoter (as described in section 5.2) which regulates the expression of a RNA barcode upon pathway activation. The use of a barcoded genetic sensor has two major advantages over currently used readout options for pooled interference screens (RNAi or CRISPR-Cas9): (1) It allows to measure cellular phenotypes other than proliferation/survival which is the case if only the bare shRNA pool complexity is analyzed. (2) It is independent of cell sorting based on a

Results

fluorescent reporter and therefore a direct quantitative readout. In order to achieve the combined approach of a pooled RNAi screen with a pathway activity readout, two libraries need to become one, the shRNA library and the sensor-coupled molecular barcode library. Each barcode within this library is controlled by the same genetic sensor and codes for an shRNA that is expressed from the same AAV vector (Figure 13A). The corresponding vector is hereafter named PATHscreener vector.

The screen itself is based on the simplified hypothesis that a stimulus (e.g. receptor agonist) triggers a signaling cascade which induces the barcoded sensor and that interference (by shRNAs) within this pathway leads to an altered sensor induction compared to shRNAs that are not targeting the pathway (Figure 13B). Sensor activities are finally measured by counting of the corresponding barcodes using NGS. The screen is based on the assumption that each cell is only infected once in order to avoid cross-contamination of multiple shRNAs and barcodes. In addition, we consider it as extremely unlikely that even at infection rates slightly greater than one per cell, by chance two shRNAs act in a synergistic or opposing fashion and may therefore compromise the screen.

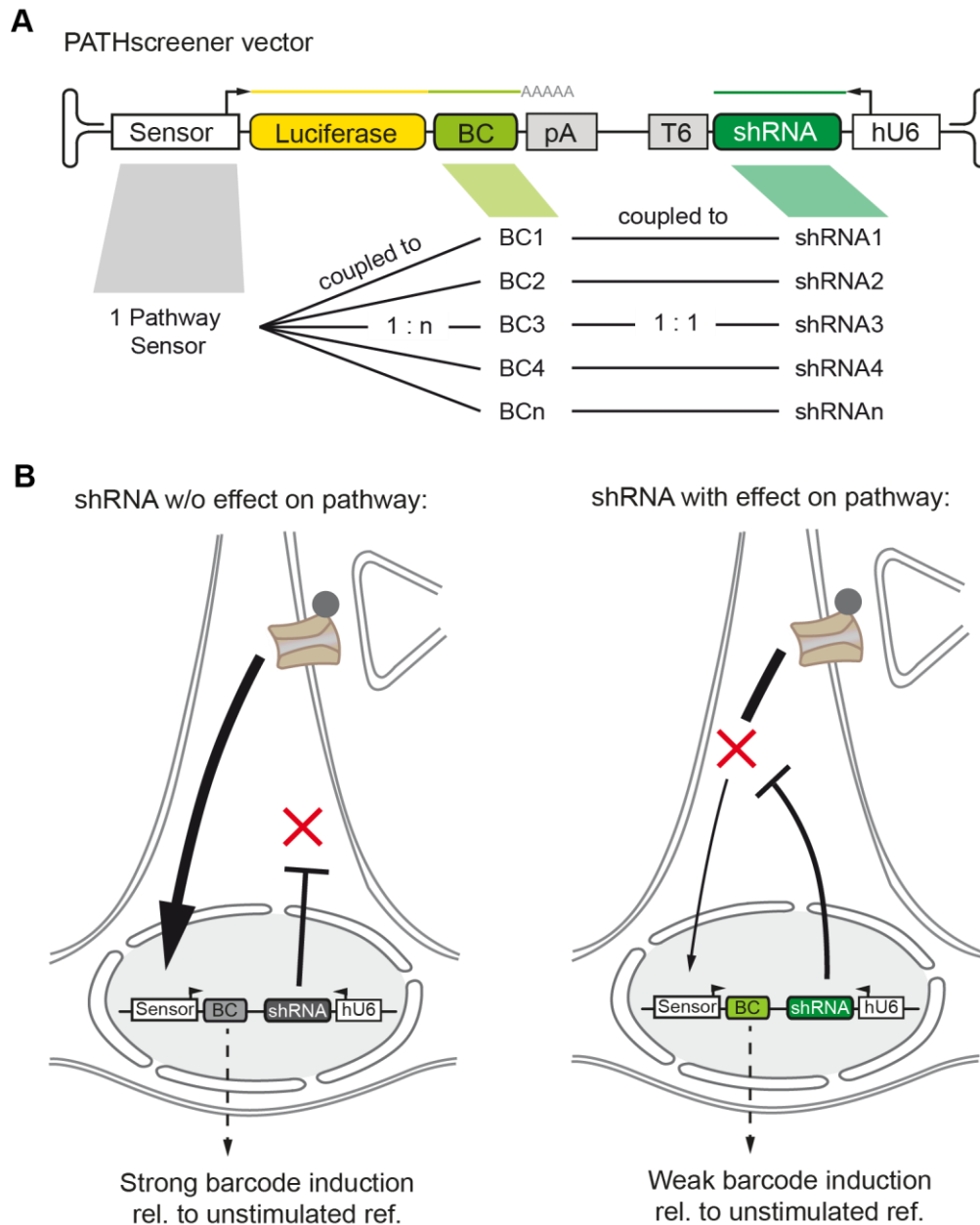


Figure 13: Principle of the sensor-based genetic interference screen.

A Map of the AAV PATHscreener vector. The connection within the library between sensor, barcodes and shRNAs is indicated below. **B** Graphical summary of the working hypothesis for the sensor-coupled RNAi screen. Interference independent of a given pathway addressed with a corresponding sensor does not affect the readout (left), whereas shRNAs targeting the signaling cascade alter sensor activity (right).

5.3.2. The shRNA expression cassette

Soon after the discovery of the post-transcriptional regulatory mechanism called RNA interference, its use as a research tool for gene expression manipulation has rapidly evolved to a gold standard technique (Mohr et al., 2014). The expression of shRNAs by a strong

Results

RNA polymerase III promoter (e.g. human U6 promoter) is the most commonly used method for stable RNAi. However, at the time when this project was initiated protocols and constructs have been published which allow shRNA expression from DNA polymerase II promoters (Li et al., 2007; Liu et al., 2010; Zuber et al., 2011). One advantage is the ability to use cell type specific promoters (please refer to section 2.4. for a detailed discussion on RNAi tools). The success and depth of a genetic interference screen relies on the efficiency of the genetic manipulation. As knockdown efficiency cannot be increased by multiple infections per cell during a pooled screen it is necessary to express optimized shRNAs from a strong promoter. In order to compare the impact of different promoters on RNAi efficiency, knockdown of a luciferase reporter by five different shRNAs driven by the hU6 promoter (hU6p or the DNA polymerase II promoters of synapsin-1 (Syn1p) or neuron-specific enolase (NSEp) were determined (Figure 14A). Overall, the hU6p-driven shRNAs showed superior knockdown efficiencies. In particular when the shRNA efficiency is suboptimal, the hU6 promoter demonstrates its impressive strength to boost the knockdown (Figure 14A, shRNA#4). Moreover, only the hU6 promoter-mediated RNAi achieved knockdown efficiencies above 90% in this test. Hence, the hU6 promoter was selected to drive the expression of the shRNA library for screening irrespective of possible limitation given the absence of cell type specificity.

In order to transduce primary neurons with the sensor-coupled shRNA library, AAV is the vector of choice as it has a natural tropism for neurons and does not evoke any cellular immune response (McCown, 2005). Whether the expression of a transgene or an shRNA is stable in primary neurons over time, was determined by infecting at DIV1 with an AAV which expresses GFP and an shRNA against Tcf4 and analyzing GFP fluorescence and Tcf4 mRNA abundance at various time points until DIV14 (Figure 14B and C). Knockdown of the Tcf4 mRNA was first detectable at four days post-infection which is also the time needed for AAV (serotype 1/2) infection until reaching its maximum. The knockdown was increasing and remained stable until DIV14. In accordance to this observation are the results obtained from GFP imaging. GFP expression is first visible at two days post-infection and increases until it stays stable over the entire time course (Figure 14C). This indicates that the AAV system is well suited for the screening approach and that the risk of losing AAV genomes or epigenetic silencing of promoters over time appears to be probably negligible.

Results

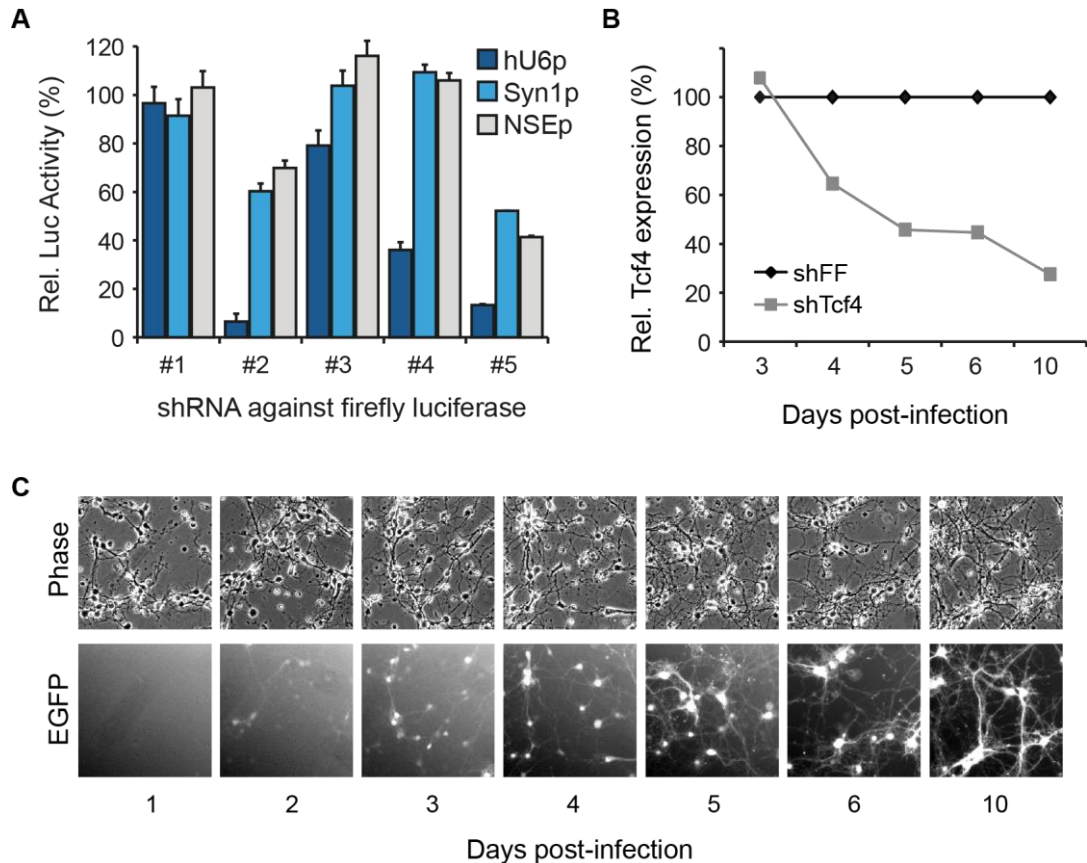


Figure 14: Efficient mRNA knockdown by hU6 promoter-driven shRNAs in neuronal cells.

A. Efficacy of five shRNAs, targeting firefly luciferase, driven by the hU6p, Syn1p, or NSEp promoter. shRNA expression plasmids were co-transfected with a luciferase reporter plasmid into PC12 cells (n=6, +-sd). **B.** Quantification of Tcf4 mRNA expression in primary neurons infected with AAVs for shRNA expression against Tcf4 or firefly luciferase as a non-targeting control on DIV1. Tcf4 mRNA was quantified at the indicated days post-infection. **C.** Longitudinal imaging of GFP expression in primary neurons infected on DIV1 with AAV-Syn1p-GFP (serotype 1/2).

In summary, the following milestones for the development of a sensor-coupled pooled RNAi screen were accomplished: (1) The E-SARE sensor gives a strong and robust induction in response to neuronal activity. (2) The hU6 promoter is the promoter of choice for efficient shRNA-mediated interference with gene expression. (3) AAVs are suitable vectors for stable transgene and shRNA expression in primary neurons. Next, the screening vector, as illustrated in figure 13A, needed to be generated and tested for functionality.

5.3.3. Combining sensor and shRNA expression

In the previous chapters the general design of the screening vector and independent validations of the barcoded E-SARE sensor and shRNA expression cassette have been presented. Next, it has been crucial to determine how both parts function in parallel and in close proximity if cloned into the same AAV backbone, which has a capacity of ~4.8 kb. This distance between the two promoters is relatively small, compared to genomic scales of promoter regions and one major concern was that the sensor might be biased due to regulatory elements of the hU6 promoter (Das et al., 1988). To address this issue the E-SARE induction upon PMA stimulation was determined in a luciferase assay with the complete AAV PATHscreener vector (containing E-SARE sensor and hU6p) or vectors where either the E-SARE sensor (w/o sensor) or the hU6p-shRNA cassette (w/o hU6p-shRNA) were deleted. Comparison of the complete PATHscreener vector with the hU6p-shRNA deletion vector ruled out the initial concerns and showed that the sensor is not compromised by the hU6 promoter (Figure 15A). Both vectors generated similar luciferase activities at baseline as well as upon stimulation by PMA.

An essentially important requirement for the pooled RNAi screen is that the sensor shows uniform inductions across different constructs with variable barcode and shRNA sequences. To test this condition 10 constructs with different barcode and shRNA sequences were cloned. E-SARE induction for each clone was tested by PMA stimulation in rat PC12 cells to minimize the risk of a true shRNA effect on the sensor activity. Overall the inductions across all clones were similar and the variance was considered acceptable (Figure 15B). None of the clones deviated more than three median absolute deviations (MAD) from the median, which is a frequently used hit criterion in high-throughput screens (Birmingham et al., 2009).

The two expression cassettes, sensor and shRNA, are directed towards each other which is defined by the library cloning procedure (described in chapter 5.4). Hence, the barcode is located downstream of the shRNA cassette, only separated by a synthetic poly-adenylation signal (SpA) and the T6 terminator (six thymidines) (see Figure 13A). Early research on the transcriptional termination from DNA polymerase III promoters has revealed that the termination is not always efficient and that run-through transcripts can occur (Campbell and Setzer, 1992). In case of the screening vector this might cause barcode transcription from the hU6 promoter (Figure 15C, dashed orange line). Since expression from the hU6 promoter is strong even slight termination inefficiency could lead to a severe contamination problem during sequencing if those barcode sequences are transcribed into cDNA. To avoid such a contamination it might be sufficient to use an oligo(dT) primer during first-strand cDNA synthesis. This primer only hybridizes with poly(A)-tails of transcripts expressed by the sensor. In addition, a comparison of random primers with oligo(dT) primers for cDNA

Results

synthesis indicated that the oligo(dT) primer is superior in this set-up and the data show that transcriptional run-through by DNA polymerase III is not a problem (Figure 15C).

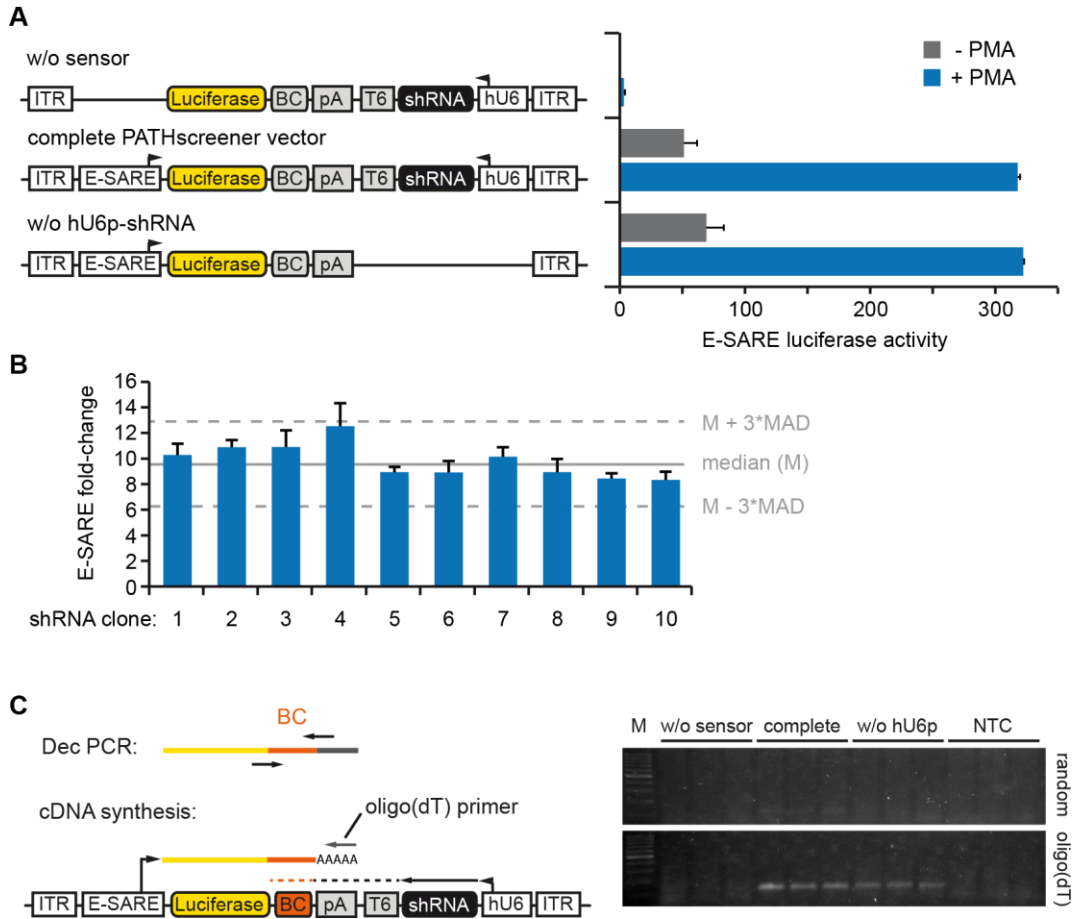


Figure 15: Functional validation of the PATHscreener vector.

A. Validation of an unbiased sensor response in the dual-expression PATHscreener vector. PC12 cells were transfected with the complete vector or a vector with an E-SARE sensor deletion or hU6p-shRNA deletion. Luciferase activity was measured for unstimulated and PMA-stimulated samples ($n=6 \pm$ sd). **B.** PC12 cells were transfected with the PATHscreener vector expressing 10 different random shRNAs. E-SARE-luciferase fold change upon PMA stimulation does not deviate more the three median absolute deviations (MAD) from the median ($n=6 \pm$ sd). **C.** Left, schematic of the vector with transcripts expressed by the sensor and by the hU6 promoter. The dashed line indicates DNA polymerase III run-through transcript. The oligo(dT) primer for cDNA synthesis is indicated as well as primer binding sites for barcode amplification at the decoding (Dec) PCR. Right, PC12 cells were transfected with the vectors shown in A and purified RNA was transcribed to cDNA either with random primers or oligo(dT) primers. A prominent Dec PCR barcode product is only detectable with cDNA transcribed using oligo(dT) primers. NTC, non-template control.

5.4. Library cloning strategy

A high quality shRNA library is the basis for successful pooled RNAi screenings. Libraries can be custom-made by high-throughput synthesis of shRNA oligonucleotides or purchased from various suppliers. Libraries can be either genome-wide or focused regarding specific groups of genes. Parameters affecting the decision between a genome-wide or focused approach are the biological question of the screen and the required cell number in order to get robust results. Common sense is that a cell number to shRNA complexity ratio of 200-1000:1 is required for robust screenings. For primary cells, cell numbers are often limited which argues for a focused library format. The aim of this study was to screen for regulators of neuronal excitation and synapse-to-nucleus signaling, hence the library should focus on signaling pathway genes in general. Such a library has been generated by Collecta as part of the Decipher project (<http://www.decipherproject.net/>). The Decipher Mouse Module 1 (MM1) shRNA library covers 4625 genes that were selected based on expert-curated pathway databases like KEGG and Reactome, the CSHL Cancer 1000 List, the Cancer Genome Atlas, FDA drug targets and MeSH. With nearly 5000 gene targets the library is perfectly sized for pooled RNAi screenings in primary neurons. The general design of the shRNA stem and loop region has been thoroughly optimized by Collecta for highest knockdown efficiencies. To make use of a high quality shRNA library design we decided to use the Decipher MM1 shRNA library and to develop a cloning strategy for repurposing of commercial shRNA libraries in a different context. The cloning strategy requires the following steps (Figure 16A): (1) PCR amplification of the hU6p-shRNA library cassette from the original shRNA plasmid library and simultaneous fusion of a minimal SpA (Levitt et al., 1989). The SpA will finally belong to the sensor cassette. (2) Fusion of the shRNA library PCR product with an oligonucleotide library containing random barcode sequences and amplification by PCR. (3) Large-scale ligation of the shRNA-barcode library insert into the sensor containing AAV backbone. (4) Sequencing of the vector region spanning the shRNA and the barcode in order to assign barcode sequences to shRNAs/gene targets (Figure 16B). The Ion Torrent PGM which was used for deep-sequencing of the final library is able to sequence fragments up to ~400bp. This implies that shRNA and barcode must be in close proximity and as a consequence both expression cassettes are facing towards each other and the SpA was selected as one of the smallest available poly-adenylation signals (Levitt et al., 1989). During library cloning, 12 individual clones were isolated and analyzed by restriction digest and Sanger sequencing. All clones passed the restriction digest, only one clone contained a mutated insert and each clone had a unique shRNA and barcode sequence. This confirmed that the protocol is delivering reliable cloning products. The cloned library contains ~25,000 unique barcodes which code for ~13,000 different shRNAs covering ~4500 genes (Table 1). Hence, after library repurposing ~97% of target genes are covered. An shRNA complexity of ~13,000 allows to perform a screen in a 15 cm cell culture dish with

10 million cells. With an infection rate of 60%, ~500 cells would be infected per shRNA on average. The barcode to shRNA ratio of ~2:1 results from a 2:1 ratio between barcode oligo and hU6p-shRNA-SpA fragment during PCR#2. This provides evidence that the cloning strategy by PCR is well tunable. A feature which makes this cloning strategy superior to protocols which are commonly used for library cloning in MPRA projects, for example. Those protocols require a barcoded backbone vector library into which an enhancer library is cloned. This usually results in higher numbers of different barcodes per enhancer. The generated E-SARE-shRNA library was successfully packaged into AAV particles (serotype 1/2) and subsequently used for screenings in primary neuron cultures.

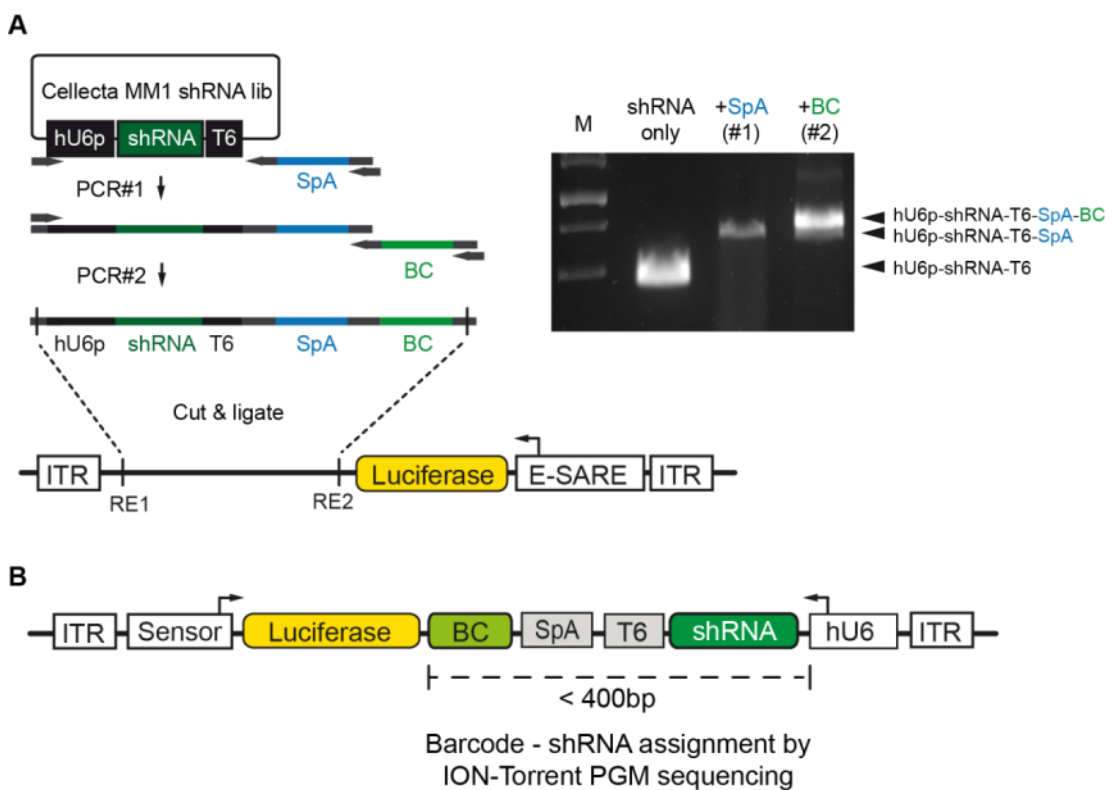


Figure 16: Generation of the PATHscreeener library.

A Cloning workflow. Left, the shRNA expression cassette is amplified by PCR and extended by the SpA. A second PCR adds the barcode (BC) to the previous PCR product. The product of PCR#2 is finally ligated into the sensor containing AAV backbone. Right, verification of the PCR products by agarose-gel electrophoresis. **B** Final cloning product. The proximity of barcode and shRNA allows the barcode – shRNA assignment by next-generation sequencing using the ION-Torrent PGM with 400bp chemistry.

Table 1: Complexity of the PATHscreeener library.

Colony no.	Barcode no.	shRNA no.	Gene no.	shRNAs/gene #
30,000	25869	12780	4467	2.9

#mean value

5.5. Sensor-based pooled RNAi screen in primary neurons

In order to broaden the cell types and cellular processes that can be studied using pooled RNAi screens towards relevant psychiatric risk pathways in primary neurons, a new barcoded genetic sensor readout has been developed. Using an AAV library that contains the E-SARE sensor and a focused shRNA library of ~4500 signaling pathway genes we aimed to perform the first pooled screen in primary neurons. The screen was designed to identify genes involved in neuronal excitation and synapse-to-nucleus signaling. The data presented in this thesis focus on two main questions. Firstly, does a pooled RNAi screen in primary neurons deliver meaningful hit lists? And secondly, is the screen reproducible?

5.5.1. Proof-of-concept screen for regulators of neuronal excitation

Initially two screens were conducted as a proof-of-concept. Those first two screens (A and B) were performed identically except that 10 or 5 million cells per sample were used, respectively. Each condition had 2-3 biological replicates. Cortical neurons were isolated from E15.5 wild-type mice and infected on DIV6 with the AAV pool at an AAV particle to cell ratio of 1000:1 (~60% infection rate). On DIV10 half of the samples were treated with TTX and APV to silence the spontaneous neuronal network activity and thereby reduce the E-SARE activity to baseline. The remaining samples were stimulated with a cocktail containing bicuculline, 4-AP, glycine and strychnine (BIC/4-AP) on DIV12 to boost synaptic activity (Figure 17 and Table 2). The RNA harvest time point for a maximal dynamic range was at 4 hours after BIC/4-AP application (Figure 18A). The kinetic of the RNA-based reporter is thus faster compared to the luciferase reporter which peaks at 8 hours after BIC/4-AP application (Figure 18B). All samples, silenced and stimulated, were subsequently lysed for total RNA purification. Barcode libraries were prepared for deep-sequencing on an Ion Torrent Proton sequencer. We hypothesized that the induction of a barcode, which codes for a hit shRNA, will be reduced or increased compared to the median induction of the total library. For hit nomination two analysis methods were applied: (1) Ranking by enhanced Z-scores of normalized fold changes between stimulated and silenced conditions and (2) a protocol analogous to differential gene expression analysis in RNA-seq using the DESeq2 package in R (Dai et al., 2014; Love et al., 2014).

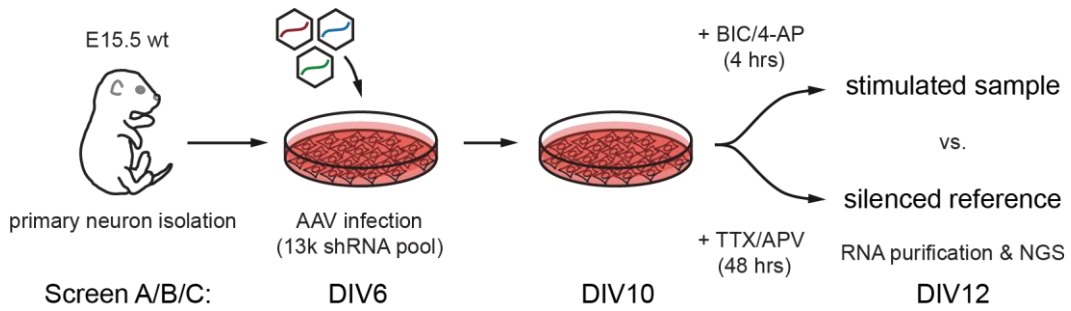


Figure 17: Screening design and workflow

Primary cortical neurons were isolated from E15.5 mice and plated in 15 cm (10 mio cells; Screen A and C) or 10 cm dishes (5 mio cells; Screen B). Neurons were infected with the AAV PATHscreeener library at DIV6. At DIV10 reference samples were treated with TTX/APV for the following 48 hours to reduce sensor activity. Neuronal activity is induced in the remaining cultures at DIV12 using a BIC/4-AP cocktail for 4 hours. Subsequently cultures were lysed and total RNA was purified and processed for next-generation sequencing.

Table 2: Screens in this thesis: A / B / C

Screen	Cell no./sample	AAV batch	Infection	Lysis	Reference condition	Test condition
A	10 mio	A59.1	DIV6	DIV12	TTX/APV	BIC/4-AP
B	5 mio	A59.1	DIV6	DIV12	TTX/APV	BIC/4-AP
C	10 mio	A59.2	DIV6	DIV12	TTX/APV	BIC/4-AP

5.5.2. Quality controls within the screening pipeline

Multiple quality control measures have been implemented into the screening workflow. Sister cultures were used to monitor the sensor activity upon neuronal silencing and stimulation with the BIC/4-AP cocktail in live cells. A ~21 fold-change of the E-SARE sensor activity was measured at the peak of induction by live cell luciferase activity recordings (Figure 18B). At the cDNA level from the actual screening samples, the sensor response was controlled by qRT-PCR using barcode flanking primers (qDec primers). Relative and absolute quantification of the barcode cDNA using qDec primers verified the E-SARE stimulation upon BIC/4-AP during the screen (Figure 18C and D). After total read count normalization of the raw data, pair-wise Pearson correlation and unsupervised hierarchical clustering was used to identify potential outlier samples. All biological replicate samples of screen A and B correlated well and samples clustered together by condition (BIC/4-AP, TTX/APV; Figure 18E). The highest correlations are observed between samples that were stimulated with BIC/4-AP.

Results

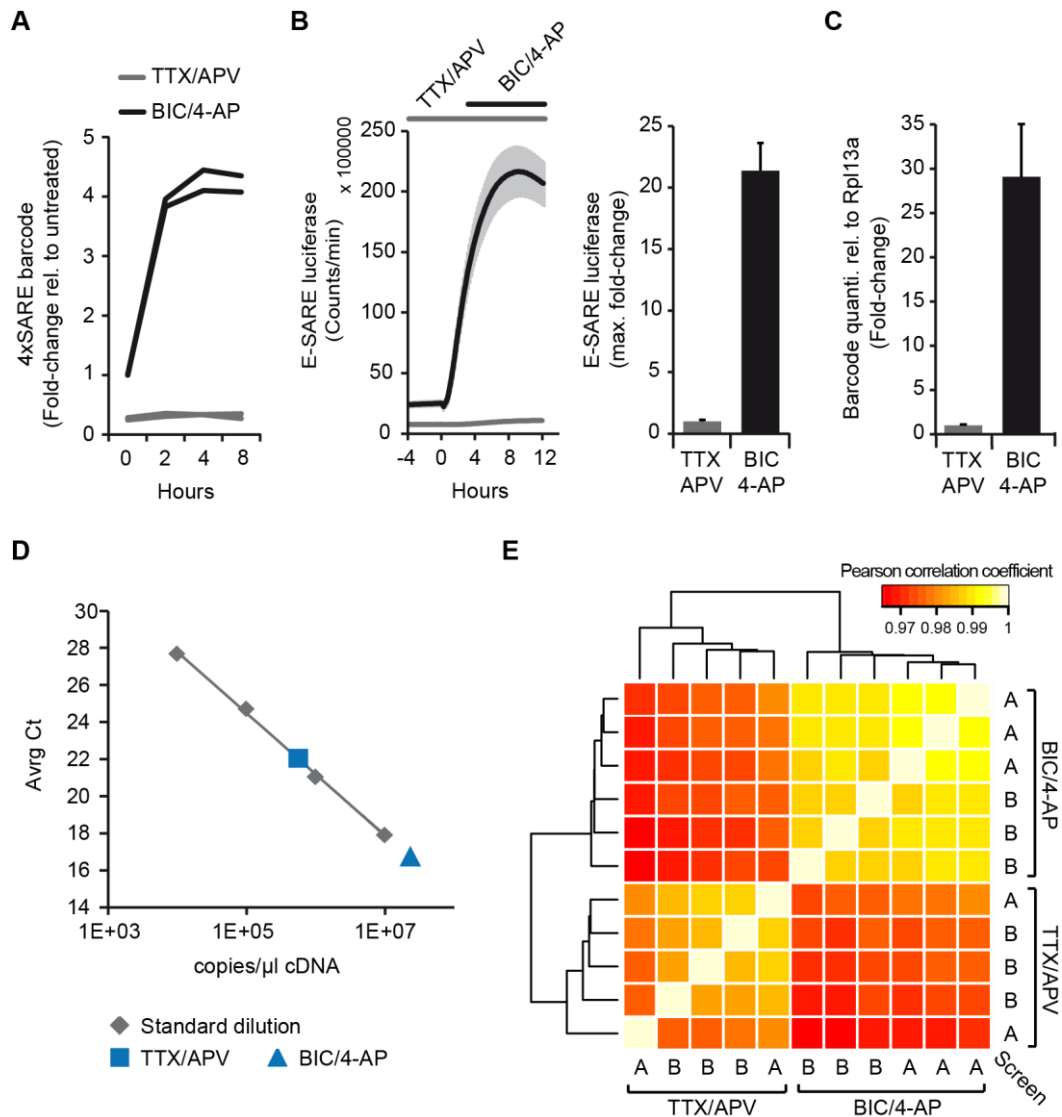


Figure 18: Quality control measures from the pooled RNAi screen.

A. Kinetics of the SARE-minMLP sensor response to TTX/APV and BIC/4-AP measured by barcode sequencing. The response for two individual barcodes is shown (average from two assay replicates; extracted from the multiplexed *cis*-regulatory sensor assay). **B.** Left, E-SARE sensor response to TTX/APV and BIC/4-AP determined by live cell luciferase activity measurement in sister cultures of screen A/B ($n=4 \pm$ sem). Right, maximal E-SARE luciferase induction by synaptic activity (time-point 8 hours of BIC/4-AP stimulation). **C, D.** Relative and absolute quantification of the barcode expression in screen A in response to TTX/APV and BIC/4-AP. **E.** Pair-wise correlation of normalized read counts from biological replicates of screen A and B. Clustering by unsupervised hierarchical clustering.

5.5.3. Hit nomination by enhanced Z-score ranking and DESeq2 analysis.

Data analysis and ranking of shRNAs and gene targets has been done by two independent methods. The knockdown effects on the E-SARE sensor activity were analyzed by an enhanced Z-score ranking and using the Bioconductor package DESeq2 (Love et al., 2014).

Results

Since absolute abundances of individual vectors vary within the library pool, barcode counts in the stimulated samples are always normalized to the barcode counts in the unstimulated reference samples (Figure 17). Both methods are based on the assumption that the majority of shRNAs within the library do not alter the induction of the E-SARE sensor in response to synaptic stimulation by BIC/4-AP. This assumption is valid if a shRNA library of high complexity, as in this case, is used and which was supported by the analysis of 10 random shRNA constructs (Figure 16B). The enhanced Z-score method analyzes the effect of a knockdown by reporting the deviation of the corresponding sensor activity from the median sensor activity of the entire pool. The advantage of the enhanced Z-score is its robustness against outliers which in this case are the hits. A negative enhanced Z-score of a shRNA means that the target gene is a positive regulator of the measured phenotype, whereas a positive enhanced Z-score identifies genes that act as negative regulators. Sensor activity in the screen can be shifted in general towards both directions, hence, positive and negative regulators can be identified. However, more shRNAs have a negative than a positive enhanced Z-score above the thresholds of 3/-3 (209 shRNAs at enhanced Z-score < -3; 111 shRNAs at enhanced Z-score > 3) and the overall amplitude is stronger at the negative scale (Figure 19A, left). Thus, the screen appears to be more sensitive for positive regulators, which is likely due to the strong stimulation applied during the screen. In order to collapse the hit list to the gene level, the shRNA with the strongest effect was selected to represent the corresponding gene target. At this level, 151 genes have an enhanced Z-score of less than -3 (Figure 19A, right) and can be considered as primary hits for positive regulators.

A second powerful analysis strategy uses the Bioconductor R package DESeq2 (Love et al., 2014). This package was originally developed for the identification of differentially expressed genes in RNA-seq experiments. Nevertheless, it has been shown that the DESeq2 package as well as the similar edgeR package are also powerful tools for hit nomination, as genetic screening data and RNA-seq data are very similar and have a negative binomial distribution (Dai et al., 2014; Parnas et al., 2015). In this study, DESeq2 was used for read count normalization between samples and identification of differentially expressed barcodes. Significance of differential expression was tested using the Wald test and corrected by multiple-testing using the Benjamini-Hochberg method (Benjamini and Hochberg, 1995). In accordance with the results from the enhanced Z-score analysis, the DESeq2 analysis identified more shRNAs where the sensor induction is significantly down-regulated (335 at a false discovery rate (FDR) < 0.05) compared to shRNAs with an enhanced sensor induction (250 at FDR < 0.05) (Figure 19B). Hit lists generated by both methods show a substantial overlap (Enh. Z-score vs. DESeq2 log₂FC 54/100; vs. DESeq2 FDR 41/100) (Figure 19C) and the use of both strategies in parallel can increase the confidence in hit nomination. The following steps of analysis are based on the enhanced Z-score ranking unless otherwise stated.

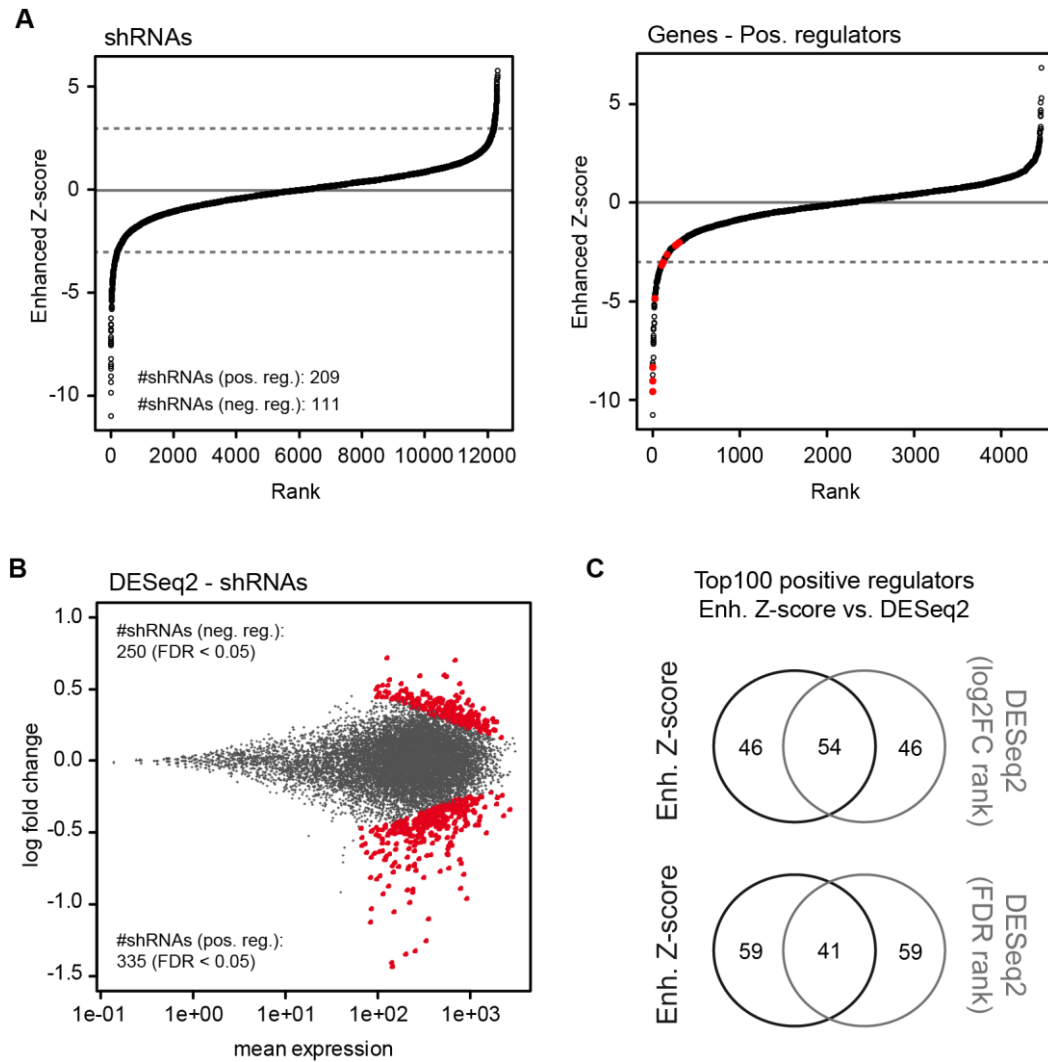


Figure 19: Enhanced Z-score and DESeq2 analysis of the pooled RNAi screen A.

A. Enhanced Z-score rankings. Left, For individual shRNAs from screen A. An enhanced Z-score of +3/-3 is indicated by a dashed line. Right, Collapsed to gene level by filtering for the shRNA with the most negative score per gene. The dashed line indicates a score of -3. Selected candidates for subsequent validation are highlighted in red. **B.** MA-plot compares for shRNAs the DESeq2 log₂ fold changes (screen A) to the mean expression of the corresponding barcode. shRNAs with differentially expressed barcodes are highlighted in red (FDR < 0.05). **C.** Overlap between the top 100 positive regulators identified by enhanced Z-score analysis and by DESeq2 analysis (either ranked by log₂ fold change or FDR). FDR was determined using the Benjamini-Hochberg method.

Next, 10 candidates for positive regulators were selected from screen A, covering an enhanced Z-score range from -2 to -10 as indicated in figure 19A (right, red dots). These candidates are components of cAMP signaling (*Adcy3*), cytokine signaling (*Il2rb*), calcium signaling (*Calm1*, *Camk2d*, *Cacna1f*, *Cacna1h*, *Tacr2*), the circadian clock (*Bhlhe40*), the postsynaptic density (*Gphn*), and a schizophrenia risk gene (*Disc1*). They were selected to test the first step of validation by performing individual knockdown experiments. For each

Results

gene the shRNA with the strongest effect in the screen was cloned into the PATHscreeener vector and tested individually for its interference in BIC-induced synaptic signaling (Figure 20). All tested shRNAs reduced the E-SARE induction compared to a non-targeting control (NTC) vector and 8 out of 10 shRNAs showed a significant effect (student's t-test, $p < 0.05$). While this is the first validation step, additional orthogonal validation tools (e.g. synapse/dendrite stainings, electrophysiology) need to be implemented into the protocol and high-content analysis of hit candidates might be a powerful strategy.

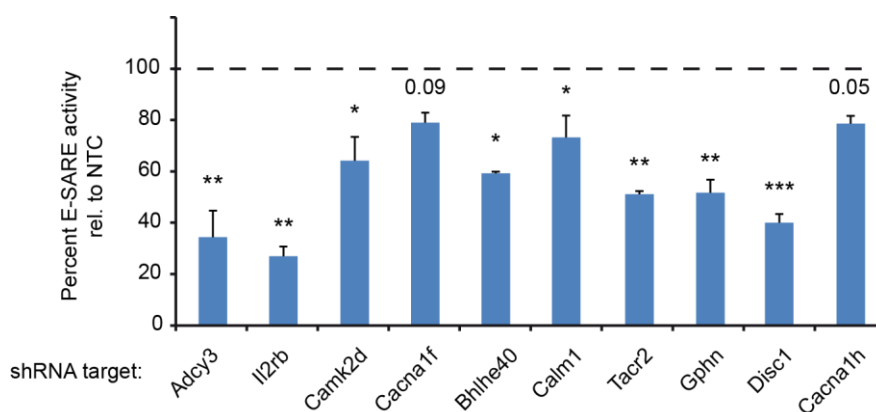


Figure 20: Individual validation of selected candidates.

E-SARE activity in response to knockdown of 10 candidate genes relative to a non-targeting control (NTC). Primary cortical neurons were infected with individual PATHscreeener vectors for 10 different shRNAs selected from screen A and a NTC vector. In accordance to the screening conditions cultures were either silenced by TTX/APV (48 hrs) or stimulated by BIC/4-AP (4 hrs) and E-SARE activity was determined by luciferase measurement ($n=3 \pm$ sd).

5.5.4. Hit ranking to biological function by KEGG and Reactome analyses

The main focus of this proof-of-concept study lies on the quality assessment of the screening results by comparison to currently available data. One would assume that in particular a knockdown of synaptic genes and genes with known function in cAMP/calcium signaling are likely to affect synapse-to-nucleus signaling and therefore alter E-SARE induction. In order to systematically interpret and validate the output of the pooled RNAi screen for regulators of neuronal excitation and synapse-to-nucleus signaling, the two manually curated pathway databases KEGG and Reactome were used as a reference (Fabregat et al., 2016; Ogata et al., 1998). This analysis has been done with the top 140 positive regulators identified in screen A. Strikingly, pathway analysis using the KEGG database revealed an enrichment of genes associated with the categories “Long-term potentiation”, “Neurotrophin signaling”, and “Calcium signaling” ($p < 0.05$, hypergeometric test, Table 3). These associations confirm that

the screen produces reliable results and can be used to identify pathway genes in primary neurons.

Table 3: KEGG Pathway analysis for the Top140 positive regulators

KEGG Pathway	R	pValue#	Genes
Long-term potentiation	4.15	0.0013	<i>Calm1, Ppp1ca, Adcy8, Araf, Camk2d, Ppp1cb, Camk4</i>
Neurotrophin signaling	2.94	0.0032	<i>Calm1, Psen1, Camk2d, Nfkbie, Pik3cd, Mapk14, Csk, Camk4, Fasl</i>
Calcium signaling	2.08	0.0374	<i>Calm1, Cacna1f, Slc25a4, Tacr2, Camk2d, Adyc8, Camk4, Adcy3</i>
Chemokine signaling	2.05	0.0406	<i>Pik3cd, Ccr5, Adyc8, Cxcr5, Xcr1, Csk, Cxcl2, Adcy3</i>
MAPK signaling	1.79	0.0519	<i>Dusp6, Cacna1f, Ppp5c, Fgf20, Fgf12, Mapk14, Fgf18, Daxx, Map3k12, Fasl</i>

R Enrichment ratio; # hypergeometric test

Along with pathways of known and well-established function in neuronal activity-dependent signaling, surprisingly, an enrichment for genes in the KEGG pathway ‘Chemokine signaling’ was found (Table 3). The top hit list for positive regulators contains the chemokine receptors CC-motif-chemokine receptor 5 (*Ccr5*), CXC-motif-chemokine receptor 5 (*Cxcr5*), and chemokine (C motif) receptor 1 (*Xcr1*), as well as, the ligand chemokine (C-X-C motif) ligand 2 (*Cxcl2*). In addition, the C-Src kinase (*Csk*), two adenylate cyclase isoforms 3 and 8 (*Adcy3/8*), and the catalytic domain delta of PI3-kinase (*Pik3cd*) have been identified as components of chemokine signaling.

A second line of evidence for the functionality of the screen comes from a pathway analysis using the Reactome pathway browser. Significant enrichments were found for multiple signaling events that involve the second messenger molecules calcium, diacylglycerol (DAG), and inositol triphosphate (IP3). In addition, the Reactome analysis reflects that in primary cortical cultures primarily the glutamatergic post-synapse is screened (Pathway: ‘Activation of NMDA receptor upon glutamate binding and postsynaptic events’, p=0.003). Finally, the Reactome pathway analysis revealed that the screen is also sensitive for perturbed neurodevelopmental processes like neurite outgrowth (Pathway: ‘NCAM signaling for neurite outgrowth’, p=0.004) (Table 4).

Table 4: Reactome Pathway analysis for the Top140 positive regulators

Pathway	pValue	FDR
Phospholipase C-mediated cascade; FGFR3/4/2/1	6.69E-05 / 7.54E-05/ 1.46E-04 / 9.14E-04	0.022
Activation of CaMK IV	4.36E-04	0.022
PLC beta mediated events	5.66E-04	0.022
G-protein mediated events	6.26E-04	0.022
CaM pathway	6.76E-04	0.022
Calmodulin induced events	6.76E-04	0.022
Ca-dependent events	8.89E-04	0.022
CaMK IV-mediated phosphorylation of CREB	9.71E-04	0.022
DAG and IP3 signaling	0.001	0.026
CREB phosphorylation through the activation of CaMKK	0.002	0.031
PLC-gamma1 signaling	0.002	0.031
Post NMDA receptor activation events	0.002	0.034
Activation of NMDA receptor upon glutamate binding and postsynaptic events	0.003	0.050
NCAM signaling for neurite outgrowth	0.004	0.062
MAPK family signaling cascade	0.005	0.076
CREB phosphorylation through the activation of adenylate cyclase	0.005	0.076

Figure 21 summarizes the major findings from screen A by mapping hit candidates along the synapse-to-nucleus route. Mapping was done using the KEGG pathway maps “Long-term potentiation”, “Glutamatergic synapse”, “Calcium signaling pathway”, “mTOR signaling pathway”, and “PI3K-Akt signaling pathway”. The map has been further complemented by a few entries based on additional literature. As expected from the KEGG and Reactome pathway analysis output many positive regulators that ranked high in the screen are involved in post-synaptic function. Along the route from the synapse to the nucleus multiple genes involved in calcium signaling, a schizophrenia risk pathway, were found (*Cacna1f/h/g/c*, *Calm1/3*, *Camk2d/g*, *Camk4*) and with *Itpr1* an IP3 receptor involved in calcium wave propagation along the dendritic ER. Besides calcium regulators, several members of the mTOR and PI3K-Akt signaling pathways, which are associated to schizophrenia and ASD as well, ranked high in the screen (e.g. *Pik3cd*, *Akt1*, *mTOR*) (Kim et al., 2009; Sawicka and Zukin, 2012). Notably, the recently identified schizophrenia risk gene *C4a*, which is member of the classical component cascade, ranked high in the screen (rank 446, screen A; rank 50, screen B) (Sekar et al., 2016).

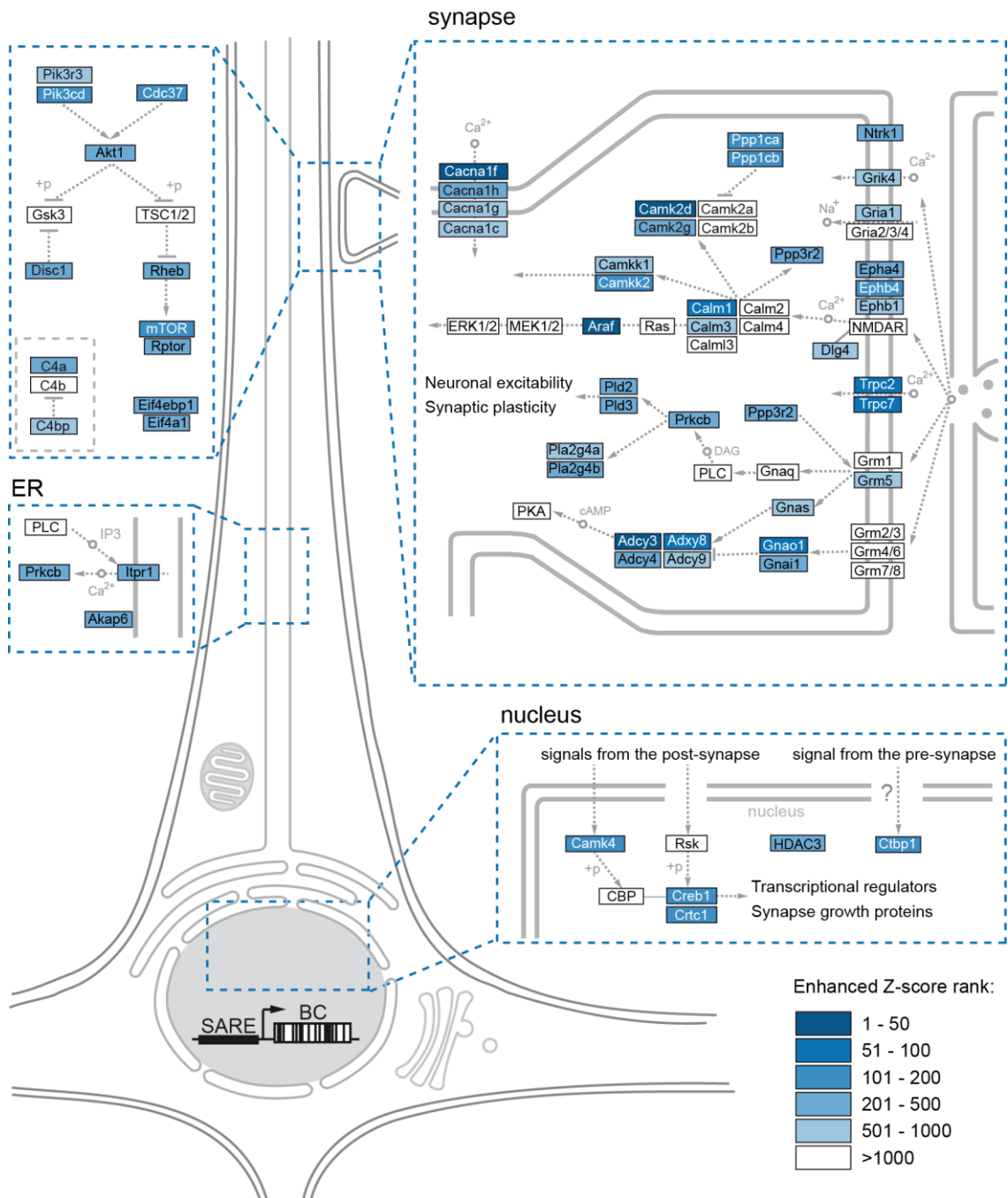


Figure 21: Screening hits along the synapse-to-nucleus pathway.

Pathway mapping of positive regulators of neuronal excitability and synapse-to-nucleus signaling based on KEGG and manual literature mining. The color code indicates the enhanced Z-score ranking in screen A.

5.5.5. Reproducibility of the screen

The robustness of a screen and consequently the reproducibility of its results should always be a major concern during assay development. Nevertheless, the issue of insufficient

reproducibility in biomedical research is frequently raised in academia and industry (Freedman et al., 2015). The presented pooled sensor-based RNAi screen in primary neurons was performed three times in total in order to estimate the degree of reproducible results. Screen A and B were performed in parallel with the same batch of primary neurons and AAV preparation. Both screen only differed in terms of cell number (screen A: 10 mio cells/sample; screen B: 5 mio cells/sample). Screen C has been carried out completely independent. This means that primary neuron cultures were prepared on another day using different embryos, a new AAV batch was used, and multiple steps of the screening protocol were performed by another experimenter (e.g. primary neuron preparation, RNA isolation, cDNA synthesis). Each screen has been completed with 2-3 internal biological replicates per condition. Comparison of the enhanced Z-scores from the entire gene level results from screen A and B displayed that both datasets correlate with a spearman-rank coefficient (ρ) of 0.567 (Figure 22A). A focused view at the top hits for positive regulators revealed a substantial overlap between screen A, B, and C. The 100 highest-ranked positive regulators from screen A and B share over 50% of genes when analyzed by DESeq2 and ranked by log2 fold-change (\log_2FC) or FDR (Figure 22B). Analysis by enhanced Z-score ranking displayed an overlap of 45 genes between screen A and B and 38 genes between screen A and C out of the top 100 (Figure 22C).

The evaluation of all three screens indicates that in particular the discovery of positive regulators of neuronal excitation under strong synaptic stimulation is reproducible.

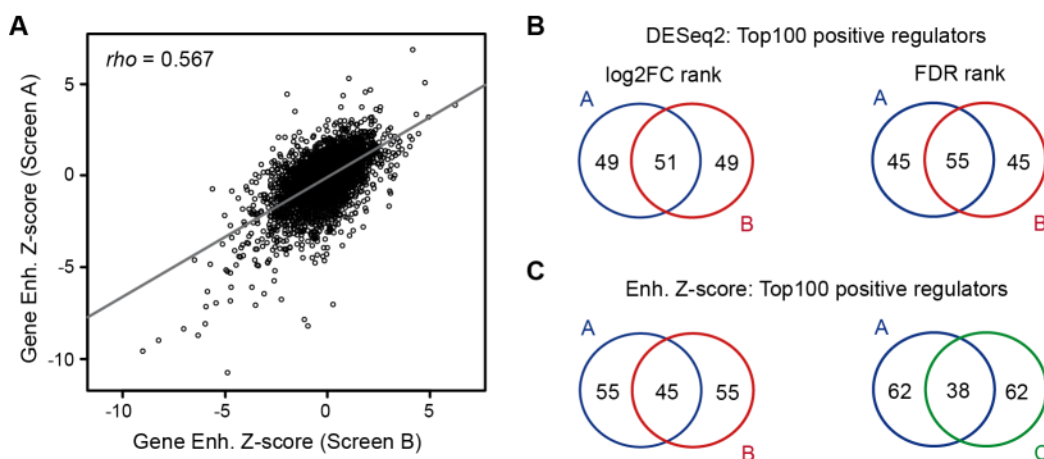


Figure 22: Reproducibility of the pooled RNAi screen in primary neurons.

A. Scatterplot of enhanced Z-scores from screen A and B. Data has been collapsed to gene level and filtered for positive regulators. The spearman-rank coefficient ρ and linear regression are indicated. **B, C.** Venn diagrams for the overlap in the hit lists generated by DESeq2 analysis (B) and enhanced Z-score ranking (C).

5.5.6. Screening for negative regulators of neuronal excitation

The identification of negative regulators of neuronal excitation and synapse-to-nucleus signaling is of great interest particularly for the discovery of new potential drug targets in order to restore hypoexcitability and synaptic function of neurons. As pointed out earlier, hit nomination for negative regulators is challenging due to a smaller dynamic range of the E-SARE sensor under strong synaptic stimulation, hence, false-positives are more likely. Consequently, datasets from screen A, B, and C were used and compared in order to evaluate the screening performance for negative regulators. As expected, the pairwise overlap as well as the overlap between all three screens is smaller than for positive regulators. Within the top 100 potential negative regulators, screen A and B shared 15 genes, screen A and C shared 11 genes, and screen B and C shared 10 genes (Figure 23). One gene is in common to the hit lists of all three screens. Among hits found in two independent screens are genes with known function in neuronal excitation and calcium/cAMP-signaling like the Na^+/H^+ antiporter *Slc9a1*, the ATPase Na^+/K^+ transporting subunit beta 3 (*Atp1b3*), and the cAMP-responsive element modulator (*Crem*) (Forrest, 2014; Gu et al., 2001; Mellström et al., 1993; Xia et al., 2003). The only gene that is shared across all three hit lists for negative regulators is *Katnb1* which encodes the noncatalytic regulatory p80 subunit of katanin, a protein complex involved in severing of microtubules (Hartman et al., 1998). Hence, *Katnb1* knockdown might stabilize neurites, thereby enhancing the excitatory input.

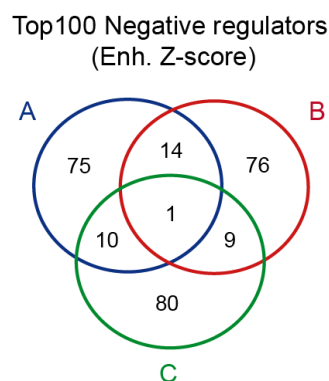


Figure 23: Comparison of identified negative regulators in screen A, B, and C.

Venn diagram showing the overlap between the top 100 potential negative regulators from screen A, B, and C identified by enhanced Z-score ranking.

5.6. Adaptation towards CRISPR-Cas9-based screening in primary neurons

Over the last three years CRISPR-Cas9 has evolved to the most popular and powerful tool not only for genome engineering but also for loss- and gain-of-function studies (Gilbert et al., 2014; Jinek et al., 2013; Larson et al., 2013). Similar to the early days of pooled RNAi screens, it is no surprise that the cancer field is again at the forefront of functional genomics screens using CRISPR-Cas9. To date, multiple pooled CRISPR-Cas9 screens have been published. Most of them have been performed in cancer cell lines but recently one screen in primary dendritic cells using a pathway readout has been published (Parnas et al., 2015; Shalem et al., 2014, 2015; Wang et al., 2014). Direct and indirect comparisons between pooled RNAi and CRISPR-Cas9 screens have indicated that CRISPR-Cas9 has superior on-target efficacy and reduced off-target activity (Evers et al., 2016a; Morgens et al., 2016; Shalem et al., 2014). Although most of the published screens are loss-of-function knockout screens, a major advancement is its use for gain-of-function studies. This for the first time allows genome-wide gain-of-function screens in mammalian cells and hence complements the loss-of-function toolbox (Koneremann et al., 2015).

Based on the acquired expertise from the proof-of-concept pooled RNAi screen in primary neurons, the adaptation towards a CRISPR-Cas9-based screening tool has been initiated. Transcriptional regulation by CRISPR-Cas9 relies on the recruitment of effector domains (e.g. p65, VP64 activator domains) into proximity of the transcriptional start site of the gene-of-interest. It has been shown that recruitment of multiple domains to the same locus enhances activation of gene expression (Koneremann et al., 2015; Tanenbaum et al., 2014). We therefore decided to use the CRISPR-Cas9-SAM (Synergistic Activation Mediator), that recruits multiple effector domains using a fusion of the sgRNA with two MS2 aptamer sequences and a second fusion of the MS2-binding domain with the effector domains (e.g. p65 and VP64) (Figure 24A). This increases the number of effector domains at the locus compared to a direct fusion of the effector domain to dCas9 (as illustrated in Figure 6B and C). Two AAV vectors have been cloned, one for dCas9 (*Streptococcus pyogenes*) expression and the second vector represents the CRISPRa PATHscreeener2.0 vector with the following modifications to the RNAi-based PATHscreeener vector: (1) The firefly luciferase was substituted by the shorter NanoLuc luciferase. (2) The shRNA is substituted by the sgRNA2.0. (3) A third expression cassette is introduced for MS2-p65-VP64 expression (Figure 24B, PATHscreeener2.0). Multiple experiments have been performed until now to validate the CRISPRa PATHscreeener2.0 vector. Expression of dCas9 and MS2-p65-VP64 from the AAV backbone has been verified by western blot (Figure 24C). Stimulation of the E-SARE sensor within the PATHscreeener2.0 backbone by PMA in HEK293 cells showed comparable inductions as with the RNAi-based PATHscreeener vector (Figures 15A and 24D). The system is able to induce expression of a luciferase reporter as well as

Results

endogenous Arc mRNA (Figure 24E and F). Primary neurons express both dCas9 and MS2-p65-VP64 after AAV infection. This has been a critical step as the AAV-dCas9 genome slightly exceeds the optimal AAV packaging capacity of 4.8 kb. Importantly both proteins are localized in the nucleus (Figure 24G).

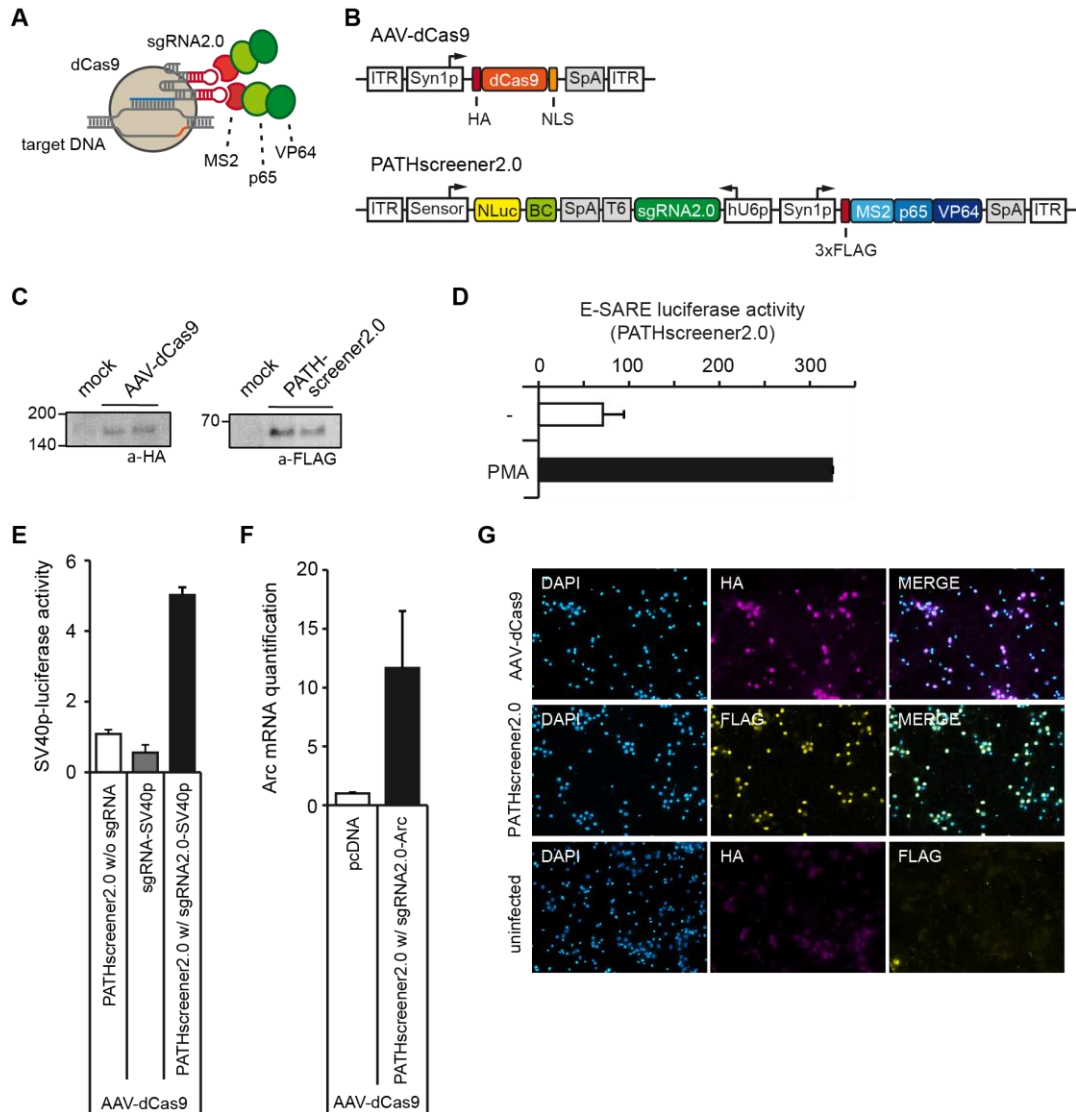


Figure 24: Adaptation towards an AAV CRISPR screening vector.

A Schematic of the CRISPRa complex comprising the target DNA bound by the inactive Cas9 (dCas9) and the sgRNA2.0 harboring two MS2 loops. MS2 loops are recruiting the MS2-binding domain fused to the p65 and VP64 transcription activator domains. **B** AAV maps of the dCas9 vector (top) and the CRISPRa-PATHscreener vector (bottom). **C** Expression validation of dCas9 and MS2-p65-VP64 in HEK293FT cells by western blot. **D** Validation of the E-SARE sensor response to PMA in the context of the CRISPRa-PATHscreener vector in HEK293 cells (n=6 +- sd). **E** Transcriptional activation of a SV40p-luciferase reporter by dCas9, MS2-p65-VP64 and sgRNA2.0-SV40 (n=6 +- sd). **F** Transcriptional activation of Arc gene expression in N2a cells by dCas9, MS2-p65-VP64 and sgRNA2.0-Arc (n=3 +- sd). **G** Validation of nuclear dCas9 and MS2-p65-VP64 localization in primary mouse neurons after AAV infection of the vectors shown in B.

6. Discussion

Experience-driven neuronal activity is shaping the brain throughout life by modulating synaptic connections and the excitability of neurons within circuits. Aberrant neuronal connectivity and activity might result from a multitude of genetic defects and is likely causative for various CNS diseases including psychiatric disorders (Grant, 2012). The underlying molecular mechanisms of neuronal activity and synaptic plasticity in health and disease can be studied using primary neuronal cultures. While research over the last decades has identified many key components of synaptic transmission, plasticity, and signaling to the nucleus, it is likely that proper neuronal function is also dependent on various other biological processes. One example is the energy metabolism and control of redox state (Sada et al., 2015; Winkler and Hirrlinger, 2015). Elucidation of the networks which affect neuronal function can be a tedious endeavor. Pooled genetic loss-of-function screens are a tool that offers a rapid and holistic view at genes with essential functions during the development of a particular cellular phenotype. Until now, no strategy for a pooled genetic screen in primary neurons has been published. The presented work describes the first proof-of-concept pooled RNAi screen in primary neurons, which is also the first screen using a post-mitotic cell type. The intention for this project was dual-purpose. Firstly, the assay should be useful for the dissection of signaling pathways. Most of the time, follow-up investigations of a screen only pursue a single candidate. This constrains the full capacity of a large-scale screen. An exception is the work by Parnas and colleagues who aimed to dissect the LPS/Tlr4-to-Tnf pathway in dendritic cells using a pooled CRISPR-Cas9 knockout screen (Parnas et al., 2015). This screen will be discussed and compared to the presented screen in more detail later. Secondly, an assay was to be delivered that complement the toolbox for psychiatric and neurodegenerative drug discovery in the future.

6.1. Advancing the current screening strategies

The current strategies for pooled genetic screens exclusively rely on a lentiviral-based approach where DNA barcodes or the shRNAs/sgRNAs itself are used for deconvolution of the cell pool by next-generation sequencing. This rather static reporter makes it indispensable to physically segregate cell populations according to their phenotype. For post-mitotic cell types or phenotypes other than proliferation it is therefore required to stain and sort cells by flow cytometry. In this work a new readout strategy for pooled genetic screens is presented which makes cell sorting unnecessary. Molecular RNA barcodes which are expressed by a pathway sensor and code for a specific shRNA allow direct deconvolution of the complete cell pool. The genetic E-SARE sensor has been empirically selected as a superior sensor for neuronal activity from a resource of 70 sensors, which is in

line with data obtained by others (Kawashima et al., 2009, 2013). This pool of genetic sensors together with additional putative sensors described in the literature represents a resource for the dissection of numerous cellular phenotypes in the future using a pooled screen. Interesting pathways/phenotypes in the context of psychiatric and neurodegenerative diseases would be antioxidant response (ARE sensor), hypoxia (HRE sensor), hippo signaling (TEAD sensor), Wnt signaling (TCF-LEF sensor), unfolded protein response (ERSE sensor), and apoptosis (TP53INP1 sensor).

An inherent risk of high-throughput screens is the false-positive hit nomination due to interference with the assay system (e.g. reporter expression) itself. For genetic screens using reporters (e.g. GFP), this risk encompasses interference with transcription, mRNA transport and stability, translation, protein folding and degradation of the reporter protein. The integration of an RNA reporter system not only generates faster kinetics but also eliminates several of the above mentioned interference points associated to the expression of a protein reporter.

6.2. Assay validity

The main focus in data analysis of this proof-of-concept screen was to assess the validity of the assay. This has been done by mapping the hit list to the KEGG and Reactome pathway databases and a literature search for associations between screen hits and psychiatric disorders.

6.2.1. Identification of genes with known function in synaptic plasticity

Pathway analysis using KEGG and Reactome databases revealed that the screening hits are enriched for genes involved in regulation of synaptic plasticity and signaling from the glutamatergic postsynapse to the nucleus. It was expected that in particular regulators of calcium and cAMP signaling could be identified to provide evidence for the validity of the screen. This was indeed the case as multiple voltage-gated calcium channel subunits, calmodulin isoforms, adenylate cyclases, calcium/calmodulin-dependent kinases and downstream transcription factors were amongst the top-ranked genes. This confirms that the approach is suitable to dissect neuronal signaling pathways. Nevertheless, the screening results did not entirely recapitulate the pathway maps found for example in the KEGG database. This might have several reasons. First of all a focused shRNA library was used which does not cover the entire mouse genome. Second, if a certain regulator is covered but does not score in the screen, the knockdown might not be effective enough to produce a measureable phenotype. A third reason, which might contribute to false negatives, is

functional redundancy of proteins, a general challenge to loss-of-function studies. While the biological space of the screen can be increased relatively easily up to a genomic scale by expanding the library, studying protein redundancy and epistasis would require applying a second genetic perturbation on top of the shRNA library. Although, this has even been done in a systematic manner by generating a double-shRNA library, it rapidly increases the library complexity to a point where screenings in primary neuron cultures are not feasible anymore (Bassik et al., 2013)

6.2.2. Hits with association to psychiatric disorders

The identification of genetic risk loci for psychiatric disorders like schizophrenia, BPD and ASD by genome-wide association studies and exome sequencing has highlighted the synapse proteome as well as several regulatory networks (e.g. calcium pathway, PI3K/Akt/mTOR pathway) as being important for the pathophysiology (Cross-Disorder Group of the Psychiatric Genomics Consortium et al., 2013; Fromer et al., 2014; Geschwind and Flint, 2015; Schizophrenia Working Group of the Psychiatric Genomics Consortium, 2014). Common variants associated with psychiatric disorders are often found in regulatory elements (e.g. enhancers), hence, altering the expression level of a gene (Maurano et al., 2012). Having the list of risk loci, it is about time to identify the genes underlying the risk association at a given locus. In patients it is the sum of numerous genetic variations which in the end might perturb brain function leading to the manifestation of psychiatric symptoms. I therefore wondered whether the knockdown of a single putative risk gene per neuron during the screen can be sufficient to generate a measureable phenotype using the E-SARE sensor. Strikingly, multiple genes are amongst the high ranking candidates which have a risk association to psychiatric disorders. Adenylate cyclase 3 (*Adcy3*), the top ranked positive regulator hit in screen A and B (enhanced Z-score rank: 2 and 1, respectively) is suggested to have a genetic association with major depressive disorder (MDD) (Wray et al., 2012). Although *Adcy3* does not yet reach genome-wide significance in GWAS, it is likely to become a significant association with increasing case-control numbers. Several genes linked to schizophrenia, BPD, and/or ASD reduced synaptically-evoked E-SARE induction. These include for example *Disc1*, members of the PI3K/Akt/mTOR pathway (*Akt1*, *mTOR*), components of the metabotropic glutamate receptor 5 complex (*Grm5*, *Aldoa*), the dual-specificity tyrosine-(Y)-phosphorylation-regulated kinase 1 A (*Dyrk1a*), and the actin binding LIM protein 1 (*Ablim1*) (Emamian et al., 2004; 2004; Kim et al., 2009; Kirov et al., 2012; Newell and Matosin, 2014; Nurnberger JI et al., 2014; Sawicka and Zukin, 2012). Notably, knockdown of multiple genes of the complement system (*C4a*, *C4bp*, *C1s*) ranked high as positive regulators. The notion that the classical complement cascade has a role in synapse biology is relatively new (Stephan et al., 2012). For a long time schizophrenia's association

to the MHC locus could not be explained and the identification of the underlying risk gene was a challenge. Only very recently, *C4a* was identified as the main risk gene at the extended MHC locus (Sekar et al., 2016). The pooled RNAi screen supports this finding and the consent between both studies argues that pooled genetic screens might facilitate the identification of risk genes at GWAS loci. With presenilin 1 (*Psen1*), a prominent risk gene for Alzheimer's disease (AD) can be found in the hit lists for positive regulators (Sherrington et al., 1995). *Psen1* encodes one out of four core proteins that form the γ -secretase complex. The γ -secretase complex is involved in the generation of amyloid-beta peptide from amyloid precursor protein (APP), which is believed to be crucial in the pathophysiology of AD (De Strooper, 2007). Other γ -secretase substrates are notch and neuroligin 1 (NRG1). Notch signaling has a known function in neurite outgrowth and the NRG1-ERBB4 pathway is associated to schizophrenia (Berezovska et al., 1999; Stefánsson et al., 2003). How exactly *Psen1* loss-of-function mutations finally contribute to AD, and which substrates are critical, remains uncertain.

6.2.3. Chemokine signaling: Growing evidence for its role in neuronal activity

Chemokine signaling is well known for its versatile function in the haematopoietic/lymphopoietic system in general, and in particular for its role in attracting leukocytes to sites of tissue lesions (Ma et al., 1999; Rossi and Zlotnik, 2000; Szekanecz and Koch, 2001). Approximately 50 chemokines and 20 chemokine receptors are described to date and the receptors are exclusively GPCRs (Bachelier et al., 2014). Chemokine receptors can either be stimulated by a single, specific ligand (e.g. XCR1 and its ligand XCL1), or by multiple different chemokines (e.g. CXCR2 with six ligands, including CXCL2) (Tran and Miller, 2003). Downstream signaling of chemokine receptors can activate various intracellular substrates, such as adenylate cyclases, phospholipases, GTPases as well as the MAPK and PI3-kinase pathways (Balkwill, 1998; Mellado et al., 2001; Neves et al., 2002). Hence, it is conceivable that chemokine-induced activation of these signaling pathways might play a regulatory role in neuronal plasticity, for instance. In the CNS, chemokine signaling has been mainly described in the context of neuroinflammation, which involves the recruitment of chemokine receptor-expressing microglia by chemokine-releasing neurons (de Haas et al., 2007; Ubogu et al., 2006). However, a body of evidence, from studies using various neuronal cell types (e.g. hippocampal, Purkinje, and dopaminergic neurons), suggests that chemokine signaling might modulate neurotransmission and synaptic plasticity (Bertollini et al., 2006; Giovannelli et al., 1998; Guyon et al., 2006; Ragozzino et al., 2002). In this case, chemokine signaling might occur between neurons or as autocrine signaling, which would be a possible scenario within a primary neuron culture during the pooled RNAi screen (de Haas et al., 2007). Amongst other components of

chemokine signaling, the screen has discovered XCR1, a chemokine receptor without a known link to neurons, as a positive regulator of neuronal activity. This finding is supported by replication in screen A and B, using both analysis methods (screen A: enhanced Z-score rank 21, FDR = 1.26e-19; screen B: enhanced Z-score rank 7, FDR = 5.47e-21). XCL1 (also known as lymphotactin) is the unique ligand for XCR1 and studies with calcium indicators in immune cells have revealed that XCR1 stimulation leads to calcium mobilization (Bachem et al., 2010; Yoshida et al., 1998, 1999). Calcium mobilization most likely results from calcium release from the ER by IP3 receptors upon activation of phospholipase C by XCR1-coupled G-proteins. Thus, it might be plausible that XCR1 contributes to calcium signaling during neuronal activity. Nevertheless, it requires additional investigations to validate this finding.

6.2.4. Comparison with the screen by Parnas et al.

Currently the most comprehensive pooled genetic screen has been published by Parnas and colleagues (Parnas et al., 2015). They have used a genome-wide CRISPR-Cas9 knockout library in order to study the response of primary mouse dendritic cells to bacterial LPS. Therefore they sorted the cell pool based on Tnf expression, which is downstream of the LPS/Tlr4 pathway. This allowed them to identify many known regulators of the Tlr4-to-Tnf pathway. In particular, CRISPR-Cas9-mediated knockout screens are believed to improve screen data quality due to higher on-target efficacy and more pronounced phenotypes compared to shRNA-mediated knockdowns (Evers et al., 2016a; Morgens et al., 2016). Although both screens differ in more aspects besides the screening technology (e.g. cell type, phenotype, readout strategy), some quality control parameters might allow a comparison. As a measure of reproducibility Parnas and colleagues present Pearson-correlation coefficients of normalized read counts between two independent screen replicates in the range of 0.45-0.54. Correlation of replicate samples of the pooled RNAi screen presented in this thesis is in all cases above 0.95. The difference probably reflects the different readout strategies and might be evidence for the robustness of a RNA barcode sensor. Both screens were analyzed by Z-score ranking and using the DESeq2 package. Parnas and colleagues describe that 50 out of the top 100 positive regulators overlap between the two analysis strategies. The same comparison was done for screen A in this thesis and 41 common genes could be found in the top 100 hit lists from both rankings (see Figure 19C). Thus, by this parameter both screens do not differ a lot. Worth mentioning is that Parnas and colleagues carried out a secondary screen where they used the same cell number as in the primary screen but infected with a 5-fold smaller sgRNA library, focusing on an extended hit list from the primary screen. This further improved the data quality and seems to be a worthwhile strategy for large-scale screens when cell numbers are limiting as in the case of many primary cell types.

6.3. Limitations of the approach

The power of pooled genetic screens lies in the rapid and straightforward identification of genes that modulate a certain phenotype. A pooled genetic screen is, however, not able to resolve temporal or spatial information. These dimensions can at least to some extent be inferred from additional data sources such as pathway and protein localization databases or need to be determined by additional experiments (Fabregat et al., 2016; Ogata et al., 1998; Sprenger et al., 2008). A second general limitation which is inherent to large-scale screening approaches using shRNA libraries is the wide range of shRNA efficacy. Although shRNA design algorithms have improved over the years, it is still necessary to include multiple shRNAs per gene into the library (Kampmann et al., 2015). In particular, with the limited access to primary cells it is thus always a tradeoff between the number of genes included in a screen and the number of shRNAs per gene. Recent findings argue that on-target efficacy of sgRNAs seems to be higher and more predictable which will be beneficial for the next generation of pooled screens in primary neuron cultures (Evers et al., 2016a; Morgens et al., 2016).

In the case of a pooled RNAi screen using the E-SARE sensor under synaptic stimulation it was expected that the screen is blind for the presynapse/axonal compartment. This is because the main signaling route is from the postsynapse along the dendrites to the cell soma and nucleus and via the axon and the presynapse to a connected neuron. Except for neurotrophin-induced signaling endosomes that translocate long distances from the presynapse to the soma, little is known about presynapse-to-nucleus signaling (Fainzilber et al., 2011). A recent study claims that during neuronal activity signaling from the presynapse to the nucleus might exist as well and that it contributes to the regulation of activity-dependent gene expression (Ivanova et al., 2015). Ivanova and colleagues found that the nuclear and the presynaptic localization of the co-repressor CtBP1 is interconnected and depends on neuronal activity and presynaptic NAD/NADH levels. In all three screens and by both analysis strategies CtBP1 is a hit as a positive regulator, supporting its function during neuronal activity. Which function CtBP1 exactly fulfills during neuronal excitation and whether the long-distance transport between presynapse and nucleus is really necessary for regulation will require further studies. Nevertheless, it might support findings of presynapse-to-nucleus signaling and that components can be identified using the pooled RNAi screen.

6.4. Future aspects of pooled genetic screens in neuroscience

This study expands the existing toolbox in functional genomics (RNAi-, CRISPR-Cas9 screens) by a new readout strategy in which pathway activities are monitored by a barcoded RNA reporter. Compared to previous strategies, pathway monitoring by a barcoded reporter

makes cell sorting dispensable. This broadens the application spectrum and facilitates the screening procedure of cell types with complex morphologies such as primary neurons, where flow cytometry is challenging and unfavorable. The assay has been validated in this proof-of-concept study and is already able to dissect neuronal regulatory networks at so far unprecedented throughput. Screening throughput can still be increased by designing genome-wide next generation libraries. Data quality might be further improved by the adaptation towards a CRISPR-Cas9 screening technology (Evers et al., 2016b). This will in addition provide access to gain-of-function screens (Koneremann et al., 2015). The corresponding AAV vector for this approach has been presented and preliminarily validated in this thesis.

As emphasized earlier, several genes with associations to psychiatric diseases have been identified by the pooled RNAi screen. The majority of common variants in psychiatric patients that have been discovered by GWAS analyses seem to lie in regulatory elements (e.g. enhancers, core promoters) (Maurano et al., 2012). Usually the most proximal gene is reported as a potential risk gene although empirical validation is missing in most cases. Mutations in enhancer and promoter regions can result in up- and down-regulation of the corresponding gene. A complementary screening approach using CRISPR-Cas9-mediated gain-of-function and shRNA- or CRISPR-Cas9-mediated loss-of-function might facilitate and accelerate the empirical identification of risk genes at genome-wide GWAS loci.

6.4.1. Importance for psychiatric drug discovery

The pharmaceutical industry has experienced reduced productivity and increasing costs for first-in-class drug discovery over the last decades (Scannell et al., 2012). Main reasons are high attrition rates for drugs during clinical trials due to lack of efficacy and safety issues. This repression is particularly visible in psychiatric drug discovery where for example most of the current medications for schizophrenia have been discovered decades ago (Agid et al., 2007; Kapur and Mamo, 2003; Papassotiropoulos and de Quervain, 2015). The lack of a primary target in many psychiatric disorders has made target-based drug discovery attempts using biochemical binding assays highly inefficient. In the last years, however, hope is emerging from the progress made with phenotypic screenings (Haggarty et al., 2016; Kaiser and Feng, 2015). Phenotypic screening describes in the best case the testing of compounds using a cellular or even *in vivo* model of the disease, under physiological conditions and with a readout that has translational validity into the clinic (Vincent et al., 2015). The increased biological relevance of the approach is believed to enhance the predictive validity and it expands the biological target space (Scannell and Bosley, 2016). Consequently, the target of a hit compound identified by phenotypic screenings is usually unknown. A recent survey on

how new medications were discovered revealed that between 1999 and 2008 FDA-approved first-in-class drugs mainly originated from phenotypic screenings (Swinney and Anthony, 2011). In the field of CNS diseases 7 out of 9 new molecular entities (NME) came from phenotypic drug discovery and many still do not have an identified target or MoA.

Genetic interference screens (RNAi, CRISPR-Cas9, arrayed or pooled) are already part of the standard repertoire for target identification during drug discovery in oncology, for example (Fennell et al., 2014; Schenone et al., 2013). Thus, the presented assay delivers the missing tool for target identification in phenotypic drug discovery for CNS diseases. As elaborated earlier functional genomics is currently experiencing a transformation from RNAi towards CRISPR-Cas9 knockout screens. However, it should not be forgotten that both screening technologies have their unique properties (Deans et al., 2016). Knockdown of a drug target using shRNAs is expected to phenocopy the inhibitory action of the drug on that target. The incomplete knockdown efficiency of shRNAs, a frequently criticized feature, allows the study of epistatic interactions between shRNA-mediated knockdown and drug-mediated inhibition of a protein. The power of both systems has been recently compared and used for target identification. This study highlighted that shRNA-mediated knockdown is well suited for the identification of essential genes for a given phenotype, whereas CRISPR-Cas9-mediated knockout is advantageous for the discovery of non-essential genes (Deans et al., 2016; Morgens et al., 2016).

7. Abbreviations

AAV	Adeno-associated virus
AD	Alzheimer disease
Adcy	Adenylate cyclase
AMPA	α -amino-3-hydroxy-5-methyl-4-isoxazole propionic acid
ASD	Autism spectrum disorder
BC	Barcode
BDNF	Brain-derived neurotrophic factor
BIC	Bicuculline
BPD	Bipolar disorder
cAMP	3',5'-cyclic adenosine monophosphate
CNS	Central nervous system
CNV	Copy number variation
CRISPR	Clustered regularly interspaced short palindromic repeats
crRNA	CRISPR RNA
DAG	Diacylglycerol
DIV	Day in vitro
E/I	Excitation-inhibition balance
ER	Endoplasmic reticulum
FACS	Fluorescence-activated cell sorting
FBS	Fetal bovine serum
FDR	False discovery rate
GPCR	G-protein coupled receptor
GWAS	Genome-wide association study
HS	Horse serum
IEG	Immediate early gene
IP3	Inositol-1,4,5-trisphosphate
iPSC	Induced pluripotent stem cell
LPS	Lipopolysaccharide
LTP/LTD	Long-term potentiation/depression
MAPK	Mitogen-activated protein kinase
MDD	Major depressive disorder
MoA	Mode of action
MPRA	Massively parallel reporter gene assay
NGS	Next-generation sequencing
NME	New molecular entity
NMDA	<i>N</i> -methyl-D-aspartate
PAM	Proximal adjacent motif

Abbreviations

PGC	Psychiatric Genomics Consortium
PMA	Phorbol-12-myristat-13-acetat
PSD	Post-synaptic density
PV	Parv-albumin
RNAi	RNA interference
sd	Standard deviation
sem	Standard error of the mean
sgRNA	Short guide RNA
shRNA	Short hairpin RNA
siRNA	Small interfering RNA
SV	Structural variant
SV40	Simian virus 40
tracrRNA	Trans-activating crRNA
VGCC	Voltage-gated calcium channel

8. References

- Abbott, L.F., and Regehr, W.G. (2004). Synaptic computation. *Nature* 431, 796–803.
- Adams, J.P., and Dudek, S.M. (2005). Late-phase long-term potentiation: getting to the nucleus. *Nat. Rev. Neurosci.* 6, 737–743.
- Agid, Y., Buzsáki, G., Diamond, D.M., Frackowiak, R., Giedd, J., Girault, J.-A., Grace, A., Lambert, J.J., Manji, H., Mayberg, H., et al. (2007). How can drug discovery for psychiatric disorders be improved? *Nat. Rev. Drug Discov.* 6, 189–201.
- Amtul, Z., and Atta-Ur-Rahman, null (2015). Neural plasticity and memory: molecular mechanism. *Rev. Neurosci.* 26, 253–268.
- Anderl, J.L., Redpath, S., and Ball, A.J. (2009). A neuronal and astrocyte co-culture assay for high content analysis of neurotoxicity. *J. Vis. Exp. JoVE.*
- Arthur, J.S.C., Fong, A.L., Dwyer, J.M., Davare, M., Reese, E., Obrietan, K., and Impey, S. (2004). Mitogen- and stress-activated protein kinase 1 mediates cAMP response element-binding protein phosphorylation and activation by neurotrophins. *J. Neurosci. Off. J. Soc. Neurosci.* 24, 4324–4332.
- Azevedo, F.A.C., Carvalho, L.R.B., Grinberg, L.T., Farfel, J.M., Ferretti, R.E.L., Leite, R.E.P., Jacob Filho, W., Lent, R., and Herculano-Houzel, S. (2009). Equal numbers of neuronal and nonneuronal cells make the human brain an isometrically scaled-up primate brain. *J. Comp. Neurol.* 513, 532–541.
- Bachelierie, F., Ben-Baruch, A., Burkhardt, A.M., Combadiere, C., Farber, J.M., Graham, G.J., Horuk, R., Sparre-Ulrich, A.H., Locati, M., Luster, A.D., et al. (2014). International Union of Basic and Clinical Pharmacology. [corrected]. LXXXIX. Update on the extended family of chemokine receptors and introducing a new nomenclature for atypical chemokine receptors. *Pharmacol. Rev.* 66, 1–79.
- Bachem, A., Güttler, S., Hartung, E., Ebstein, F., Schaefer, M., Tannert, A., Salama, A., Movassaghi, K., Opitz, C., Mages, H.W., et al. (2010). Superior antigen cross-presentation and XCR1 expression define human CD11c+CD141+ cells as homologues of mouse CD8+ dendritic cells. *J. Exp. Med.* 207, 1273–1281.
- Bading, H. (2013). Nuclear calcium signalling in the regulation of brain function. *Nat. Rev. Neurosci.* 14, 593–608.
- Bading, H., Hardingham, G.E., Johnson, C.M., and Chawla, S. (1997). Gene regulation by nuclear and cytoplasmic calcium signals. *Biochem. Biophys. Res. Commun.* 236, 541–543.
- Baj, G., Patrizio, A., Montalbano, A., Sciancalepore, M., and Tongiorgi, E. (2014). Developmental and maintenance defects in Rett syndrome neurons identified by a new mouse staging system in vitro. *Front. Cell. Neurosci.* 8, 18.
- Balkwill, F. (1998). The molecular and cellular biology of the chemokines. *J. Viral Hepat.* 5, 1–14.
- Barco, A., Patterson, S.L., Patterson, S., Alarcon, J.M., Gromova, P., Mata-Roig, M., Morozov, A., and Kandel, E.R. (2005). Gene expression profiling of facilitated L-LTP in VP16-CREB mice reveals that BDNF is critical for the maintenance of LTP and its synaptic capture. *Neuron* 48, 123–137.

References

- Bartos, M., Vida, I., and Jonas, P. (2007). Synaptic mechanisms of synchronized gamma oscillations in inhibitory interneuron networks. *Nat. Rev. Neurosci.* *8*, 45–56.
- Bassett, A.S., Marshall, C.R., Lionel, A.C., Chow, E.W.C., and Scherer, S.W. (2008). Copy number variations and risk for schizophrenia in 22q11.2 deletion syndrome. *Hum. Mol. Genet.* *17*, 4045–4053.
- Bassik, M.C., Lebbink, R.J., Churchman, L.S., Ingolia, N.T., Patena, W., LeProust, E.M., Schuldiner, M., Weissman, J.S., and McManus, M.T. (2009). Rapid Creation and Quantitative Monitoring of High Coverage shRNA Libraries. *Nat. Methods* *6*, 443–445.
- Bassik, M.C., Kampmann, M., Lebbink, R.J., Wang, S., Hein, M.Y., Poser, I., Weibezahn, J., Horlbeck, M.A., Chen, S., Mann, M., et al. (2013). A systematic mammalian genetic interaction map reveals pathways underlying ricin susceptibility. *Cell* *152*, 909–922.
- Bayés, A., van de Lagemaat, L.N., Collins, M.O., Croning, M.D.R., Whittle, I.R., Choudhary, J.S., and Grant, S.G.N. (2011). Characterization of the proteome, diseases and evolution of the human postsynaptic density. *Nat. Neurosci.* *14*, 19–21.
- Bengtson, C.P., Freitag, H.E., Weislogel, J.-M., and Bading, H. (2010). Nuclear calcium sensors reveal that repetition of trains of synaptic stimuli boosts nuclear calcium signaling in CA1 pyramidal neurons. *Biophys. J.* *99*, 4066–4077.
- Benjamini, Y., and Hochberg, Y. (1995). Controlling the False Discovery Rate: A Practical and Powerful Approach to Multiple Testing. *J. R. Stat. Soc. Ser. B Methodol.* *57*, 289–300.
- Benke, T.A., Lüthi, A., Isaac, J.T., and Collingridge, G.L. (1998). Modulation of AMPA receptor unitary conductance by synaptic activity. *Nature* *393*, 793–797.
- Berezovska, O., McLean, P., Knowles, R., Frosh, M., Lu, F.M., Lux, S.E., and Hyman, B.T. (1999). Notch1 inhibits neurite outgrowth in postmitotic primary neurons. *Neuroscience* *93*, 433–439.
- Berridge, M.J. (1998). Neuronal calcium signaling. *Neuron* *21*, 13–26.
- Bertollini, C., Ragozzino, D., Gross, C., Limatola, C., and Eusebi, F. (2006). Fractalkine/CX3CL1 depresses central synaptic transmission in mouse hippocampal slices. *Neuropharmacology* *51*, 816–821.
- Birmingham, A., Selfors, L.M., Forster, T., Wrobel, D., Kennedy, C.J., Shanks, E., Santoyo-Lopez, J., Dunican, D.J., Long, A., Kelleher, D., et al. (2009). Statistical Methods for Analysis of High-Throughput RNA Interference Screens. *Nat. Methods* *6*, 569–575.
- Black, J.E., Kodish, I.M., Grossman, A.W., Klintsova, A.Y., Orlovskaya, D., Vostrikov, V., Uranova, N., and Greenough, W.T. (2004). Pathology of layer V pyramidal neurons in the prefrontal cortex of patients with schizophrenia. *Am. J. Psychiatry* *161*, 742–744.
- Borchert, G.M., Lanier, W., and Davidson, B.L. (2006). RNA polymerase III transcribes human microRNAs. *Nat. Struct. Mol. Biol.* *13*, 1097–1101.
- Botvinnik, A., Wichert, S.P., Fischer, T.M., and Rossner, M.J. (2010). Integrated analysis of receptor activation and downstream signaling with EXTassays. *Nat Meth* *7*, 74–80.
- Bouard, D., Alazard-Dany, N., and Cosset, F.-L. (2009). Viral vectors: from virology to transgene expression. *Br. J. Pharmacol.* *157*, 153–165.

References

- Boutros, M., Heigwer, F., and Laufer, C. (2015). Microscopy-Based High-Content Screening. *Cell* 163, 1314–1325.
- Brami-Cherrier, K., Lavaur, J., Pagès, C., Arthur, J.S.C., and Caboche, J. (2007). Glutamate induces histone H3 phosphorylation but not acetylation in striatal neurons: role of mitogen- and stress-activated kinase-1. *J. Neurochem.* 101, 697–708.
- Brennand, K.J., Simone, A., Jou, J., Gelboin-Burkhart, C., Tran, N., Sangar, S., Li, Y., Mu, Y., Chen, G., Yu, D., et al. (2011). Modelling schizophrenia using human induced pluripotent stem cells. *Nature* 473, 221–225.
- Brincat, S.L., and Miller, E.K. (2015). Frequency-specific hippocampal-prefrontal interactions during associative learning. *Nat. Neurosci.* 18, 576–581.
- Bullmore, E., and Sporns, O. (2009). Complex brain networks: graph theoretical analysis of structural and functional systems. *Nat. Rev. Neurosci.* 10, 186–198.
- Caicedo, J.C., Singh, S., and Carpenter, A.E. (2016). Applications in image-based profiling of perturbations. *Curr. Opin. Biotechnol.* 39, 134–142.
- Campbell, F.E., and Setzer, D.R. (1992). Transcription termination by RNA polymerase III: uncoupling of polymerase release from termination signal recognition. *Mol. Cell. Biol.* 12, 2260–2272.
- Carthew, R.W., and Sontheimer, E.J. (2009). Origins and Mechanisms of miRNAs and siRNAs. *Cell* 136, 642–655.
- Charles A Janeway, J., Travers, P., Walport, M., and Shlomchik, M.J. (2001). The major histocompatibility complex and its functions.
- Chawla, S. (2002). Regulation of gene expression by Ca²⁺ signals in neuronal cells. *Eur. J. Pharmacol.* 447, 131–140.
- Chawla, S., Hardingham, G.E., Quinn, D.R., and Bading, H. (1998). CBP: a signal-regulated transcriptional coactivator controlled by nuclear calcium and CaM kinase IV. *Science* 281, 1505–1509.
- Chendrimada, T.P., Gregory, R.I., Kumaraswamy, E., Norman, J., Cooch, N., Nishikura, K., and Shiekhattar, R. (2005). TRBP recruits the Dicer complex to Ago2 for microRNA processing and gene silencing. *Nature* 436, 740–744.
- Chowdhury, S., Shepherd, J.D., Okuno, H., Lyford, G., Petralia, R.S., Plath, N., Kuhl, D., Huganir, R.L., and Worley, P.F. (2006). Arc/Arg3.1 interacts with the endocytic machinery to regulate AMPA receptor trafficking. *Neuron* 52, 445–459.
- Citri, A., and Malenka, R.C. (2008). Synaptic plasticity: multiple forms, functions, and mechanisms. *Neuropsychopharmacol. Off. Publ. Am. Coll. Neuropsychopharmacol.* 33, 18–41.
- Collins, S.R., Weissman, J.S., and Krogan, N.J. (2009). From information to knowledge: new technologies for defining gene function. *Nat. Methods* 6, 721–723.
- Cross-Disorder Group of the Psychiatric Genomics Consortium, Lee, S.H., Ripke, S., Neale, B.M., Faraone, S.V., Purcell, S.M., Perlis, R.H., Mowry, B.J., Thapar, A., Goddard, M.E., et al. (2013). Genetic relationship between five psychiatric disorders estimated from genome-wide SNPs. *Nat. Genet.* 45, 984–994.

References

- Curtis, D.R., Duggan, A.W., Felix, D., and Johnston, G.A. (1970). GABA, bicuculline and central inhibition. *Nature* 226, 1222–1224.
- Dai, Z., Sheridan, J.M., Gearing, L.J., Moore, D.L., Su, S., Wormald, S., Wilcox, S., O'Connor, L., Dickins, R.A., Blewitt, M.E., et al. (2014). edgeR: a versatile tool for the analysis of shRNA-seq and CRISPR-Cas9 genetic screens. *F1000Research* 3, 95.
- Darnell, J.C., Van Driesche, S.J., Zhang, C., Hung, K.Y.S., Mele, A., Fraser, C.E., Stone, E.F., Chen, C., Fak, J.J., Chi, S.W., et al. (2011). FMRP Stalls Ribosomal Translocation on mRNAs Linked to Synaptic Function and Autism. *Cell* 146, 247–261.
- Das, G., Henning, D., Wright, D., and Reddy, R. (1988). Upstream regulatory elements are necessary and sufficient for transcription of a U6 RNA gene by RNA polymerase III. *EMBO J.* 7, 503–512.
- Deans, R.M., Morgens, D.W., Ökesli, A., Pillay, S., Horlbeck, M.A., Kampmann, M., Gilbert, L.A., Li, A., Mateo, R., Smith, M., et al. (2016). Parallel shRNA and CRISPR-Cas9 screens enable antiviral drug target identification. *Nat. Chem. Biol.* 12, 361–366.
- De Strooper, B. (2007). Loss-of-function presenilin mutations in Alzheimer disease. *Talking Point on the role of presenilin mutations in Alzheimer disease. EMBO Rep.* 8, 141–146.
- Deltcheva, E., Chylinski, K., Sharma, C.M., Gonzales, K., Chao, Y., Pirzada, Z.A., Eckert, M.R., Vogel, J., and Charpentier, E. (2011). CRISPR RNA maturation by trans-encoded small RNA and host factor RNase III. *Nature* 471, 602–607.
- Diehl, P., Tedesco, D., and Chenchik, A. (2014). Use of RNAi screens to uncover resistance mechanisms in cancer cells and identify synthetic lethal interactions. *Drug Discov. Today Technol.* 11, 11–18.
- Dimos, J.T., Rodolfa, K.T., Niakan, K.K., Weisenthal, L.M., Mitsumoto, H., Chung, W., Croft, G.F., Saphier, G., Leibel, R., Goland, R., et al. (2008). Induced pluripotent stem cells generated from patients with ALS can be differentiated into motor neurons. *Science* 321, 1218–1221.
- Dobrunz, L.E., and Stevens, C.F. (1997). Heterogeneity of release probability, facilitation, and depletion at central synapses. *Neuron* 18, 995–1008.
- Dolmetsch, R. (2003). Excitation-transcription coupling: signaling by ion channels to the nucleus. *Sci. STKE Signal Transduct. Knowl. Environ.* 2003, PE4.
- Dolmetsch, R.E., Pajvani, U., Fife, K., Spotts, J.M., and Greenberg, M.E. (2001). Signaling to the nucleus by an L-type calcium channel-calmodulin complex through the MAP kinase pathway. *Science* 294, 333–339.
- Ebert, D.H., and Greenberg, M.E. (2013). Activity-dependent neuronal signalling and autism spectrum disorder. *Nature* 493, 327–337.
- Ebinu, J.O., Bottorff, D.A., Chan, E.Y., Stang, S.L., Dunn, R.J., and Stone, J.C. (1998). RasGRP, a Ras guanyl nucleotide- releasing protein with calcium- and diacylglycerol-binding motifs. *Science* 280, 1082–1086.
- Emamian, E.S., Hall, D., Birnbaum, M.J., Karayiorgou, M., and Gogos, J.A. (2004). Convergent evidence for impaired AKT1-GSK3beta signaling in schizophrenia. *Nat. Genet.* 36, 131–137.

References

- Engelman, H.S., and MacDermott, A.B. (2004). Presynaptic ionotropic receptors and control of transmitter release. *Nat. Rev. Neurosci.* *5*, 135–145.
- Evers, B., Jastrzebski, K., Heijmans, J.P.M., Grenrum, W., Beijersbergen, R.L., and Bernards, R. (2016a). CRISPR knockout screening outperforms shRNA and CRISPRi in identifying essential genes. *Nat. Biotechnol.*
- Evers, B., Jastrzebski, K., Heijmans, J.P.M., Grenrum, W., Beijersbergen, R.L., and Bernards, R. (2016b). CRISPR knockout screening outperforms shRNA and CRISPRi in identifying essential genes. *Nat. Biotechnol.*
- Fabregat, A., Sidiropoulos, K., Garapati, P., Gillespie, M., Hausmann, K., Haw, R., Jassal, B., Jupe, S., Korninger, F., McKay, S., et al. (2016). The Reactome pathway Knowledgebase. *Nucleic Acids Res.* *44*, D481-487.
- Fainzilber, M., Budnik, V., Segal, R.A., and Kreutz, M.R. (2011). From synapse to nucleus and back again—communication over distance within neurons. *J. Neurosci. Off. J. Soc. Neurosci.* *31*, 16045–16048.
- Farnsworth, C.L., Freshney, N.W., Rosen, L.B., Ghosh, A., Greenberg, M.E., and Feig, L.A. (1995). Calcium activation of Ras mediated by neuronal exchange factor Ras-GRF. *Nature* *376*, 524–527.
- Farr, C.D., Gafken, P.R., Norbeck, A.D., Doneanu, C.E., Stapels, M.D., Barofsky, D.F., Minami, M., and Saugstad, J.A. (2004). Proteomic analysis of native metabotropic glutamate receptor 5 protein complexes reveals novel molecular constituents. *J. Neurochem.* *91*, 438–450.
- Fatt, P., and Katz, B. (1953). The electrical properties of crustacean muscle fibres. *J. Physiol.* *120*, 171–204.
- Fennell, M., Xiang, Q., Hwang, A., Chen, C., Huang, C.-H., Chen, C.-C., Pelosof, R., and Garippa, R.J. (2014). Impact of RNA-guided technologies for target identification and deconvolution. *J. Biomol. Screen.* *19*, 1327–1337.
- Filipowicz, W., Bhattacharyya, S.N., and Sonenberg, N. (2008). Mechanisms of post-transcriptional regulation by microRNAs: are the answers in sight? *Nat. Rev. Genet.* *9*, 102–114.
- Fire, A., Xu, S., Montgomery, M.K., Kostas, S.A., Driver, S.E., and Mello, C.C. (1998). Potent and specific genetic interference by double-stranded RNA in *Caenorhabditis elegans*. *Nature* *391*, 806–811.
- Flavell, S.W., Cowan, C.W., Kim, T.-K., Greer, P.L., Lin, Y., Paradis, S., Griffith, E.C., Hu, L.S., Chen, C., and Greenberg, M.E. (2006). Activity-dependent regulation of MEF2 transcription factors suppresses excitatory synapse number. *Science* *311*, 1008–1012.
- Forrest, M.D. (2014). The sodium-potassium pump is an information processing element in brain computation. *Front. Physiol.* *5*, 472.
- Frank, F., Sonenberg, N., and Nagar, B. (2010). Structural basis for 5'-nucleotide base-specific recognition of guide RNA by human AGO2. *Nature* *465*, 818–822.
- Franke, B., Stein, J.L., Ripke, S., Anttila, V., Hibar, D.P., van Hulzen, K.J.E., Arias-Vasquez, A., Smoller, J.W., Nichols, T.E., Neale, M.C., et al. (2016). Genetic influences on schizophrenia and subcortical brain volumes: large-scale proof of concept. *Nat. Neurosci.* *19*, 420–431.

References

- Freedman, L.P., Cockburn, I.M., and Simcoe, T.S. (2015). The Economics of Reproducibility in Preclinical Research. *PLoS Biol.* 13, e1002165.
- Fromer, M., Pocklington, A.J., Kavanagh, D.H., Williams, H.J., Dwyer, S., Gormley, P., Georgieva, L., Rees, E., Palta, P., Ruderfer, D.M., et al. (2014). De novo mutations in schizophrenia implicate synaptic networks. *Nature* 506, 179–184.
- Garner, A.R., Rowland, D.C., Hwang, S.Y., Baumgaertel, K., Roth, B.L., Kentros, C., and Mayford, M. (2012). Generation of a synthetic memory trace. *Science* 335, 1513–1516.
- Geschwind, D.H., and Flint, J. (2015). Genetics and genomics of psychiatric disease. *Science* 349, 1489–1494.
- Giaever, G., Shoemaker, D.D., Jones, T.W., Liang, H., Winzeler, E.A., Astromoff, A., and Davis, R.W. (1999). Genomic profiling of drug sensitivities via induced haploinsufficiency. *Nat Genet* 21, 278–283.
- Giaever, G., Chu, A.M., Ni, L., Connelly, C., Riles, L., Veronneau, S., Dow, S., Lucau-Danila, A., Anderson, K., Andre, B., et al. (2002). Functional profiling of the *Saccharomyces cerevisiae* genome. *Nature* 418, 387–391.
- Gilbert, L.A., Horlbeck, M.A., Adamson, B., Villalta, J.E., Chen, Y., Whitehead, E.H., Guimaraes, C., Panning, B., Ploegh, H.L., Bassik, M.C., et al. (2014). Genome-Scale CRISPR-Mediated Control of Gene Repression and Activation. *Cell*.
- Gille, H., Kortenjann, M., Thomae, O., Moomaw, C., Slaughter, C., Cobb, M.H., and Shaw, P.E. (1995). ERK phosphorylation potentiates Elk-1-mediated ternary complex formation and transactivation. *EMBO J.* 14, 951–962.
- Giovannelli, A., Limatola, C., Ragozzino, D., Mileo, A.M., Ruggieri, A., Ciotti, M.T., Mercanti, D., Santoni, A., and Eusebi, F. (1998). CXC chemokines interleukin-8 (IL-8) and growth-related gene product alpha (GROalpha) modulate Purkinje neuron activity in mouse cerebellum. *J. Neuroimmunol.* 92, 122–132.
- Grant, S.G.N. (2012). Synaptopathies: diseases of the synaptome. *Curr. Opin. Neurobiol.* 22, 522–529.
- Greenberg, M.E., Greene, L.A., and Ziff, E.B. (1985). Nerve growth factor and epidermal growth factor induce rapid transient changes in proto-oncogene transcription in PC12 cells. *J. Biol. Chem.* 260, 14101–14110.
- Greer, P.L., and Greenberg, M.E. (2008). From synapse to nucleus: calcium-dependent gene transcription in the control of synapse development and function. *Neuron* 59, 846–860.
- Gregory, R.I., Chendrimada, T.P., Cooch, N., and Shiekhattar, R. (2005). Human RISC Couples MicroRNA Biogenesis and Posttranscriptional Gene Silencing. *Cell* 123, 631–640.
- Gu, X.Q., Yao, H., and Haddad, G.G. (2001). Increased neuronal excitability and seizures in the Na(+)/H(+) exchanger null mutant mouse. *Am. J. Physiol. Cell Physiol.* 281, C496-503.
- Guidotti, A., Auta, J., Davis, J.M., Di-Giorgi-Gerevini, V., Dwivedi, Y., Grayson, D.R., Impagnatiello, F., Pandey, G., Pesold, C., Sharma, R., et al. (2000). Decrease in reelin and glutamic acid decarboxylase67 (GAD67) expression in schizophrenia and bipolar disorder: a postmortem brain study. *Arch. Gen. Psychiatry* 57, 1061–1069.

References

- Guyon, A., Skrzydelsi, D., Rovère, C., Rostène, W., Parsadaniantz, S.M., and Nahon, J.L. (2006). Stromal cell-derived factor-1 α modulation of the excitability of rat substantia nigra dopaminergic neurones: presynaptic mechanisms. *J. Neurochem.* 96, 1540–1550.
- de Haas, A.H., van Weering, H.R.J., de Jong, E.K., Boddeke, H.W.G.M., and Biber, K.P.H. (2007). Neuronal Chemokines: Versatile Messengers In Central Nervous System Cell Interaction. *Mol. Neurobiol.* 36, 137–151.
- Habela, C.W., Song, H., and Ming, G.-L. (2016). Modeling synaptogenesis in schizophrenia and autism using human iPSC derived neurons. *Mol. Cell. Neurosci.* 73, 52–62.
- Haenschel, C., Bittner, R.A., Waltz, J., Haertling, F., Wibrall, M., Singer, W., Linden, D.E.J., and Rodriguez, E. (2009). Cortical oscillatory activity is critical for working memory as revealed by deficits in early-onset schizophrenia. *J. Neurosci. Off. J. Soc. Neurosci.* 29, 9481–9489.
- Haggarty, S.J., Silva, M.C., Cross, A., Brandon, N.J., and Perlis, R.H. (2016). Advancing drug discovery for neuropsychiatric disorders using patient-specific stem cell models. *Mol. Cell. Neurosci.*
- Hardingham, G.E., Chawla, S., Johnson, C.M., and Bading, H. (1997). Distinct functions of nuclear and cytoplasmic calcium in the control of gene expression. *Nature* 385, 260–265.
- Hardingham, G.E., Arnold, F.J., and Bading, H. (2001). A calcium microdomain near NMDA receptors: on switch for ERK-dependent synapse-to-nucleus communication. *Nat. Neurosci.* 4, 565–566.
- Harrill, J.A., Robinette, B.L., and Mundy, W.R. (2011). Use of high content image analysis to detect chemical-induced changes in synaptogenesis in vitro. *Toxicol. Vitro Int. J. Publ. Assoc. BIBRA* 25, 368–387.
- Hartman, J.J., Mahr, J., McNally, K., Okawa, K., Iwamatsu, A., Thomas, S., Cheesman, S., Heuser, J., Vale, R.D., and McNally, F.J. (1998). Katanin, a microtubule-severing protein, is a novel AAA ATPase that targets to the centrosome using a WD40-containing subunit. *Cell* 93, 277–287.
- Henley, J.M., and Wilkinson, K.A. (2016). Synaptic AMPA receptor composition in development, plasticity and disease. *Nat. Rev. Neurosci.*
- Hensch, T.K. (2005). Critical period plasticity in local cortical circuits. *Nat. Rev. Neurosci.* 6, 877–888.
- Hensel, M., Shea, J., Gleeson, C., Jones, M., Dalton, E., and Holden, D. (1995). Simultaneous identification of bacterial virulence genes by negative selection. *Science* 269, 400–403.
- Homayoun, H., and Moghaddam, B. (2007a). Fine-tuning of awake prefrontal cortex neurons by clozapine: comparison with haloperidol and N-desmethylclozapine. *Biol. Psychiatry* 61, 679–687.
- Homayoun, H., and Moghaddam, B. (2007b). NMDA receptor hypofunction produces opposite effects on prefrontal cortex interneurons and pyramidal neurons. *J. Neurosci. Off. J. Soc. Neurosci.* 27, 11496–11500.
- Hong, L.E., Summerfelt, A., Buchanan, R.W., O'Donnell, P., Thaker, G.K., Weiler, M.A., and Lahti, A.C. (2010). Gamma and delta neural oscillations and association with clinical

References

- symptoms under subanesthetic ketamine. *Neuropsychopharmacol. Off. Publ. Am. Coll. Neuropsychopharmacol.* **35**, 632–640.
- Hsu, P.D., Lander, E.S., and Zhang, F. (2014). Development and Applications of CRISPR-Cas9 for Genome Engineering. *Cell* **157**, 1262–1278.
- Hunsberger, J.G., Efthymiou, A.G., Malik, N., Behl, M., Mead, I.L., Zeng, X., Simeonov, A., and Rao, M. (2015). Induced Pluripotent Stem Cell Models to Enable In Vitro Models for Screening in the Central Nervous System. *Stem Cells Dev.* **24**, 1852–1864.
- Igarashi, K.M. (2015). Plasticity in oscillatory coupling between hippocampus and cortex. *Curr. Opin. Neurobiol.* **35**, 163–168.
- Impey, S., Fong, A.L., Wang, Y., Cardinaux, J.R., Fass, D.M., Obrietan, K., Wayman, G.A., Storm, D.R., Soderling, T.R., and Goodman, R.H. (2002). Phosphorylation of CBP mediates transcriptional activation by neural activity and CaM kinase IV. *Neuron* **34**, 235–244.
- Ivanova, D., Dirks, A., Montenegro-Venegas, C., Schöne, C., Altmann, W.D., Marini, C., Frischknecht, R., Schanze, D., Zenker, M., Gundelfinger, E.D., et al. (2015). Synaptic activity controls localization and function of CtBP1 via binding to Bassoon and Piccolo. *EMBO J.* **34**, 1056–1077.
- Jaffe, D.B., and Brown, T.H. (1994). Metabotropic glutamate receptor activation induces calcium waves within hippocampal dendrites. *J. Neurophysiol.* **72**, 471–474.
- Jeyabalan, N., and Clement, J.P. (2016). SYNGAP1: Mind the Gap. *Front. Cell. Neurosci.* **10**, 32.
- Jinek, M., Chylinski, K., Fonfara, I., Hauer, M., Doudna, J.A., and Charpentier, E. (2012). A programmable dual-RNA-guided DNA endonuclease in adaptive bacterial immunity. *Science* **337**, 816–821.
- Jinek, M., East, A., Cheng, A., Lin, S., Ma, E., and Doudna, J. (2013). RNA-programmed genome editing in human cells. *eLife* **2**, e00471.
- Kaiser, T., and Feng, G. (2015). Modeling psychiatric disorders for developing effective treatments. *Nat. Med.* **21**, 979–988.
- Kampmann, M., Horlbeck, M.A., Chen, Y., Tsai, J.C., Bassik, M.C., Gilbert, L.A., Villalta, J.E., Kwon, S.C., Chang, H., Kim, V.N., et al. (2015). Next-generation libraries for robust RNA interference-based genome-wide screens. *Proc. Natl. Acad. Sci. U. S. A.* **112**, E3384–E3391.
- Kandel, E.R. (2001). The Molecular Biology of Memory Storage: A Dialogue Between Genes and Synapses. *Science* **294**, 1030–1038.
- Kapur, S., and Mamo, D. (2003). Half a century of antipsychotics and still a central role for dopamine D2 receptors. *Prog. Neuropsychopharmacol. Biol. Psychiatry* **27**, 1081–1090.
- Karayorgou, M., Simon, T.J., and Gogos, J.A. (2010). 22q11.2 microdeletions: linking DNA structural variation to brain dysfunction and schizophrenia. *Nat. Rev. Neurosci.* **11**, 402–416.
- Kawashima, T., Okuno, H., Nonaka, M., Adachi-Morishima, A., Kyo, N., Okamura, M., Takemoto-Kimura, S., Worley, P.F., and Bito, H. (2009). Synaptic activity-responsive element in the Arc/Arg3.1 promoter essential for synapse-to-nucleus signaling in activated neurons. *Proc. Natl. Acad. Sci. U. S. A.* **106**, 316–321.

References

- Kawashima, T., Kitamura, K., Suzuki, K., Nonaka, M., Kamijo, S., Takemoto-Kimura, S., Kano, M., Okuno, H., Ohki, K., and Bito, H. (2013). Functional labeling of neurons and their projections using the synthetic activity-dependent promoter E-SARE. *Nat. Methods* 10, 889–895.
- Khvorova, A., Reynolds, A., and Jayasena, S.D. (2003). Functional siRNAs and miRNAs exhibit strand bias. *Cell* 115, 209–216.
- Kim, J.Y., Duan, X., Liu, C.Y., Jang, M.-H., Guo, J.U., Pow-anpongkul, N., Kang, E., Song, H., and Ming, G. (2009). DISC1 regulates new neuron development in the adult brain via modulation of AKT-mTOR signaling through KIAA1212. *Neuron* 63, 761–773.
- Kim, M.J., Dunah, A.W., Wang, Y.T., and Sheng, M. (2005). Differential roles of NR2A- and NR2B-containing NMDA receptors in Ras-ERK signaling and AMPA receptor trafficking. *Neuron* 46, 745–760.
- Kim, T.-K., Hemberg, M., Gray, J.M., Costa, A.M., Bear, D.M., Wu, J., Harmin, D.A., Laptewicz, M., Barbara-Haley, K., Kuersten, S., et al. (2010). Widespread transcription at neuronal activity-regulated enhancers. *Nature* 465, 182–187.
- Kirov, G., Pocklington, A.J., Holmans, P., Ivanov, D., Ikeda, M., Ruderfer, D., Moran, J., Chambert, K., Toncheva, D., Georgieva, L., et al. (2012). De novo CNV analysis implicates specific abnormalities of postsynaptic signalling complexes in the pathogenesis of schizophrenia. *Mol. Psychiatry* 17, 142–153.
- Kolomeets, N.S., Orlovskaya, D.D., Rachmanova, V.I., and Uranova, N.A. (2005). Ultrastructural alterations in hippocampal mossy fiber synapses in schizophrenia: a postmortem morphometric study. *Synap. N. Y. N* 57, 47–55.
- Kombian, S.B., Mougnot, D., and Pittman, Q.J. (1997). Dendritically released peptides act as retrograde modulators of afferent excitation in the supraoptic nucleus in vitro. *Neuron* 19, 903–912.
- Konermann, S., Brigham, M.D., Trevino, A.E., Joung, J., Abudayyeh, O.O., Barcena, C., Hsu, P.D., Habib, N., Gootenberg, J.S., Nishimasu, H., et al. (2015). Genome-scale transcriptional activation by an engineered CRISPR-Cas9 complex. *Nature* 517, 583–588.
- Krey, J.F., Paşca, S.P., Shcheglovitov, A., Yazawa, M., Schwemberger, R., Rasmusson, R., and Dolmetsch, R.E. (2013). Timothy syndrome is associated with activity-dependent dendritic retraction in rodent and human neurons. *Nat. Neurosci.* 16, 201–209.
- Kuwajima, G., Futatsugi, A., Niinobe, M., Nakanishi, S., and Mikoshiba, K. (1992). Two types of ryanodine receptors in mouse brain: skeletal muscle type exclusively in Purkinje cells and cardiac muscle type in various neurons. *Neuron* 9, 1133–1142.
- Larson, M.H., Gilbert, L.A., Wang, X., Lim, W.A., Weissman, J.S., and Qi, L.S. (2013). CRISPR interference (CRISPRi) for sequence-specific control of gene expression. *Nat. Protoc.* 8, 2180–2196.
- Lee, Y., Ahn, C., Han, J., Choi, H., Kim, J., Yim, J., Lee, J., Provost, P., Rådmark, O., Kim, S., et al. (2003). The nuclear RNase III Drosha initiates microRNA processing. *Nature* 425, 415–419.
- Lee, Y., Kim, M., Han, J., Yeom, K.-H., Lee, S., Baek, S.H., and Kim, V.N. (2004). MicroRNA genes are transcribed by RNA polymerase II. *EMBO J.* 23, 4051–4060.

References

- Leenay, R.T., Maksimchuk, K.R., Slotkowski, R.A., Agrawal, R.N., Gomaa, A.A., Briner, A.E., Barrangou, R., and Beisel, C.L. (2016). Identifying and Visualizing Functional PAM Diversity across CRISPR-Cas Systems. *Mol. Cell* 62, 137–147.
- Levinson, D.F., Duan, J., Oh, S., Wang, K., Sanders, A.R., Shi, J., Zhang, N., Mowry, B.J., Olincy, A., Amin, F., et al. (2011). Copy number variants in schizophrenia: confirmation of five previous findings and new evidence for 3q29 microdeletions and VIPR2 duplications. *Am. J. Psychiatry* 168, 302–316.
- Levitt, N., Briggs, D., Gil, A., and Proudfoot, N.J. (1989). Definition of an efficient synthetic poly(A) site. *Genes Dev.* 3, 1019–1025.
- Li, B., Tadross, M.R., and Tsien, R.W. (2016). Sequential ionic and conformational signaling by calcium channels drives neuronal gene expression. *Science* 351, 863–867.
- Li, L., Lin, X., Khvorova, A., Fesik, S.W., and Shen, Y. (2007). Defining the optimal parameters for hairpin-based knockdown constructs. *RNA N. Y. N* 13, 1765–1774.
- Liu, B., Xu, H., Paton, J.F.R., and Kasparov, S. (2010). Cell- and region-specific miR30-based gene knock-down with temporal control in the rat brain. *BMC Mol. Biol.* 11, 93.
- Llinás, R., Steinberg, I.Z., and Walton, K. (1976). Presynaptic calcium currents and their relation to synaptic transmission: voltage clamp study in squid giant synapse and theoretical model for the calcium gate. *Proc. Natl. Acad. Sci. U. S. A.* 73, 2918–2922.
- Love, M.I., Huber, W., and Anders, S. (2014). Moderated estimation of fold change and dispersion for RNA-seq data with DESeq2. *Genome Biol.* 15, 550.
- Luo, J., Emanuele, M.J., Li, D., Creighton, C.J., Schlabach, M.R., Westbrook, T.F., Wong, K.-K., and Elledge, S.J. (2009). A Genome-wide RNAi Screen Identifies Multiple Synthetic Lethal Interactions with the Ras Oncogene. *Cell* 137, 835–848.
- Lüscher, C., and Malenka, R.C. (2012). NMDA receptor-dependent long-term potentiation and long-term depression (LTP/LTD). *Cold Spring Harb. Perspect. Biol.* 4.
- Ma, H., Groth, R.D., Cohen, S.M., Emery, J.F., Li, B., Hoedt, E., Zhang, G., Neubert, T.A., and Tsien, R.W. (2014). γ CaMKII shuttles Ca^{2+} /CaM to the nucleus to trigger CREB phosphorylation and gene expression. *Cell* 159, 281–294.
- Ma, Q., Jones, D., and Springer, T.A. (1999). The chemokine receptor CXCR4 is required for the retention of B lineage and granulocytic precursors within the bone marrow microenvironment. *Immunity* 10, 463–471.
- Maier, R., Moser, G., Chen, G.-B., Ripke, S., Cross-Disorder Working Group of the Psychiatric Genomics Consortium, Coryell, W., Potash, J.B., Scheftner, W.A., Shi, J., Weissman, M.M., et al. (2015). Joint analysis of psychiatric disorders increases accuracy of risk prediction for schizophrenia, bipolar disorder, and major depressive disorder. *Am. J. Hum. Genet.* 96, 283–294.
- Malenka, R.C., and Nicoll, R.A. (1993). NMDA-receptor-dependent synaptic plasticity: multiple forms and mechanisms. *Trends Neurosci.* 16, 521–527.
- Malik, A.N., Vierbuchen, T., Hemberg, M., Rubin, A.A., Ling, E., Couch, C.H., Stroud, H., Spiegel, I., Farh, K.K.-H., Harmin, D.A., et al. (2014). Genome-wide identification and characterization of functional neuronal activity-dependent enhancers. *Nat. Neurosci.* 17, 1330–1339.

References

- Marín, O. (2012). Interneuron dysfunction in psychiatric disorders. *Nat. Rev. Neurosci.* *13*, 107–120.
- Martin, S.J., Grimwood, P.D., and Morris, R.G. (2000). Synaptic plasticity and memory: an evaluation of the hypothesis. *Annu. Rev. Neurosci.* *23*, 649–711.
- Maurano, M.T., Humbert, R., Rynes, E., Thurman, R.E., Haugen, E., Wang, H., Reynolds, A.P., Sandstrom, R., Qu, H., Brody, J., et al. (2012). Systematic localization of common disease-associated variation in regulatory DNA. *Science* *337*, 1190–1195.
- Mayer, M.L., Westbrook, G.L., and Guthrie, P.B. (1984). Voltage-dependent block by Mg²⁺ of NMDA responses in spinal cord neurones. *Nature* *309*, 261–263.
- Mayr, B., and Montminy, M. (2001). Transcriptional regulation by the phosphorylation-dependent factor CREB. *Nat. Rev. Mol. Cell Biol.* *2*, 599–609.
- McBurney, R.N., and Neering, I.R. (1987). Neuronal calcium homeostasis. *Trends Neurosci.* *10*, 164–169.
- McClure, C., Cole, K.L.H., Wulff, P., Klugmann, M., and Murray, A.J. (2011). Production and titering of recombinant adeno-associated viral vectors. *J. Vis. Exp. JoVE* e3348.
- McCown, T.J. (2005). Adeno-associated virus (AAV) vectors in the CNS. *Curr. Gene Ther.* *5*, 333–338.
- McLennan, H. (1981). Actions of the optical isomers of 2-amino-5-phosphonovalerate as antagonists of excitatory amino acids. *Eur. J. Pharmacol.* *73*, 97–99.
- Mellado, M., Rodríguez-Frade, J.M., Vila-Coro, A.J., Fernández, S., Martín de Ana, A., Jones, D.R., Torán, J.L., and Martínez-A, C. (2001). Chemokine receptor homo- or heterodimerization activates distinct signaling pathways. *EMBO J.* *20*, 2497–2507.
- Mellström, B., Naranjo, J.R., Foulkes, N.S., Lafarga, M., and Sassone-Corsi, P. (1993). Transcriptional response to cAMP in brain: specific distribution and induction of CREM antagonists. *Neuron* *10*, 655–665.
- Melnikov, A., Murugan, A., Zhang, X., Tesileanu, T., Wang, L., Rogov, P., Feizi, S., Gnirke, A., Callan, C.G., Kinney, J.B., et al. (2012). Systematic dissection and optimization of inducible enhancers in human cells using a massively parallel reporter assay. *Nat. Biotechnol.* *30*, 271–277.
- Mertens, J., Wang, Q.-W., Kim, Y., Yu, D.X., Pham, S., Yang, B., Zheng, Y., Diffenderfer, K.E., Zhang, J., Soltani, S., et al. (2015). Differential responses to lithium in hyperexcitable neurons from patients with bipolar disorder. *Nature* *527*, 95–99.
- Mertens, J., Marchetto, M.C., Bardy, C., and Gage, F.H. (2016). Evaluating cell reprogramming, differentiation and conversion technologies in neuroscience. *Nat. Rev. Neurosci.* *advance online publication*.
- Meves, H., and Pichon, Y. (1975). Proceedings: Effects of 4-aminopyridine on the potassium current in internally perfused giant axons of the squid. *J. Physiol.* *251*, 60P–62P.
- Mohr, S.E., Smith, J.A., Shamu, C.E., Neumüller, R.A., and Perrimon, N. (2014). RNAi screening comes of age: improved techniques and complementary approaches. *Nat. Rev. Mol. Cell Biol.* *15*, 591–600.

References

- Moiani, A., Paleari, Y., Sartori, D., Mezzadra, R., Miccio, A., Cattoglio, C., Cocchiarella, F., Lidonnici, M.R., Ferrari, G., and Mavilio, F. (2012). Lentiviral vector integration in the human genome induces alternative splicing and generates aberrant transcripts. *J. Clin. Invest.* *122*, 1653–1666.
- Montminy, M. (1997). Transcriptional regulation by cyclic AMP. *Annu. Rev. Biochem.* *66*, 807–822.
- Morgan, J.I., Cohen, D.R., Hempstead, J.L., and Curran, T. (1987). Mapping patterns of *c-fos* expression in the central nervous system after seizure. *Science* *237*, 192–197.
- Morgens, D.W., Deans, R.M., Li, A., and Bassik, M.C. (2016). Systematic comparison of CRISPR/Cas9 and RNAi screens for essential genes. *Nat. Biotechnol.*
- Murphy, T.H., Worley, P.F., and Baraban, J.M. (1991). L-type voltage-sensitive calcium channels mediate synaptic activation of immediate early genes. *Neuron* *7*, 625–635.
- Nagappan, G., and Lu, B. (2005). Activity-dependent modulation of the BDNF receptor TrkB: mechanisms and implications. *Trends Neurosci.* *28*, 464–471.
- Nakai, H., Yant, S.R., Storm, T.A., Fuess, S., Meuse, L., and Kay, M.A. (2001). Extrachromosomal recombinant adeno-associated virus vector genomes are primarily responsible for stable liver transduction in vivo. *J. Virol.* *75*, 6969–6976.
- Nakamura, T., Barbara, J.G., Nakamura, K., and Ross, W.N. (1999). Synergistic release of Ca²⁺ from IP₃-sensitive stores evoked by synaptic activation of mGluRs paired with backpropagating action potentials. *Neuron* *24*, 727–737.
- Narahashi, T., Anderson, N.C., and Moore, J.W. (1966). Tetrodotoxin does not block excitation from inside the nerve membrane. *Science* *153*, 765–767.
- Neves, S.R., Ram, P.T., and Iyengar, R. (2002). G Protein Pathways. *Science* *296*, 1636–1639.
- Newell, K.A., and Matosin, N. (2014). Rethinking metabotropic glutamate receptor 5 pathological findings in psychiatric disorders: implications for the future of novel therapeutics. *BMC Psychiatry* *14*, 23.
- Ngo, V.N., Davis, R.E., Lamy, L., Yu, X., Zhao, H., Lenz, G., Lam, L.T., Dave, S., Yang, L., Powell, J., et al. (2006). A loss-of-function RNA interference screen for molecular targets in cancer. *Nature* *441*, 106–110.
- Nicholas, C.R., Chen, J., Tang, Y., Southwell, D.G., Chalmers, N., Vogt, D., Arnold, C.M., Chen, Y.-J.J., Stanley, E.G., Elefanty, A.G., et al. (2013). Functional Maturation of hPSC-Derived Forebrain Interneurons Requires an Extended Timeline and Mimics Human Neural Development. *Cell Stem Cell* *12*, 573–586.
- Nicol, X., and Gaspar, P. (2014). Routes to cAMP: shaping neuronal connectivity with distinct adenylate cyclases. *Eur. J. Neurosci.* *39*, 1742–1751.
- Nieland, T.J.F., Logan, D.J., Saulnier, J., Lam, D., Johnson, C., Root, D.E., Carpenter, A.E., and Sabatini, B.L. (2014). High content image analysis identifies novel regulators of synaptogenesis in a high-throughput RNAi screen of primary neurons. *PLoS One* *9*, e91744.
- Nowak, L., Bregestovski, P., Ascher, P., Herbet, A., and Prochiantz, A. (1984). Magnesium gates glutamate-activated channels in mouse central neurones. *Nature* *307*, 462–465.

References

- Nugent, F.S., Penick, E.C., and Kauer, J.A. (2007). Opioids block long-term potentiation of inhibitory synapses. *Nature* *446*, 1086–1090.
- Nurnberger Jr, Koller DL, Jung J, and et al (2014). Identification of pathways for bipolar disorder: A meta-analysis. *JAMA Psychiatry* *71*, 657–664.
- Ofengeim, D., Shi, P., Miao, B., Fan, J., Xia, X., Fan, Y., Lipinski, M.M., Hashimoto, T., Polydoro, M., Yuan, J., et al. (2012). Identification of small molecule inhibitors of neurite loss induced by A β peptide using high content screening. *J. Biol. Chem.* *287*, 8714–8723.
- Ogata, H., Goto, S., Fujibuchi, W., and Kanehisa, M. (1998). Computation with the KEGG pathway database. *Biosystems* *47*, 119–128.
- Paddison, P.J., Silva, J.M., Conklin, D.S., Schlabach, M., Li, M., Aruleba, S., Baliya, V., O’Shaughnessy, A., Gnoj, L., Scobie, K., et al. (2004). A resource for large-scale RNA-interference-based screens in mammals. *Nature* *428*, 427–431.
- Papassotiropoulos, A., and de Quervain, D.J.F. (2015). Failed drug discovery in psychiatry: time for human genome-guided solutions. *Trends Cogn. Sci.* *19*, 183–187.
- Park, H., and Poo, M. (2013). Neurotrophin regulation of neural circuit development and function. *Nat. Rev. Neurosci.* *14*, 7–23.
- Parnas, O., Jovanovic, M., Eisenhaure, T.M., Herbst, R.H., Dixit, A., Ye, C.J., Przybylski, D., Platt, R.J., Tirosh, I., Sanjana, N.E., et al. (2015). A Genome-wide CRISPR Screen in Primary Immune Cells to Dissect Regulatory Networks. *Cell* *162*, 675–686.
- Paulsen, B. da S., da Silveira, M.S., Galina, A., and Rehen, S.K. (2013). Pluripotent stem cells as a model to study oxygen metabolism in neurogenesis and neurodevelopmental disorders. *Arch. Biochem. Biophys.* *534*, 3–10.
- Penzes, P., Cahill, M.E., Jones, K.A., VanLeeuwen, J.-E., and Woolfrey, K.M. (2011). Dendritic spine pathology in neuropsychiatric disorders. *Nat Neurosci* *14*, 285–293.
- Pfenning, A.R., Schwartz, R., and Barth, A.L. (2007). A comparative genomics approach to identifying the plasticity transcriptome. *BMC Neurosci.* *8*, 20.
- Plath, N., Ohana, O., Dammermann, B., Errington, M.L., Schmitz, D., Gross, C., Mao, X., Engelsberg, A., Mahlke, C., Welzl, H., et al. (2006). Arc/Arg3.1 is essential for the consolidation of synaptic plasticity and memories. *Neuron* *52*, 437–444.
- Pratt, J., Winchester, C., Dawson, N., and Morris, B. (2012). Advancing schizophrenia drug discovery: optimizing rodent models to bridge the translational gap. *Nat. Rev. Drug Discov.* *11*, 560–579.
- Purcell, S.M., Moran, J.L., Fromer, M., Ruderfer, D., Solovieff, N., Roussos, P., O’Dushlaine, C., Chambert, K., Bergen, S.E., Kähler, A., et al. (2014). A polygenic burden of rare disruptive mutations in schizophrenia. *Nature* *506*, 185–190.
- Qi, L.S., Larson, M.H., Gilbert, L.A., Doudna, J.A., Weissman, J.S., Arkin, A.P., and Lim, W.A. (2013). Repurposing CRISPR as an RNA-guided platform for sequence-specific control of gene expression. *Cell* *152*, 1173–1183.
- Radio, N.M. (2012). Neurite outgrowth assessment using high content analysis methodology. *Methods Mol. Biol. Clifton NJ* *846*, 247–260.

References

- Ragozzino, D., Renzi, M., Giovannelli, A., and Eusebi, F. (2002). Stimulation of chemokine CXC receptor 4 induces synaptic depression of evoked parallel fibers inputs onto Purkinje neurons in mouse cerebellum. *J. Neuroimmunol.* *127*, 30–36.
- Rajewsky, N. (2006). microRNA target predictions in animals. *Nat. Genet.* *38 Suppl*, S8-13.
- Redmond, L. (2008). Translating neuronal activity into dendrite elaboration: signaling to the nucleus. *Neurosignals* *16*, 194–208.
- Ripke, S., O'Dushlaine, C., Chambert, K., Moran, J.L., Kähler, A.K., Akterin, S., Bergen, S.E., Collins, A.L., Crowley, J.J., Fromer, M., et al. (2013). Genome-wide association analysis identifies 13 new risk loci for schizophrenia. *Nat. Genet.* *45*, 1150–1159.
- Rodríguez-Tornos, F.M., San Aniceto, I., Cubelos, B., and Nieto, M. (2013). Enrichment of conserved synaptic activity-responsive element in neuronal genes predicts a coordinated response of MEF2, CREB and SRF. *PLoS One* *8*, e53848.
- Rossi, D., and Zlotnik, A. (2000). The biology of chemokines and their receptors. *Annu. Rev. Immunol.* *18*, 217–242.
- Rubinson, D.A., Dillon, C.P., Kwiatkowski, A.V., Sievers, C., Yang, L., Kopinja, J., Rooney, D.L., Zhang, M., Ihrig, M.M., McManus, M.T., et al. (2003). A lentivirus-based system to functionally silence genes in primary mammalian cells, stem cells and transgenic mice by RNA interference. *Nat. Genet.* *33*, 401–406.
- Sabatini, B.L., Oertner, T.G., and Svoboda, K. (2002). The life cycle of Ca²⁺ ions in dendritic spines. *Neuron* *33*, 439–452.
- Sada, N., Lee, S., Katsu, T., Otsuki, T., and Inoue, T. (2015). Epilepsy treatment. Targeting LDH enzymes with a stiripentol analog to treat epilepsy. *Science* *347*, 1362–1367.
- Sala, C., Futai, K., Yamamoto, K., Worley, P.F., Hayashi, Y., and Sheng, M. (2003). Inhibition of dendritic spine morphogenesis and synaptic transmission by activity-inducible protein Homer1a. *J. Neurosci. Off. J. Soc. Neurosci.* *23*, 6327–6337.
- Sarkar, A., Marchetto, M.C., and Gage, F.H. (2015). Synaptic activity: An emerging player in schizophrenia. *Brain Res.*
- Saunders, J.A., Gandal, M.J., and Siegel, S.J. (2012). NMDA antagonists recreate signal-to-noise ratio and timing perturbations present in schizophrenia. *Neurobiol. Dis.* *46*, 93–100.
- Sawicka, K., and Zukin, R.S. (2012). Dysregulation of mTOR signaling in neuropsychiatric disorders: therapeutic implications. *Neuropsychopharmacol. Off. Publ. Am. Coll. Neuropsychopharmacol.* *37*, 305–306.
- Scannell, J.W., and Bosley, J. (2016). When Quality Beats Quantity: Decision Theory, Drug Discovery, and the Reproducibility Crisis. *PLoS One* *11*, e0147215.
- Scannell, J.W., Blanckley, A., Boldon, H., and Warrington, B. (2012). Diagnosing the decline in pharmaceutical R&D efficiency. *Nat. Rev. Drug Discov.* *11*, 191–200.
- Schena, M., Shalon, D., Davis, R.W., and Brown, P.O. (1995). Quantitative Monitoring of Gene Expression Patterns with a Complementary DNA Microarray. *Science* *270*, 467–470.
- Schenone, M., Dančák, V., Wagner, B.K., and Clemons, P.A. (2013). Target identification and mechanism of action in chemical biology and drug discovery. *Nat. Chem. Biol.* *9*, 232–240.

References

- Schilling, K., Luk, D., Morgan, J.I., and Curran, T. (1991). Regulation of a fos-lacZ fusion gene: a paradigm for quantitative analysis of stimulus-transcription coupling. *Proc. Natl. Acad. Sci. U. S. A.* 88, 5665–5669.
- Schizophrenia Working Group of the Psychiatric Genomics Consortium (2014). Biological insights from 108 schizophrenia-associated genetic loci. *Nature* 511, 421–427.
- Schlabach, M.R., Luo, J., Solimini, N.L., Hu, G., Xu, Q., Li, M.Z., Zhao, Z., Smogorzewska, A., Sowa, M.E., Ang, X.L., et al. (2008). Cancer proliferation gene discovery through functional genomics. *Science* 319, 620–624.
- Schmittgen, T.D., and Livak, K.J. (2008). Analyzing real-time PCR data by the comparative CT method. *Nat. Protoc.* 3, 1101–1108.
- Schulte, J., Sepp, K.J., Wu, C., Hong, P., and Littleton, J.T. (2011). High-content chemical and RNAi screens for suppressors of neurotoxicity in a Huntington's disease model. *PLoS One* 6, e23841.
- Schwarz, D.S., Hutvagner, G., Du, T., Xu, Z., Aronin, N., and Zamore, P.D. (2003). Asymmetry in the assembly of the RNAi enzyme complex. *Cell* 115, 199–208.
- Segal, M. (2005). Dendritic spines and long-term plasticity. *Nat. Rev. Neurosci.* 6, 277–284.
- Sekar, A., Bialas, A.R., de Rivera, H., Davis, A., Hammond, T.R., Kamitaki, N., Tooley, K., Presumey, J., Baum, M., Van Doren, V., et al. (2016). Schizophrenia risk from complex variation of complement component 4. *Nature* 530, 177–183.
- Selemon, L.D., and Goldman-Rakic, P.S. (1999). The reduced neuropil hypothesis: a circuit based model of schizophrenia. *Biol. Psychiatry* 45, 17–25.
- Shalem, O., Sanjana, N.E., Hartenian, E., Shi, X., Scott, D.A., Mikkelsen, T.S., Heckl, D., Ebert, B.L., Root, D.E., Doench, J.G., et al. (2014). Genome-scale CRISPR-Cas9 knockout screening in human cells. *Science* 343, 84–87.
- Shalem, O., Sanjana, N.E., and Zhang, F. (2015). High-throughput functional genomics using CRISPR-Cas9. *Nat. Rev. Genet.* 16, 299–311.
- Shalin, S.C., Hernandez, C.M., Dougherty, M.K., Morrison, D.K., and Sweatt, J.D. (2006). Kinase suppressor of Ras1 compartmentalizes hippocampal signal transduction and subserves synaptic plasticity and memory formation. *Neuron* 50, 765–779.
- Sharma, K., Schmitt, S., Bergner, C.G., Tyanova, S., Kannaiyan, N., Manrique-Hoyos, N., Kongi, K., Cantuti, L., Hanisch, U.-K., Philips, M.-A., et al. (2015). Cell type- and brain region-resolved mouse brain proteome. *Nat. Neurosci.* 18, 1819–1831.
- Sheng, M., and Greenberg, M.E. (1990). The regulation and function of c-fos and other immediate early genes in the nervous system. *Neuron* 4, 477–485.
- Shepherd, J.D., Rumbaugh, G., Wu, J., Chowdhury, S., Plath, N., Kuhl, D., Huganir, R.L., and Worley, P.F. (2006). Arc/Arg3.1 mediates homeostatic synaptic scaling of AMPA receptors. *Neuron* 52, 475–484.
- Sherrington, R., Rogaev, E.I., Liang, Y., Rogaeva, E.A., Levesque, G., Ikeda, M., Chi, H., Lin, C., Li, G., Holman, K., et al. (1995). Cloning of a gene bearing missense mutations in early-onset familial Alzheimer's disease. *Nature* 375, 754–760.

References

- Silva, J.M., Marran, K., Parker, J.S., Silva, J., Golding, M., Schlabach, M.R., Elledge, S.J., Hannon, G.J., and Chang, K. (2008). Profiling essential genes in human mammary cells by multiplex RNAi screening. *Science* 319, 617–620.
- Sindreu, C.B., Scheiner, Z.S., and Storm, D.R. (2007). Ca²⁺-stimulated adenylyl cyclases regulate ERK-dependent activation of MSK1 during fear conditioning. *Neuron* 53, 79–89.
- Sohal, V.S., Zhang, F., Yizhar, O., and Deisseroth, K. (2009). Parvalbumin neurons and gamma rhythms enhance cortical circuit performance. *Nature* 459, 698–702.
- Song, J., Bergen, S.E., Kuja-Halkola, R., Larsson, H., Landén, M., and Lichtenstein, P. (2015). Bipolar disorder and its relation to major psychiatric disorders: a family-based study in the Swedish population. *Bipolar Disord.* 17, 184–193.
- Spiegel, I., Mardinly, A.R., Gabel, H.W., Bazinet, J.E., Couch, C.H., Tzeng, C.P., Harmin, D.A., and Greenberg, M.E. (2014). Npas4 regulates excitatory-inhibitory balance within neural circuits through cell-type-specific gene programs. *Cell* 157, 1216–1229.
- Sprenger, J., Lynn Fink, J., Karunaratne, S., Hanson, K., Hamilton, N.A., and Teasdale, R.D. (2008). LOCATE: a mammalian protein subcellular localization database. *Nucleic Acids Res.* 36, D230–D233.
- St Clair, D., Blackwood, D., Muir, W., Carothers, A., Walker, M., Spowart, G., Gosden, C., and Evans, H.J. (1990). Association within a family of a balanced autosomal translocation with major mental illness. *Lancet Lond. Engl.* 336, 13–16.
- Steen, R.G., Mull, C., McClure, R., Hamer, R.M., and Lieberman, J.A. (2006). Brain volume in first-episode schizophrenia: systematic review and meta-analysis of magnetic resonance imaging studies. *Br. J. Psychiatry J. Ment. Sci.* 188, 510–518.
- Stefánsson, H., Thorgeirsson, T.E., Gulcher, J.R., and Stefánsson, K. (2003). Neuregulin 1 in schizophrenia: out of Iceland. *Mol. Psychiatry* 8, 639–640.
- Stefansson, H., Ophoff, R.A., Steinberg, S., Andreassen, O.A., Cichon, S., Rujescu, D., Werge, T., Pietiläinen, O.P.H., Mors, O., Mortensen, P.B., et al. (2009). Common variants conferring risk of schizophrenia. *Nature* 460, 744–747.
- von Stein, A., and Sarnthein, J. (2000). Different frequencies for different scales of cortical integration: from local gamma to long range alpha/theta synchronization. *Int. J. Psychophysiol. Off. J. Int. Organ. Psychophysiol.* 38, 301–313.
- Stephan, A.H., Barres, B.A., and Stevens, B. (2012). The complement system: an unexpected role in synaptic pruning during development and disease. *Annu. Rev. Neurosci.* 35, 369–389.
- Stewart, S.A., DYKXHOORN, D.M., PALLISER, D., MIZUNO, H., YU, E.Y., AN, D.S., SABATINI, D.M., CHEN, I.S.Y., HAHN, W.C., SHARP, P.A., et al. (2003). Lentivirus-delivered stable gene silencing by RNAi in primary cells. *RNA* 9, 493–501.
- Stuart, G., Spruston, N., Sakmann, B., and Häusser, M. (1997). Action potential initiation and backpropagation in neurons of the mammalian CNS. *Trends Neurosci.* 20, 125–131.
- Sullivan, P.F., Kendler, K.S., and Neale, M.C. (2003). Schizophrenia as a complex trait: evidence from a meta-analysis of twin studies. *Arch. Gen. Psychiatry* 60, 1187–1192.

References

- Sweet, R.A., Henteleff, R.A., Zhang, W., Sampson, A.R., and Lewis, D.A. (2009). Reduced dendritic spine density in auditory cortex of subjects with schizophrenia. *Neuropsychopharmacol. Off. Publ. Am. Coll. Neuropsychopharmacol.* 34, 374–389.
- Swinney, D.C., and Anthony, J. (2011). How were new medicines discovered? *Nat. Rev. Drug Discov.* 10, 507–519.
- Szekanecz, Z., and Koch, A.E. (2001). Chemokines and angiogenesis. *Curr. Opin. Rheumatol.* 13, 202–208.
- Takahashi, K., and Yamanaka, S. (2006). Induction of pluripotent stem cells from mouse embryonic and adult fibroblast cultures by defined factors. *Cell* 126, 663–676.
- Tanenbaum, M.E., Gilbert, L.A., Qi, L.S., Weissman, J.S., and Vale, R.D. (2014). A protein tagging system for signal amplification in gene expression and fluorescence imaging. *Cell* 159, 635–646.
- Tang, B., Wang, T., Wan, H., Han, L., Qin, X., Zhang, Y., Wang, J., Yu, C., Berton, F., Francesconi, W., et al. (2015). Fmr1 deficiency promotes age-dependent alterations in the cortical synaptic proteome. *Proc. Natl. Acad. Sci. U. S. A.* 112, E4697-4706.
- Tennessen, J.A., Bigham, A.W., O'Connor, T.D., Fu, W., Kenny, E.E., Gravel, S., McGee, S., Do, R., Liu, X., Jun, G., et al. (2012). Evolution and functional impact of rare coding variation from deep sequencing of human exomes. *Science* 337, 64–69.
- Thomson, A.M. (2000). Facilitation, augmentation and potentiation at central synapses. *Trends Neurosci.* 23, 305–312.
- Tian, J., Ma, K., and Saaem, I. (2009). Advancing high-throughput gene synthesis technology. *Mol. Biosyst.* 5, 714–722.
- Topol, A., Zhu, S., Tran, N., Simone, A., Fang, G., and Brennand, K.J. (2015). Altered WNT Signaling in Human Induced Pluripotent Stem Cell Neural Progenitor Cells Derived from Four Schizophrenia Patients. *Biol. Psychiatry* 78, e29-34.
- Tran, P.B., and Miller, R.J. (2003). Chemokine receptors: signposts to brain development and disease. *Nat. Rev. Neurosci.* 4, 444–455.
- Ubogu, E.E., Cossoy, M.B., and Ransohoff, R.M. (2006). The expression and function of chemokines involved in CNS inflammation. *Trends Pharmacol. Sci.* 27, 48–55.
- Uhlhaas, P.J., and Singer, W. (2012). Neuronal dynamics and neuropsychiatric disorders: toward a translational paradigm for dysfunctional large-scale networks. *Neuron* 75, 963–980.
- Vacic, V., McCarthy, S., Malhotra, D., Murray, F., Chou, H.-H., Peoples, A., Makarov, V., Yoon, S., Bhandari, A., Corominas, R., et al. (2011). Duplications of the neuropeptide receptor gene VIPR2 confer significant risk for schizophrenia. *Nature* 471, 499–503.
- Varela, F., Lachaux, J.P., Rodriguez, E., and Martinerie, J. (2001). The brainweb: phase synchronization and large-scale integration. *Nat. Rev. Neurosci.* 2, 229–239.
- Verkhatsky, A. (2004). Endoplasmic reticulum calcium signaling in nerve cells. *Biol. Res.* 37, 693–699.
- Vincent, F., Loria, P., Pregel, M., Stanton, R., Kitching, L., Nocka, K., Doyonnas, R., Stepan, C., Gilbert, A., Schroeter, T., et al. (2015). Developing predictive assays: the phenotypic screening “rule of 3.” *Sci. Transl. Med.* 7, 293ps15.

References

- Wagner, B.K., and Schreiber, S.L. (2016). The Power of Sophisticated Phenotypic Screening and Modern Mechanism-of-Action Methods. *Cell Chem. Biol.* 23, 3–9.
- Wang, H., and Storm, D.R. (2003). Calmodulin-regulated adenylyl cyclases: cross-talk and plasticity in the central nervous system. *Mol. Pharmacol.* 63, 463–468.
- Wang, X.J., and Buzsáki, G. (1996). Gamma oscillation by synaptic inhibition in a hippocampal interneuronal network model. *J. Neurosci. Off. J. Soc. Neurosci.* 16, 6402–6413.
- Wang, T., Wei, J.J., Sabatini, D.M., and Lander, E.S. (2014). Genetic screens in human cells using the CRISPR-Cas9 system. *Science* 343, 80–84.
- Watanabe, S., Hong, M., Lasser-Ross, N., and Ross, W.N. (2006). Modulation of calcium wave propagation in the dendrites and to the soma of rat hippocampal pyramidal neurons. *J. Physiol.* 575, 455–468.
- Waters, J., Schaefer, A., and Sakmann, B. (2005). Backpropagating action potentials in neurones: measurement, mechanisms and potential functions. *Prog. Biophys. Mol. Biol.* 87, 145–170.
- Wen, Z., Nguyen, H.N., Guo, Z., Lalli, M.A., Wang, X., Su, Y., Kim, N.-S., Yoon, K.-J., Shin, J., Zhang, C., et al. (2014). Synaptic dysregulation in a human iPSC cell model of mental disorders. *Nature* 515, 414–418.
- West, A.E., and Greenberg, M.E. (2011). Neuronal activity-regulated gene transcription in synapse development and cognitive function. *Cold Spring Harb. Perspect. Biol.* 3.
- West, A.E., Griffith, E.C., and Greenberg, M.E. (2002). Regulation of transcription factors by neuronal activity. *Nat. Rev. Neurosci.* 3, 921–931.
- Whittington, M.A., Traub, R.D., and Jefferys, J.G. (1995). Synchronized oscillations in interneuron networks driven by metabotropic glutamate receptor activation. *Nature* 373, 612–615.
- Wiegert, J.S., and Bading, H. (2011). Activity-dependent calcium signaling and ERK-MAP kinases in neurons: a link to structural plasticity of the nucleus and gene transcription regulation. *Cell Calcium* 49, 296–305.
- Wiegert, J.S., Bengtson, C.P., and Bading, H. (2007). Diffusion and not active transport underlies and limits ERK1/2 synapse-to-nucleus signaling in hippocampal neurons. *J. Biol. Chem.* 282, 29621–29633.
- Williams, R.W., and Herrup, K. (1988). The control of neuron number. *Annu. Rev. Neurosci.* 11, 423–453.
- Winkler, U., and Hirrlinger, J. (2015). Crosstalk of Signaling and Metabolism Mediated by the NAD(+)/NADH Redox State in Brain Cells. *Neurochem. Res.* 40, 2394–2401.
- Winzler, E.A., Shoemaker, D.D., Astromoff, A., Liang, H., Anderson, K., Andre, B., Bangham, R., Benito, R., Boeke, J.D., Bussey, H., et al. (1999). Functional Characterization of the *S. cerevisiae* Genome by Gene Deletion and Parallel Analysis. *Science* 285, 901–906.
- Wray, N.R., Pergadia, M.L., Blackwood, D.H.R., Penninx, B.W.J.H., Gordon, S.D., Nyholt, D.R., Ripke, S., MacIntyre, D.J., McGhee, K.A., Maclean, A.W., et al. (2012). Genome-wide association study of major depressive disorder: new results, meta-analysis, and lessons learned. *Mol. Psychiatry* 17, 36–48.

References

- Xia, Y., Zhao, P., Xue, J., Gu, X.Q., Sun, X., Yao, H., and Haddad, G.G. (2003). Na⁺-channel expression and neuronal function in the Na⁺/H⁺ exchanger 1 null mutant mouse. *J. Neurophysiol.* *89*, 229–236.
- Xia, Z., Dudek, H., Miranti, C.K., and Greenberg, M.E. (1996). Calcium influx via the NMDA receptor induces immediate early gene transcription by a MAP kinase/ERK-dependent mechanism. *J. Neurosci. Off. J. Soc. Neurosci.* *16*, 5425–5436.
- Xing, J., Ginty, D.D., and Greenberg, M.E. (1996). Coupling of the RAS-MAPK pathway to gene activation by RSK2, a growth factor-regulated CREB kinase. *Science* *273*, 959–963.
- Yi, R., Qin, Y., Macara, I.G., and Cullen, B.R. (2003). Exportin-5 mediates the nuclear export of pre-microRNAs and short hairpin RNAs. *Genes Dev.* *17*, 3011–3016.
- Yizhar, O., Fenno, L.E., Prigge, M., Schneider, F., Davidson, T.J., O'Shea, D.J., Sohal, V.S., Goshen, I., Finkelstein, J., Paz, J.T., et al. (2011). Neocortical excitation/inhibition balance in information processing and social dysfunction. *Nature* *477*, 171–178.
- Yoshida, T., Imai, T., Kakizaki, M., Nishimura, M., Takagi, S., and Yoshie, O. (1998). Identification of single C motif-1/lymphotactin receptor XCR1. *J. Biol. Chem.* *273*, 16551–16554.
- Yoshida, T., Izawa, D., Nakayama, T., Nakahara, K., Kakizaki, M., Imai, T., Suzuki, R., Miyasaka, M., and Yoshie, O. (1999). Molecular cloning of mXCR1, the murine SCM-1/lymphotactin receptor. *FEBS Lett.* *458*, 37–40.
- Zeng, Y., and Cullen, B.R. (2004). Structural requirements for pre-microRNA binding and nuclear export by Exportin 5. *Nucleic Acids Res.* *32*, 4776–4785.
- Zhang, S.-J., Zou, M., Lu, L., Lau, D., Ditzel, D.A.W., Delucinge-Vivier, C., Aso, Y., Descombes, P., and Bading, H. (2009). Nuclear calcium signaling controls expression of a large gene pool: identification of a gene program for acquired neuroprotection induced by synaptic activity. *PLoS Genet.* *5*, e1000604.
- Zhu, J.J., Qin, Y., Zhao, M., Van Aelst, L., and Malinow, R. (2002). Ras and Rap control AMPA receptor trafficking during synaptic plasticity. *Cell* *110*, 443–455.
- Zilberter, Y. (2000). Dendritic release of glutamate suppresses synaptic inhibition of pyramidal neurons in rat neocortex. *J. Physiol.* *528*, 489–496.
- Zuber, J., McJunkin, K., Fellmann, C., Dow, L.E., Taylor, M.J., Hannon, G.J., and Lowe, S.W. (2011). Toolkit for evaluating genes required for proliferation and survival using tetracycline-regulated RNAi. *Nat. Biotechnol.* *29*, 79–83.
- Zucker, R.S., and Regehr, W.G. (2002). Short-term synaptic plasticity. *Annu. Rev. Physiol.* *64*, 355–405.

9. Acknowledgement

First of all, I want to thank Prof. Dr. Moritz Rossner for his supervision and his support over the last years. I am very grateful that I got the opportunity to do cutting-edge science and develop under his supervision into a passionate scientist with a strong interest in assay development.

I want to highlight the exceptional team spirit of the entire department for Molecular Neurobiology. This has been very important for the success of this project. In particular, I would like to give credit to Dr. Sven Wichert, Dr. Michael Wehr, Dr. Ben Brankatschk, and Nirmal Raman Kannaiyan, as they were always open for help and invaluable feedback, as well as great times outside the lab.

For proof-reading my thesis, I would in particular like to thank Dr. Michael Wehr and Dr. Ben Brankatschk.

Since many people have been involved in this project, I would like to extend my thanks to Beate Kauschat for her great assistance with the primary neuron cultures and to Dr. Sabrina Galinski, Stefanie Behrens, and Karin Neumeier for running the NGS facility.

I am grateful to my thesis committee members, Prof. Dr. Nils Brose and Dr. Camin Dean for the input during the committee meetings.

Curriculum vitae

Personal data

Name	Alexander Herholt
Date of birth	16.05.1986
Place of birth	Bielefeld
Nationality	German

Education

2012 – current	Graduate student GGNB Graduate School “Molecular Physiology of the Brain” Molecular Neurobiology, Department of Psychiatry, Ludwig-Maximilians-University Munich 2012-2014 Max-Planck-Institute of Experimental Medicine Göttingen, Department of Neurogenetics, Research group Gene expression and signaling
2011 – 2012	Research associate Max-Planck-Institute of Experimental Medicine Göttingen, Department of Neurogenetics, Research group Gene expression and signaling
2011	M. Sc. in Developmental, Neural, and Behavioral Biology
2009 – 2011	M.Sc. study in Developmental, Neural, and Behavioral Biology Georg-August University Göttingen
2009	B.Sc. in Biology
2006 – 2009	B.Sc. study in Biology Georg-August University Göttingen
2005 – 2006	Social service
2005	Abitur Martin-Niemöller Gesamtschule Bielefeld

Publications

Willig KI, Steffens H, Gregor C, Herholt A, Rossner MJ, Hell SW (2014)
Nanoscopy of filamentous actin in cortical dendrites of a living mouse.
Biophysical journal 106(1), L01-L03